

Biosensors, customisation, and prototyping

Citation for published version (APA):

Rogosic, R. (2023). *Biosensors, customisation, and prototyping: How to make point of care diagnostics more relevant*. [Doctoral Thesis, Maastricht University]. Maastricht University. <https://doi.org/10.26481/dis.20230404rr>

Document status and date:

Published: 01/01/2023

DOI:

[10.26481/dis.20230404rr](https://doi.org/10.26481/dis.20230404rr)

Document Version:

Publisher's PDF, also known as Version of record

Please check the document version of this publication:

- A submitted manuscript is the version of the article upon submission and before peer-review. There can be important differences between the submitted version and the official published version of record. People interested in the research are advised to contact the author for the final version of the publication, or visit the DOI to the publisher's website.
- The final author version and the galley proof are versions of the publication after peer review.
- The final published version features the final layout of the paper including the volume, issue and page numbers.

[Link to publication](#)

General rights

Copyright and moral rights for the publications made accessible in the public portal are retained by the authors and/or other copyright owners and it is a condition of accessing publications that users recognise and abide by the legal requirements associated with these rights.

- Users may download and print one copy of any publication from the public portal for the purpose of private study or research.
- You may not further distribute the material or use it for any profit-making activity or commercial gain
- You may freely distribute the URL identifying the publication in the public portal.

If the publication is distributed under the terms of Article 25fa of the Dutch Copyright Act, indicated by the "Taverne" license above, please follow below link for the End User Agreement:

www.umlib.nl/taverne-license

Take down policy

If you believe that this document breaches copyright please contact us at:

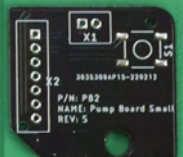
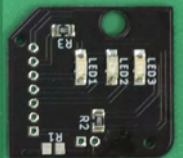
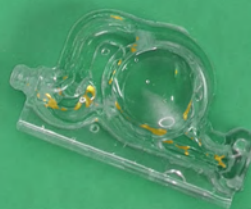
repository@maastrichtuniversity.nl

providing details and we will investigate your claim.

BIOSENSORS, CUSTOMISATION AND PROTOTYPING: HOW TO MAKE POINT OF CARE DIAGNOSTICS MORE RELEVANT

Renato Rogosic

2023



BIOSENSORS, CUSTOMISATION AND PROTOTYPING: HOW TO MAKE POINT OF CARE DIAGNOSTICS MORE RELEVANT

Dissertation

To obtain the degree of Doctor at Maastricht University,
on the authority of the Rector Magnificus, Prof. Dr. P. Habibovic,
in accordance with the decision of the Board of Deans,
to be defended in public
on the 4th of April, at 16:00

by

Renato Rogosic

Promotor

Dr. Bart van Grinsven
Prof. Dr. Thomas Cleij

Copromotor

Dr. Kasper Eersels

Assessment Committee

Prof. Dr. Mark Winands (Chair)
Prof. Dr. Ronald Thoelen
Prof. Dr. Theodor Doll
Dr. Jules Harings
Dr. Christopher Pawley

© Renato Rogosic, Maastricht 2023.

All rights reserved. No part of this publication may be reproduced, stored in a retrieval system or transmitted in any form or by any means, electronic, mechanical, photocopying, recording or otherwise, without prior written permission of the author.

Contents

1	Introduction	1
1.1	From Rapid Prototyping (RP) to Rapid Manufacturing (RM)	3
1.2	Rapid Manufacturing	8
1.3	Point of care diagnostics	18
1.4	Outline and aim of the thesis	24
2	The Liberalization of Microfluidics - Form2 Benchtop 3D Printing as an Affordable Alternative to Established Manufacturing Methods	37
2.1	Introduction	40
2.2	Materials and Methods	44
2.3	Results	46
2.4	Discussion	49
2.5	Conclusion	51
3	Studying the effect of Adhesive Layer Composition on MIP-based Thermal Biosensing	57
3.1	Introduction	60
3.2	Experimental Section	62
3.3	Results	65
3.4	Discussion	68
3.5	Conclusion	70
4	Cost-effective, Scalable and Smartphone-controlled 3D-Printed Syringe Pump - From Lab Bench to Point of Care Biosensing Applications	75
4.1	Introduction	78
4.2	Materials and Methods	79
4.3	Validation and Characterization	83
4.4	Discussion and Conclusion	87

Contents

5	Modular Science Kit as a support platform for STEM learning in primary and secondary school	103
5.1	Introduction	106
5.2	Materials and Hazards	108
5.3	The experiencing phase	110
5.4	The learning phase	113
5.5	Conclusion	115
6	General Discussion	151
	Summary	159
	Valorization	163
	Published work	167
	Curriculum Vitae	171
	Acknowledgments	173

1

Introduction

Chapter preface

The first chapter of the thesis starts with the introduction of the concepts of rapid prototyping (RP) and rapid manufacturing (RM). It provides the reader with a historical contextualization, guiding through the main technologies that enabled the rise of this new type of production process. Particular focus is given to the impact of rapid prototyping, and rapid manufacturing, on the design cycle and industrial manufacturing processes. Engineering and economic advantages are discussed in relation to the design cycle, with real world examples of industries using 3D printing, the main RP and RM technique discussed in this thesis. After a general introduction, attention is given to the medical industry, describing the main areas of utilization of 3D printing in this field. Rapid manufacturing is contextualized with regard to personalization of medicine and the crucial role it gained. The chapter continues by moving from medical applications to educational and research environments and to socially relevant projects, in which 3D printing is the main manufacturing process. As it will be seen in chapters 4 and 5, educational applications of 3D printing are an important part of the work developed. Finally, the chapter introduces the concept of biosensors, their main commercial applications (focusing on Point of Care devices) and gives an insight on how RM could improve their commercial valorization. The goal of the introduction chapter is to contextualize the works described in the thesis, which are of various nature, but have a common underlying goal: the use of modern RP and RM (mainly 3D printing) as powerful tool for research, education and medical applications. The concluding parts of the introduction briefly describe the aim of each chapter, and the thesis as a whole.

1.1 From Rapid Prototyping (RP) to Rapid Manufacturing (RM)

Rapid prototyping is a term that describes a variety of techniques that share common features used in well-defined phases of product development. Generally, these shared features are the use of a Computer Aided Design/Manufacturing (CAD/CAM) system, the translation of the computer-modelled design into a format supported by the machine used in the rapid prototyping technique of choice, and finally the fabrication of the desired part. The complete process is performed in a relatively short time and at reduced cost. Rapid prototyping manufacturing processes are divided into compressive, subtractive and additive processes. While compressive and subtractive processes are the more traditional approaches (e.g. molding, rapid machining), at present, additive manufacturing, and in particular 3D printing, is the most commonly used technique [1]. In additive manufacturing, after creating the CAD model, the object is exported in a .STL file (stands for stereo lithography, and it is an approximation of the solid with combinations of polygons) and finally the “slicing” of the model into cross-sectional layers. These layers are then consecutively materialized in order to fabricate the solid [2].

Additive manufacturing, as we know it today, started to develop in the 1980s : Hideo Kodama was the first, in 1981, to use UV light to cure liquid polymers in order to create solid objects [3]. Similarly, a patent from Charles Hull in 1984, claimed the right for “A system for generating three-dimensional objects by creating successive adjacent cross-sections of the object, being automatically formed and integrated together to provide a step-wise laminar build-up of the desired object” [4]. This process is called stereo lithography and Charles Hull is credited to be its father. In 1989, Scott Crump patented a technology that over the years became the most widely used technology for rapid prototyping in the world: fused deposition modelling (FDM) [5]. Both FDM machines and stereo lithography machines fall today under the umbrella term “3D printers”. Since then, a plethora of similar technologies have been developed, some of which have been abandoned while others managed to reach the market and became commercially successful [6]. Today,

rapid prototyping techniques are used to improve efficiency during some stages of the design cycle (Figure 1.2) in a multitude of industries. The most commonly used machine in additive manufacturing, is the 3D printer [7]. In the early 1990s, a 3D printer would cost several hundreds of thousands of dollars, while today we can buy a high-end desktop 3D printer for a few thousand dollars [8]. While it might seem like an incredible technological leap, it is important to understand that in the early 2000s, a conceptual change happened in the 3D printing industry. Since the birth of additive manufacturing, big industries were the main beneficiary from these technologies, using 3D printing to reduce prototyping costs.



Figure 1.1: The prototyping revolution. A typical RP workstation including a computer with a CAD software and a slicing software, a prototyping tool and different materials. Adapted from zortrax.com

This was due to various factors such as the need for expensive and delicate machines, training costs for personnel, limited range of materials and low quality of final object. Over the years, the technical improvements allowed to 3D print objects with better mechanical properties and more aesthetically pleasant finishing at a fraction of the price [9]. Better aesthetics together with the possibility to use materials with a wide range of properties created the perfect environment for

the spread of 3D printing among thousands of smaller companies, self-employed professionals as well as millions of DIY enthusiasts and artists. The boom that 3D printing experienced in the last decade lays its grounds on another technological development of the late 20th century: Computer Aided Design (CAD) [10].

The invention of CAD dates back to the middle of the past century. Many researchers and inventors were working on similar concepts in those years, however, there are few milestones often cited as inventions that paved the way for the development of CAD as we know it today. One of these milestones dates to 1963, when Ivan Sutherland published his PhD thesis. In his work, he developed “Sketchpad”, a program that allowed drafters to draw with a light pen on a CRT monitor [11]. This was the first program that allowed for graphical communication between man and machine, and a pioneering effort in the field of human-computer interaction. Similarly, Patrick J. Hanratty’s PRONTO [12] (Program for Numerical Tooling Operations, 1957) was the first Computer Numerical Controlled (CNC) programming system developed. The program worked by taking as input punch-cards and translating them into digital instructions that the machine tool controller needed to operate the machine tool. Last but not least, Pierre Bézier’s UNISURF CAD, was a computer aided design tool used at Renault in the early 1960s to shape the car body. Traditionally, car designs started on a drawing board and the design process had to go through various stages and iterations of clay models and machined prototypes. Particularly complicated and time-consuming was the process of designing the curves of the car’s bodies. A solution came at the end of the 1950s with the invention of the Bézier curves. These curves are parametric equations that allow a computer to draw lines in an elegant and numerically efficient way. Bézier’s curves are based on the De Cateljau’s Algorithm, however Bézier patented a parametric method used to represent curves with a computer. Similarly to 3D printing, in the early years of CAD/CAM, this technology was a tool for heavy industry. However, the emergence of UNIX workstations and later the development of new PCs, marked the beginning of large-scale adoption of CAD [13]. Slowly, the technology started to become accessible to a wide pool of engineers and consumers. In today’s industry, it is difficult to imagine a production

process of a good that does not involve CAD software in one of its phases. Even artists in the fashion industry rely on 3D CAD software to design test and review their creations [14, 15].

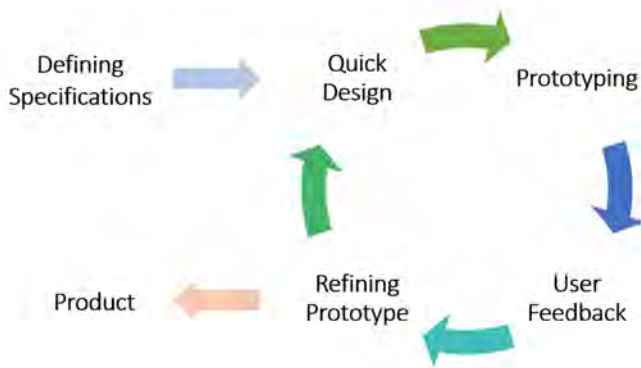


Figure 1.2: The product design cycle. The first step is the definition of the product specifications. Following a draft and a first prototype, user feedback is collected and analysed. Based on this feedback, the prototype is refined, and the cycle can be re-entered or finished if the product meets the requirements.

Accessible designing tools and rapid prototyping machines have changed the design cycle of products in all types of industries. Skilled model makers that had to transform 2D drawings into a prototype have been substituted by CAD designers and 3D printers. Rapid prototyping has shortened the time to market and the development costs considerably [16]. It has also changed the way functional parts are designed: since the advent of RP, the complexity of products that reach the markets have increased [17]. The flexibility in fabrication technology allows product designers to overcome the complexity constraints that characterized previous prototyping and fabrication methods. This translates into highly optimized parts that can respect multiple specifications, but also in products that are more aesthetically appealing. The development process of a new product is made of sequence of parallel and serial activities: for example, the parallel development of the mechanical, electrical and software designs or the sequential improvement and expansion of each of these design segments. In industry, it is common

to assemble the prototypes of the product at various stages of the design process to get a better picture of development direction. This type of development process is called waterfall development process or stage-gate process, as it provide evaluation stages at which design features can be stopped. The costs and timelines of the completion of all the activities associated to a new product development are a burden for the companies which generally adopt optimization strategies [18]. As the development process goes on, the prototypes built evolve from simple models to assemblies that closely resemble the final product. Similarly, the functionality of the models evolve with the process, as early prototypes have limited functionality. An important process that is often neglected by product designers along the design process is the customer acceptance testing. While external influences can slow down the process and add costs, they are obviously very important to the success of the commercialization of the final product. Some companies relegate the customer input in the development of a product only to the latest stages of the process. This would be done for multiple reasons: to keep the product confidential, but also because producing a functional prototype with adequate characteristics for commercialization would be extremely expensive. It is clear that this process potentially hinders the efficacy of the customer acceptance testing. With the advent of RP, it became possible to use CAD models and fabrication techniques such as additive manufacturing to drastically reduce times and costs of prototyping, creating fully working prototypes, closely resembling the final product.

Over the last three decades, the development in technologies and materials, created the perfect conditions for a slow transition, in some industrial areas, from RP to Rapid Manufacturing (RM) [19]. In contrast to RP, which is seen as the initial step in a bigger production process, RM takes the process one step forward and can be defined as 'the use of CAD-based automated additive manufacturing process to construct parts that are used directly as finished products or components' [20]. The crucial difference is that while RP techniques are not designed to create fully functional parts, goods produced through RM respect all the product specifications required. This allows companies to use fully functional prototypes, fabricated with the same materials and processes that will be used in production. This not only gives the

possibility to have a highly representative set of opinions in the customer validation process, but rapid manufacturing also allows economically viable production of articles that are fully optimized toward the final purpose [21]. While in mass production and in prototyping processes there are always design or functionality constraints, with RM articles can be produced almost 100% in respect of specifications. This feature is extremely useful in various situations. Examples can be small batch production of prototypes, one-off custom-made products, or in some applications of mass-customization. As the name suggests, mass customization (MC) is a manufacturing technique that combines the possibility to produce in a flexible and customized way, satisfying the individual needs of different clients, while maintaining the low costs associated with mass production. Concepts of mass customization are applied across different fields (software companies, consulting, automotive...) and companies that successfully implement this technique can build a strategic advantage over competitors [22]. Traditional mass production has the benefit of the economy of scale, but the growth in demand for customized products is a strong incentive for the implementation of MC in specific applications [23]. MC is not a novel concept as it has been conceptualized decades ago and since it has been implemented and optimized. The main limitation that MC demonstrated is the inevitable increase in cost and lead-time compared to classical mass production. Some of these drawbacks can be balanced by the benefits of rapid manufacturing techniques. Mass production remains the main technique of fabrication of goods in our economies, but RM rapidly evolved and expanded, becoming today a successful production method that can be implemented in parallel to classical mass production techniques [24, 25]. There are important niches in today's industry that benefit from RM and similarly to the revolution that RP brought to many areas of our society, RM, with its broad potential of application, has changed the way we think, design and produce.

1.2 Rapid Manufacturing

Customization means the tailoring of a product to the specific needs of a customer. At one end of the spectrum of customization, we can find the process of developing a product for one single individual, making that

product virtually unique. At the other end, however, customization can also be intended as the modification of a feature of an otherwise standard product, for example changing the colour or the size of a product. This is also referred to as “modularization” which is the production of modules that can be assembled in different configurations [26]. In this way, it is still possible to achieve some degree of customization of a product while maintaining the economies of mass production (Figure 1.3). In fact, the process of customization is postponed, maintaining

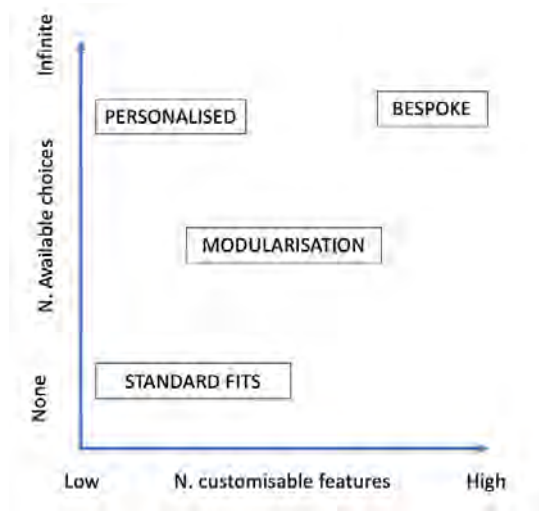


Figure 1.3: Trade off between customizable features and different available choices.

low costs even for a considerable number of customizable features. Automotive manufacturers typically adopted the modularization approach as part of their commitment towards MC [27, 28]. Rapid manufacturing has the potential to improve modularization thanks to its flexibility and can be thus integrated in the production methods used in different types of industry [29]A clear example of the potential industrial impact of this approach, is given by car manufacturers that are already producing high-end products in “limited” batches with RM (Figure 1.4). Similarly, during the recent COVID-19 crisis, the potential of additive manufacturing has been on display following logistics problems

of supply chains and shortages of products fabricated with traditional manufacturing methods [30, 31]. On demand manufacturing responded promptly by supplying personal protection equipment (PPE), medical devices and testing accessories all around the world [32, 33] (Figure 1.5).

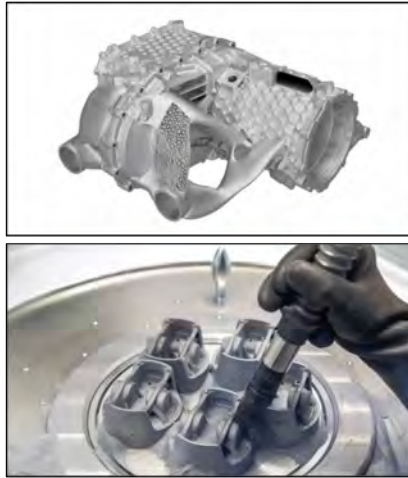


Figure 1.4: Rapid manufacturing: Thanks to the possibility to optimize the design without manufacturing limitations, Porsche is using 3D printing of metal components to manufacture functional part in some of their cars. In the upper picture, a casing for the electric motor of the new Porsche Tycan and in the lower picture, high performance pistons from the 911 GT2 RS. Adapted from newsroom.porsche.com

Thanks to RM's characteristics, its application is ideal in medical device manufacturing. Creating products that have an infinite number of choices for one or more features, allows adapting the medical device for patient-specific needs [34].

1.2.1 Medical Applications

The medical device industry is rapidly evolving towards personalized medicine and personalized medical devices, a process in which

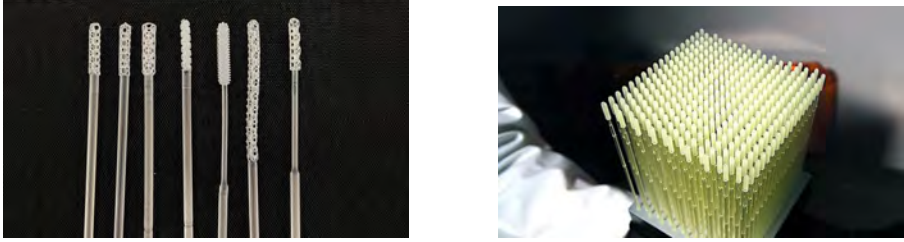


Figure 1.5: Nasal swabs printed with resin 3D printers and used for collection of samples for COVID-19 rapid testing. Adapted from formlabs.com

customization is essential [35, 36]. Each patient has different needs that have to be addressed individually, and thus each product requires on-demand design, prototyping and fabrication. Classical mass production techniques make this process economically and logistically impractical. RP and RM, on the contrary, unlocked the potential for the development of personalized medicine. Today, additive manufacturing plays an important role in surgery where it is used in a broad range of applications including maxillofacial surgery [37], orthodontics [38], cardiology [39], neurosurgery [40], vascular surgery [41], ophthalmology [42], orthopaedic surgery [43], plastic surgery [44]. One of the first usages of additive manufacturing in the medical field has been the creation of personalized pre-surgical studies and for preoperative planning. By integrating clinical and imaging data from the patient, the engineers are able to build an accurate physical model of the area operated on, allowing the physician to train and evaluate the best therapeutic procedure. It has been demonstrated that pre-surgical planning potentially reduces time spent in the operating room and overall increases the success rate of the procedure [45, 46].

In addition to surgery, many other fields in the medical world are advancing through additive manufacturing. RM allows producing patient specific tools for the intervention based on the patient's anatomy [48] as well as 3D printed prostheses in a rapid and cost-effective manner. Cranial defects, for example, are often treated with custom-made cranial vaults and today RM is the golden standard for producing such parts (Figure 1.6). RM also allow to flexibly chose the best suited material.

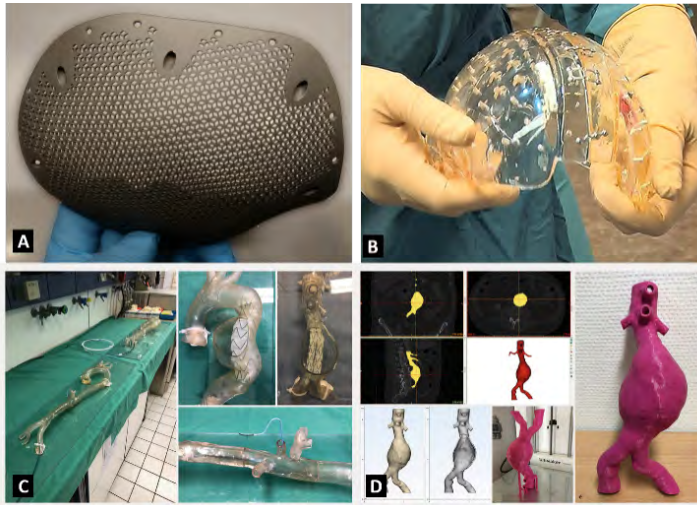


Figure 1.6: Medical applications of RM. A and B are cranial vaults custom built to fit the cranial patient specific anatomy with 3D printing. C and D are 3D printed models of pathological circulatory segments. Adapted from xilloc.com and [47]

While titanium and ceramics are the main materials used in medical applications, polymers and plastics have also been investigated as cost-effective alternatives [49]. An interesting and rapidly developing field of application of RM is the study of the vascular system. RP allows producing many complex structures that mimic the human blood vessels and use them as testing setups to evaluate the efficacy of treatments. Rapid fabrication techniques can even be used for polymeric 3D printed *in vivo* implants [47]. While applications with polymers are still mainly experimental [50, 51], *in vivo* implants of metal 3D printed parts is a well established procedure [52]. Patient specific parts for orthopaedics are used to treat defects or tumours (Figure 1.7). The process starts with the acquisition of images and 3D computer reconstruction. Thanks to modern techniques available, doctors can obtain 3D models of the patient's anatomy starting from computer tomography (CT, MDCT) and magnetic resonance imaging (MRI). Post-processing software use the DICOM files extracted to render the volume of interest, usually by



Figure 1.7: Patient specific parts for orthopedics. From left to right: image acquisition and reconstructions, 3D printed metal implant, assembly and functional implant. Adapted from materialise.com

image segmentation [48]. Finally, the 3D file is converted into an STL file by CAD software. With the final step completed, the part is ready to be 3D printed, inspected, post-processed and ultimately implanted in the patient.

Medical education is another field in which rapid manufacturing and in particular 3D printing is enabling progress, innovation, and collaboration between fields [53]. 3D printing allows visualizing concepts and gives a more practical side to classes. Examples are the fabrication of anatomical models with highlighted features or custom-made details. Patient specific models are useful to improve the understanding of specific diseases, fostering learning and performance [54]. The safety and reproducibility of the anatomical models, in comparison with cadaver dissection, together with the possibility to fabricate rapidly models from a vast data-set of images, makes 3D printing an essential tool for today's medical schools [55].

3D printing and additive manufacturing, in general, had a profound influence on our society. Today, understanding the functioning of such machines and having the ability to use them, are considered necessary skills to be competitive in the job market [56]. Educational systems are conforming to this drive, and 3D printing is an ever more and more

common tool found in primary and secondary schools around the world [57].

1.2.2 RM for education and research

STEM (Science, Technology, engineering and mathematics) education is today a central focus in the majority of educational systems worldwide [58, 59]. STEM is promoted and implemented because there is the need to give to pupils applied skills that can be used in the rapidly changing job market. RP is the perfect supporting technology for STEM classes, as it can be used to teach multidisciplinary concepts. In recent years 3D printing has been used in different types of classes and courses, including chemistry [60], biology [61], physics and mathematics [62]. The hands-on approach that 3D printing brings to classes, together with the broad range of applications and the wide accessibility, made this technology widespread in today's schools [63]. In primary and secondary schools, 3D printing is mainly used as a pedagogical tool for visual-tactile-learning [56]. Higher education and research institutions have not been left out from the RP revolution. Rapid prototyping is empowering researchers and students all around the world. Since the spread of 3D printing and RM, a movement of people that develop their own analytical instruments or modify commercially available ones, has risen [64, 65].

Developing such devices not only allows equipping a laboratory maintaining relatively low expenditure, but also to create highly flexible and customized machines suited specifically for the researcher's need. Concomitantly, recent decades saw the rise of open source hardware and software. Electronic boards such as Arduino or Raspberry Pi, together with webspaces such as GitHub and Thingiverse, allow quick information and file exchange between people that can build on top of each other's innovation [66, 67]. In the true spirit of RP and RM, researchers, lab technicians or hobbyists can create prototypes using off the shelf components and integrating them with rapidly built hardware, cutting development costs and times. In literature, it is possible to find open source projects for fluorescent microscopes and imaging devices [61], microfluidic pumps [68, 69], spectrophotometers [70, 71] and cell growth live-monitoring devices [72].

The above-mentioned benefits are even more emphasized in

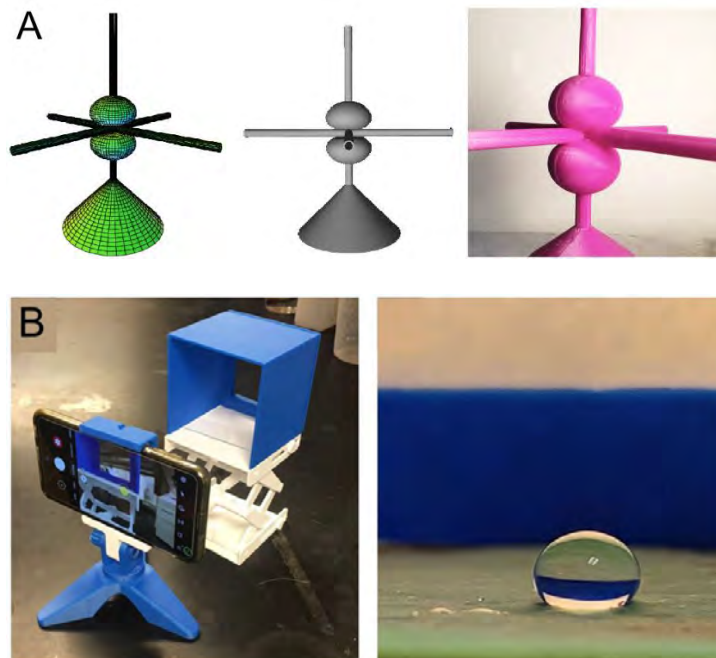


Figure 1.8: 3D printing in education. A. atomic orbitals visualized with 3D printing models. B. setup for measurement of contact angle with a smartphone. Adapted from [57, 60]

environments with low resources. While in first world countries RP and RM improved or optimized the existing high-tech practices in the above-mentioned fields, in low resource settings these technologies are true enablers. Very often, researchers in low or middle-income countries struggle to equip their labs with even the most basic instrumentation needed to perform their research. Non-profit organizations such as *Seeding Labs* (<https://seedinglabs.org/>) have the goal to foster science in settings with limited resources by providing tools, equipment, training and connections needed at a highly discounted rate when compared to off the shelf laboratory equipment. As they state, “all locations are selected for having limited resources but limitless potential”. Seeding

labs works on different levels: they provide laboratory equipment through their program *Instrumental Access*, and it also has a vast library of educational videos (TeleScience program) with procedures/tips and explanations for the most common assays, research techniques and activities performed in a laboratory. Similar initiatives are being undertaken around the world, some of them rather than institutions, to address directly the communities and the people that are most in need. Examples are initiatives such as *Not Impossible* or *Biomakers*. Not impossible is a Foundation involved in many projects aimed at improving the quality of life of people around the world. One of their project had the goal to 3D print a prosthetic arm for a 16 years old victim of a bomb in South Sudan. Mick Ebeling, the founder of the Not-Impossible Foundation, ended up establishing a small 3D printing lab for prosthesis fabrication in the small village, enabling the trained locals to provide access to affordable prosthetic for those most in need (*Project Daniel*, <https://www.notimpossible.com/projects/project-daniel>).

1.2.3 Use of RM in point of care

The possibility to fabricate with low costs and high flexibility, as well as to overcome basic logistical problems by producing on the spot, allows a vast audience of patients to be able to benefit from medical services that would otherwise be out of reach. The above mentioned-examples have a strong emotional charge and are socially meaningful. Such initiatives should be incentivized and promoted by first-world institutions, and the fact that RP and RM have a central role as enabling technologies, is already a strong drive for the further development and implementation of their use in medical applications. Traditionally, the biomedical market is a highly regulated and controlled industry that often requires long times to introduce radical innovations. However, it is a field characterized by continuous research and huge investments. Furthermore, the recent COVID-19 pandemic showed our health system's weaknesses and low flexibility. A clear example was showcased during the first wave of COVID-19 cases that struck northern Italy in February-March 2020, when several hospitals reached critical capacity. One hospital in particular ran out of a specific valve that is used in a respiration-aid machine. A local engineering and prototyping

company designed and printed 100 valves with a 3D printer in a couple of days, supplying the hospital until the new batch of valves arrived [73] (Figure 1.9).



Figure 1.9: Rapid manufacturing for medical applications. 3D printed valves for respiratory aid machines. Adapted from [bbc.com/news/technology-51911070](https://www.bbc.com/news/technology-51911070)

In regions of Spain and Switzerland, hospitals 3D printed the nasopharyngeal (NP) swabs with biocompatible and autoclavable resin, addressing the shortage of rapid COVID-19 tests. Many other projects and ideas came out from the online makers' community during the two years of the pandemic [74]. The majority of such projects never reached the market or the application phase. However, they demonstrate the interest of the community and the potential for future development. Especially the diagnosis market, was put under incredible strain during the pandemic. The need to respond to the crisis, pushed biomedical companies and healthcare systems to start performing diagnosis test at scales larger than ever before. Driven by this need, traditional production systems and logistics chains were disrupted [75]. Additive manufacturing provided relief in some cases, shortening the production times and logistical processes [76, 77].

1.3 Point of care diagnostics

Point-of-care diagnostics (PoC) have become increasingly important in recent years. The commercial success of PoC test can be attributed to some of their key characteristics. For example, they are very simple and can be used without any prior training, following basic instructions. They accept untreated samples and give a result in a matter of minutes. Interpretation of the test must be easy and unambiguous, for example, by visualizing a stripe of colour on a paper substrate. PoC devices should have contained dimensions and ideally be made from inexpensive materials and with simple designs [78, 79]. Thanks to these characteristics, PoC devices are advantageous over lab analysis techniques regarding time and costs, and thus also to patient compliance [80]. Although a number of PoC tests, based on different strategies, have been developed over the years, this thesis will focus on the use of RM and RP to mass produce biosensor technologies for PoC application.

1.3.1 Biosensors in Point of Care diagnostics

Biosensors are a category of devices used to detect a biological, physical, or chemical target by integrating a biological receptor into the sensor design. The basic functioning of a biosensor can be broken down to three levels: the sampling, the recognition, and the transducer or read-out [81].

Biosensors take their name from the biological matter that is used as the receptor. There are various types of biosensors, based on the type of biological receptor used (e.g. enzyme-based, immunosensors, cell-based, DNA-based). Biosensors are usually specialized in detecting a single target, making them highly accurate and selective. The majority and most used biosensor-based PoC diagnostic test are disposable, although there are more complex instruments that use chips or cartridges (Figure 1.10) [82, 83]. The low-cost and user-friendly nature of biosensors make them very suitable to be used in PoC applications [84, 85]. However, an often disregarded aspect in the analytical process is the sampling of the analyte. Many assays require sample pre-treatment, for example with sample concentration or isolation of a specific target among a complex matrix [86]. Even those samples that do not need pre-treatment. still rely

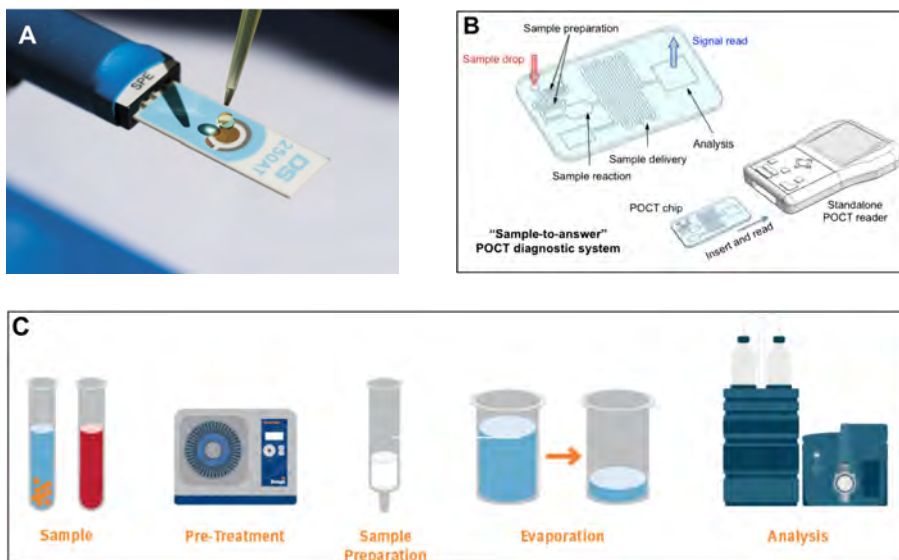


Figure 1.10: A) Typical example of biosensor. All the three characteristic elements of a biosensor are visible: sampling (achieved through precision pipetting of a liquid drop), receptor (screen printed electrode), and transducer (impedimetric readout). Adapted from revistapesquisa.fapesp.br. B) example of Point-of-care testing (POCT) system, relying on microfluidic flow cell for sample processing. Adapted from [100] C) example of sample preparation for LC-MS/MS or GC-MS. Often the sample needs to be pre-treated before analysis, making the sampling a crucial part of the analytical process. Adapted from sampleprep.biotage.com/biofluidssampleprep.

on sample extraction, handling and coupling with the sensor core. These procedures introduce two main criticalities: potential mishandling (e.g. contamination or invalidation), and sample dissipation, which leads to a higher initial sample volume required [87]. PoC devices have promising characteristics that could solve these issues. Examples are the integration of fully automated microfluidic disposable flowcells, in which the sample is conditioned and transported [88]. Integrating disposable cartridges that fully contain the sample could reduce waste, costs and sample volume required [89]. 3D printing gives the possibility to researchers to

develop innovative solutions, and adapt them to various applications. Research has focused, in the last decade, on integrating the benefits of low volume samples (microfluidics) with PoC applications (Figure 1.11). Many of these research works, include the design of readout technologies that are fabricated with 3D printing [90], thanks to previously discussed advantages that this technology has.

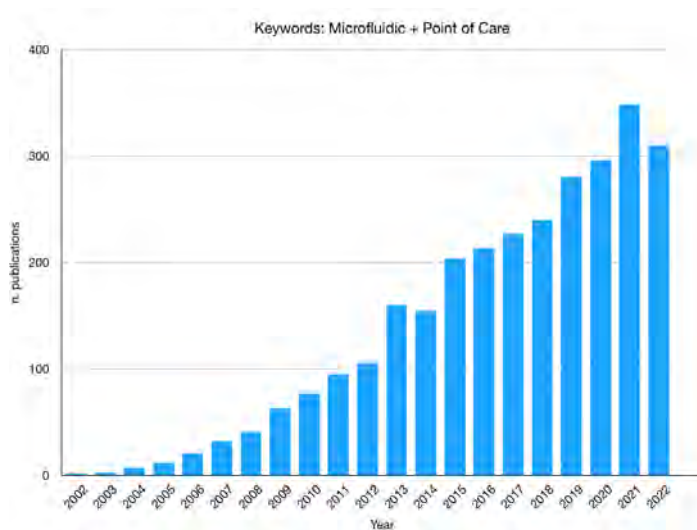


Figure 1.11: Number of publications per year containing the keywords microfluidics and point of care.

Among the commercially successful examples of biosensors in medical diagnosis and therapy, and in particular of PoC biosensors, is the glucose meter, a device that has massively increased the quality of life of diabetic patients since their implementation in diabetes treatment [91, 92]. The origin of diabetes care and monitoring can be traced to the beginning of the 20th century, thanks to Stanley Rossiter Benedict, who developed a colorimetric assay for urine glucose content [93]. Improvements on the technique followed around the middle of the century, with an important breakthrough in 1965, when Dextrostix was developed. It was the first enzymatic blood glucose test strip, based on glucose oxidase [94]. The latter is an enzyme that catalyses the oxidation of glucose to gluconic

acid and hydrogen peroxide. Adding peroxidase and a chromogenic oxygen acceptor, results in the formation of a coloured compound, thus allowing colorimetric reading. In the 1970s, attempts have been made to use automatic glucose meters combined with the Dextrostix strip. However, their accuracy was low. The major breakthrough in glucose self-monitoring was the invention of the Clark electrode that would lead into the amperometric glucometers that diabetes patients still use today. It allows them to accurately monitor their blood glucose levels at regular time intervals and adjust their diet or insulin therapy accordingly [95]. Continuous Glucose Monitoring (CGM) is the next big step in the technology development for diabetes care. In the beginning of the 21st century, new types of wearable, compact and wireless sensors, were developed and coupled with portable pumps for insulin. Nowadays, unequivocal evidence exists, supporting the importance of CGM, cementing this category of devices as some of the most successful PoC on the market [96].

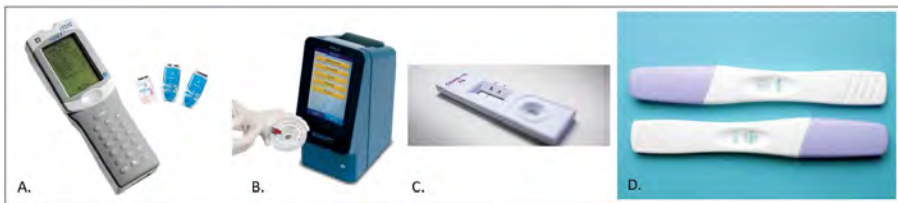


Figure 1.12: Different types of point of care diagnostics. A. i-STAT blood analysis device. B. Piccolo blood analysis device based on disk shaped cartridges. C. LFIA test for COVID-19. D. LFIA pregnancy test. Adapted from [82, 84].

Another important category of biosensor, that has achieved a lot of commercial success, are the so-called immunosensors and assays. These PoC devices are based on antibodies to bind the desired antigen and on various readout methods to give a qualitatively or quantitatively result of the binding [97]. The development of lab-based immunoassays such as radio immunoassay (RIA) first and the enzyme-linked immunoassay (ELISA) later, paved the way for the development of the first PoC diagnosis tools [98]. A major breakthrough in commercializing immunoassays for PoC application was the advent of so-called lateral flow immunoassay (LFIA). This technology represented a great

innovation that until today is the base of the majority of PoC diagnostic tools [99]. Briefly, LFIA tests are strips of various functionalized materials sandwiched together. The strip is divided in sequential different sections, the first one being the sample pad. Here the sample is added and the absorption process starts. The sample travels by capillarity force to the next area, the conjugate pad, in which the conjugated labels and antibodies are present. If the sample contains the target, the immobilized conjugated antibodies and labels will bind to the target and continue to migrate along the strip. As the sample moves along the device, it enters the nitrocellulose membrane section, where a series of binding agents are immobilized along the test lines. Here the binding reagents will bind to the target (if present in the sample) and a visible coloured line will form on the surface of the strip (Figure 1.13). LFIAs have been used for decades for home pregnancy testing and, more recently, for the diagnosis of viral infections such as Covid-19. This shows that sampling strategies and their potentially positive effect on patient compliance and user-friendliness are often over-looked, but just as important as the specificity or sensitivity of a PoC test.

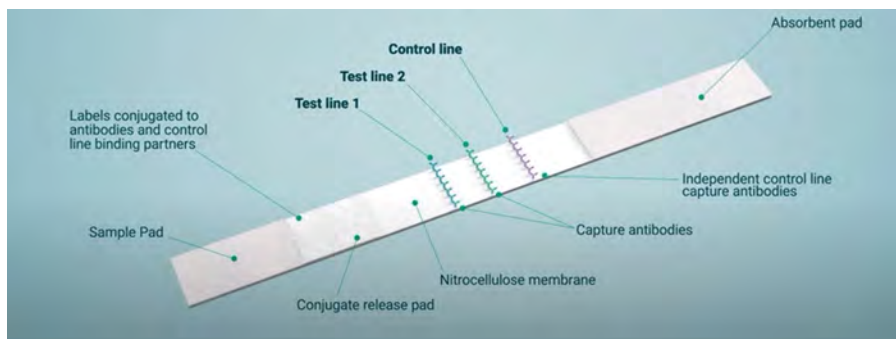


Figure 1.13: Schematic functioning of lateral flow immunoassays. The sample is deposited on the sample pad, following it moves through the conjugate release pad, the nitrocellulose membrane and finally into the absorbent pad. Adapted from abingdonhealth.com.

In this respect, it is worth mentioning that other sampling strategies such as finger stick and venipuncture formats have also led to the development of assays for HIV. In addition, oral sample tests detecting

HIV- 1/2 antibodies are also present on the market and have received CLIA clearance. These tests are potentially beneficial, as they are easier to perform and less invasive for the patients and can be used in home settings with ease [100].

The main drawback associated with PoC usage, is the absence of professional personnel control over the testing procedure [101]. This leads to a potential risk of an incorrect testing procedure, or even misinterpretation of the test result [102, 103]. This can be mitigated by assuring that tests are as user-friendly as possible and by providing clear and straightforward informative materials on the test [104]. PoCs are powerful instruments that empower the patient, functioning especially well as a first line of diagnosis thanks to its practical advantages [105, 106]. High income countries have a capillary network of analysis laboratories and hospitals, thus easily addressing situation in which PoC fail or are not sufficient. The reasons that drive PoC development and implementation in such environments are minimization of healthcare systems costs, efficient data collection and continuous patient tracking [107]. In contrast, low income countries often lack the healthcare backbone that would allow healthcare providers to respond adequately to the sanitary needs of the population [108, 109]. Furthermore, often the same countries are the ones that have the highest incidence of infectious diseases, which can have a heavy impact on the economic and societal setup [110]. Malaria, Tuberculosis, and HIV are only some of the most known diseases that heavily impact low income countries every year [111, 112, 113]. Accurate disease diagnosis is crucial in such settings, as it is essential for proper treatment and improving patient prognosis. PoC diagnostics could potentially have an enormous positive effect on the cumulative well-being of populations in low income countries [114]. The low costs, mobility and often user-friendliness of PoC devices would allow increasing the diagnosis rates and thus the response to the disease. PoC diagnostics would allow for readily available results that would lead to faster and more accurate clinical decisions and referrals, which, in turn, would lead to a better treatment and better prognosis for the patient [115].

Although commercialization of PoC devices has been exploited in selected specific fields (e.g. diabetes care, pregnancy tests, and more recently COVID-19 tests), they are yet to fulfil their full economic

potential [116]. The reasons are various and complex, including societal factors such as fragmented governmental policy commitment, inadequate investments, and lacking infrastructure [117, 118, 119]. While many of these problems are difficult to tackle, another important bottleneck is the need to rapidly produce user-friendly, handheld sampling tools that allow for swift implementation of the PoC test. The design of a sampler in function of mass production is often overlooked in biosensor research and leads to many promising technologies not reaching the market. RM and RP could have a positive influence on this issue, offering researchers and engineers more affordable and flexible tools, in the early stages of research and development [120, 121]. Exploiting these tools, by creating smarter, more cost-effective, and adaptable devices, could accelerate biosensor R&D and lead to quicker valorization of technologies that potentially benefit a large pool of people, in various fields of application.

1.4 Outline and aim of the thesis

The research work presented in this thesis, focuses on investigating the potentially positive impact of 3D printing in designing tools for use in biosensor research and STEM education. While scientific research is a fundamental element of the thesis, the approach adopted in this work focuses on the practical engineering aspects. The thesis bundles my four interdisciplinary, peer-reviewed, published studies, aimed at addressing this overarching research question. Although the papers have been minimally adapted to fit this thesis, they remain largely as published. In **Chapter 2** the use of the Form2, one of the most commercially widespread SLA 3D printers for hobbyists and enthusiasts, in producing fluidic samplers for application in e.g. biosensor research is studied. Capabilities of the machine are evaluated and discussed concerning the use of different materials and applications, focusing on the printing of molds for microfluidic flow cells. Building on the findings of this study, **Chapter 3**, uses such a 3D printed flow cell, and studies its use in a biosensor application. The flow cell is used to conduct a simple experiment that illustrates the impact of the adhesive layer used to immobilize the recognition element on biosensor performance. In **Chapter 4**, 3D printing is used to construct a low-cost syringe

pump, which can be customized specifically in terms of the envisioned biosensor or analytical application, offering a low-cost alternative to most commercially available options. In addition, the use of this syringe pump as part of a tool kit to facilitate STEM education is also demonstrated. **Chapter 5**, finally addresses the entire overarching research question by tying up the findings of the previous chapters, combining 3D printing of flow cells and syringe pumps, to create a tool for education in science, technology, engineering, and mathematics (STEM). In particular, this chapter describes how 3D printing can be used to develop a modular toy kit that can be used to build and perform visually attractive science experiments. This work leads to research valorization in the form of the startup Flui.Go Science, that I founded in order to provide primary and secondary school teacher with scientific tool kits to accelerate STEM education. The final part of the empirical cycle, demonstrating that the kit actually stimulates the learning process in the target, was done by an external researcher at the *Open University Netherlands* to avoid a commercial conflict-of-interest. The results of their study will however be discussed in a dedicated section, the post-face of **Chapter 5** as their conclusions are instrumental to illustrate the impact of the thesis.

Bibliography

- [1] PM Dickens. Research developments in rapid prototyping. *Proceedings of the Institution of Mechanical Engineers, Part B: Journal of Engineering Manufacture*, 209(4):261–266, 1995.
- [2] D White. *Rapid Prototyping Processes*, pages 8003–8009. 2001.
- [3] H Kodama. Automatic method for fabricating a three-dimensional plastic model with photo-hardening polymer. *Review of scientific instruments*, 52(11):1770–1773, 1981.
- [4] SS Crump. Device and method for creating three-dimensional object. *Patent US4575330A*, 1984.
- [5] CW Hull. Apparatus for production of three-dimensional objects by stereolithography. *Patent US4575330B1*, 1989.
- [6] CA Gonzalez Lengua. *History of Rapid Prototyping*, pages 3–7. 2017.
- [7] A Su and SJ Al'Aref. Chapter 1 - history of 3d printing. In Subhi J. Al'Aref, Bobak Mosadegh, Simon Dunham, and James K. Min, editors, *3D Printing Applications in Cardiovascular Medicine*, pages 1–10. 2018.
- [8] A. Savini and G.G. Savini. A short history of 3d printing, a technological revolution just started. In *2015 ICOHTEC/IEEE International History of High-Technologies and their Socio-Cultural Contexts Conference (HISTELCON)*, pages 1–8, 2015.
- [9] B Panda, MJ Lin, Ian Gibson, and CK Chua. The disruptive evolution of 3d printing. In *Proceedings of the International Conference on Progress in Additive Manufacturing*, pages 152–157, 2016.
- [10] S Junk and C Kuen. Review of open source and freeware cad systems for use with 3d-printing. *Procedia CIRP*, 50:430–435, 2016. 26th CIRP Design Conference.
- [11] IE Sutherland. Sketchpad a man-machine graphical communication system. *Simulation*, 2(5):R–3–R–20, 1964.

- [12] S Tornincasa and F Di Monaco. The future and the evolution of cad. In *Proceedings of the 14th international research/expert conference: trends in the development of machinery and associated technology*, volume 1, pages 11–18.
- [13] I Nuñez, T Matute, R Herrera, J Keymer, T Marzullo, T Rudge, and F Federici. Low cost and open source multi-fluorescence imaging system for teaching and research in biology and bioengineering. *PLOS ONE*, 12(11), 2017.
- [14] T Spahiu, E Shehi, and E Piperi. Advanced cad/cam systems for garment design and simulation. In *6th International Conference of Textile*.
- [15] A Dwivedi and A Dwivedi. Role of computer and automation in design and manufacturing for mechanical and textile industries: Cad/cam. *International Journal of Innovative Technology and Exploring Engineering (IJITEE)*, 3(3):8, 2013.
- [16] AK Kamrani and EA Nasr. *Rapid prototyping: theory and practice*, volume 6. 2006.
- [17] R Hague, I Campbell, and P Dickens. Implications on design of rapid manufacturing. *Proceedings of the Institution of Mechanical Engineers, Part C: Journal of Mechanical Engineering Science*, 217(1):25–30, 2003.
- [18] RG Cooper, SJ Edgett, and EJ Kleinschmidt. Optimizing the stage-gate process: What best-practice companies do—i. *Research-Technology Management*, 45(5):21–27, 2002.
- [19] GN Levy, R Schindel, and JP Kruth. Rapid manufacturing and rapid tooling with layer manufacturing (lm) technologies, state of the art and future perspectives. *CIRP Annals*, 52(2):589–609, 2003.
- [20] N Hopkinson, R Hague, and P Dickens. *Introduction to Rapid Manufacturing*, pages 1–4. 2005.
- [21] D Pham and SS Dimov. *Rapid manufacturing: the technologies and applications of rapid prototyping and rapid tooling*. 2012.
- [22] B Pine Ii, B Victor, and A Boynton. Making mass customization work. *Harvard Business Review*, 71, 1993.
- [23] CWL Hart. Mass customization: conceptual underpinnings, opportunities and limits. *International Journal of Service Industry Management*, 6(2):36–45, 1995.
- [24] D Cormier, O Harrysson, and T Mahale. Rapid manufacturing in the 21st century. *Journal of the Chinese Institute of Industrial Engineers*, 20(3):193–203, 2003.
- [25] M Ruffo, C Tuck, and R Hague. Cost estimation for rapid manufacturing - laser sintering production for low to medium volumes. *Proceedings of the Institution of Mechanical Engineers, Part B: Journal of Engineering Manufacture*, 220(9):1417–1427, 2006.

-
- [26] F Salvador, C Forza, and M Rungtusanatham. Modularity, product variety, production volume, and component sourcing: theorizing beyond generic prescriptions. *Journal of Operations Management*, 20(5):549–575, 2002.
- [27] TB Christensen. Modularised eco-innovation in the auto industry. *Journal of Cleaner Production*, 19(2-3):212–220, 2011.
- [28] MA Sellitto, FL Nunes, and DRF Valadares. Factors that contribute to the use of modularisation in the automotive industry: A survey in brazil. *South African Journal of Industrial Engineering*, 29(4):33–44, 2018.
- [29] C Tuck and R Hague. The pivotal role of rapid manufacturing in the production of cost-effective customised products. *International Journal of Mass Customization*, 1(2):360–373, 2006.
- [30] Q Qi, F Tao, Y Cheng, J Cheng, and AYC Nee. New it driven rapid manufacturing for emergency response. *Journal of Manufacturing Systems*, 60:928–935, 2021.
- [31] J Holmström, J Partanen, J Tuomi, and M Walter. Rapid manufacturing in the spare parts supply chain: Alternative approaches to capacity deployment. *Journal of manufacturing technology management*, 2010.
- [32] AD Pasha, J Urbanic, B Hedrick, H Ramezani, and O Jianu. Leveraging advanced design and novel rapid manufacturing solutions to respond to the covid-19 pandemic. *Comput. Aided. Des. Appl*, 19:755–778, 2022.
- [33] MJ Antonini, D Plana, S Srinivasan, L Atta, A Achanta, H Yang, AK Cramer, J Freake, MS Sinha, and SH Yu. A crisis-responsive framework for medical device development applied to the covid-19 pandemic. *Frontiers in digital health*, 3:617106, 2021.
- [34] D Eyers and K Dotchev. Technology review for mass customisation using rapid manufacturing. *Assembly Automation*, 2010.
- [35] A Harvey, A Brand, ST Holgate, LV Kristiansen, H Lehrach, A Palotie, and B Prainsack. The future of technologies for personalised medicine. *New biotechnology*, 29(6):625–633, 2012.
- [36] G Tan, N Ioannou, E Mathew, AD Tagalakakis, DAL Conceptualisation, and C Conceptualisation. 3d printing in ophthalmology: From medical implants to personalised medicine. *International Journal of Pharmaceutics*, page 122094, 2022.
- [37] K Igawa, U Chung, and Y Tei. [custom-made artificial bones fabricated by an inkjet printing technology]. *Clinical calcium*, 18(12):1737–1743, 2008.
- [38] K Torabi, E Farjood, and S Hamedani. Rapid prototyping technologies and their applications in prosthodontics, a review of literature. *Journal of dentistry (Shiraz, Iran)*, 16(1):1–9, 2015.
- [39] M Vukicevic, B Mosadegh, J K Min, and SH Little. Cardiac 3d printing and its future directions. *JACC: Cardiovascular Imaging*, 10(2):171–184, 2017.

- [40] M Randazzo, JM Pisapia, N Singh, and JP Thawani. 3d printing in neurosurgery: a systematic review. *Surgical neurology international*, 7(Suppl 33):S801, 2016.
- [41] P Hangge, Y Pershad, AA Witting, H Albadawi, and R Oklu. Three-dimensional (3d) printing and its applications for aortic diseases. *Cardiovascular diagnosis and therapy*, 8(Suppl 1):S19, 2018.
- [42] W Huang and X Zhang. 3d printing: print the future of ophthalmology. *Investigative ophthalmology & visual science*, 55(8):5380–5381, 2014.
- [43] F Auricchio and S Marconi. 3d printing: clinical applications in orthopaedics and traumatology. *EFORT open reviews*, 1(5):121–127, 2016.
- [44] MP Chae, WM Rozen, PG McMenemy, MW Findlay, RT Szychal, and DJ Hunter-Smith. Emerging applications of bedside 3d printing in plastic surgery. *Frontiers in surgery*, 2:25, 2015.
- [45] E Perica and Z Sun. Patient-specific three-dimensional printing for pre-surgical planning in hepatocellular carcinoma treatment. *Quantitative imaging in medicine and surgery*, 7(6):668, 2017.
- [46] EK O'Brien, DB Wayne, KA Barsness, WC McGaghie, and JH Barsuk. Use of 3d printing for medical education models in transplantation medicine: a critical review. *Current Transplantation Reports*, 3(1):109–119, 2016.
- [47] AJ Melchiorri, N Hibino, CA Best, T Yi, YU Lee, CA Kraynak, LK Kimerer, A Krieger, P Kim, CK Breuer, and JP Fisher. 3d-printed biodegradable polymeric vascular grafts. *Advanced healthcare materials*, 5(3):319–325, 2016.
- [48] KC. Wong. 3d-printed patient-specific applications in orthopedics. *Orthopedic research and reviews*, 8:57, 2016.
- [49] A De La Peña, J De La Peña-Brambila, J Pérez-De La Torre, M Ochoa, and GJ Gallardo. Low-cost customized cranioplasty using a 3d digital printing model: a case report. *3D Printing in Medicine*, 4(1):4, 2018.
- [50] D Bozukova, C Pagnouille, R Jérôme, and C Jérôme. Polymers in modern ophthalmic implants—historical background and recent advances. *Materials Science and Engineering: R: Reports*, 69(6):63–83, 2010.
- [51] HM Wache, DJ Tartakowska, A Hentrich, and MH Wagner. Development of a polymer stent with shape memory effect as a drug delivery system. *Journal of Materials Science: Materials in Medicine*, 14(2):109–112, 2003.
- [52] X Hu, Y Chen, W Cai, M Cheng, W Yan, and W Huang. Computer-aided design and 3d printing of hemipelvic endoprosthesis for personalized limb-salvage reconstruction after periacetabular tumor resection. *Bioengineering*, 9(8):400, 2022.
- [53] S Hartmut. 3d printing—risks and opportunities. *Institute for Applied Ecology*, 23, 2013.
- [54] KR Rosen. The history of medical simulation. *J Crit Care*, 23(2):157–66, 2008.

-
- [55] K Wang, C Wu, Z Qian, C Zhang, B Wang, and MA Vannan. Dual-material 3d printed metamaterials with tunable mechanical properties for patient-specific tissue-mimicking phantoms. *Additive Manufacturing*, 12: 31–37, 2016.
- [56] Y Sun and Q Li. The application of 3d printing in stem education. In *2018 IEEE International Conference on Applied System Invention (ICASI)*, pages 1115–1118, 2018.
- [57] S Ford and T Minshall. Where and how 3d printing is used in teaching and education. *Additive Manufacturing*, 25:131–150, 2019.
- [58] L Madden, J Beyers, and S O’Brien. The importance of stem education in the elementary grades: Learning from pre-service and novice teachers’ perspectives. *The Electronic Journal for Research in Science & Mathematics Education*, 20(5), 2016.
- [59] RN Hafni, T Herman, E Nurlaelah, and L Mustikasari. The importance of science, technology, engineering, and mathematics (stem) education to enhance students’ critical thinking skill in facing the industry 4.0. In *Journal of Physics: Conference Series*, volume 1521, page 042040. IOP Publishing, 2020.
- [60] T Tabassum, M Iloska, D Scuereb, N Taira, C Jin, V Zaitsev, F Afshar, and T Kim. Development and application of 3d printed mesoreactors in chemical engineering education. *Journal of Chemical Education*, 95(5):783–790, 2018.
- [61] A Maia Chagas, LL Prieto-Godino, AB Arrenberg, and T Baden. The €100 lab: A 3d-printable open-source platform for fluorescence microscopy, optogenetics, and accurate temperature control during behaviour of zebrafish, drosophila, and caenorhabditis elegans. *PLOS Biology*, 15(7), 2017.
- [62] Y Sun and Q Li. The application of 3d printing in mathematics education. In *2017 12th International Conference on Computer Science and Education (ICCSE)*, pages 47–50.
- [63] E Buehler, SK Kane, and A Hurst. Abc and 3d: opportunities and obstacles to 3d printing in special education environments. In *Proceedings of the 16th international ACM SIGACCESS conference on Computers & accessibility*, pages 107–114, 2014.
- [64] A Ambrosi and M Pumera. 3d-printing technologies for electrochemical applications. *Chemical Society Reviews*, 45(10):2740–2755, 2016.
- [65] G Salentijn, PE Oomen, M Grajewski, and E Verpoorte. Fused deposition modeling 3d printing for (bio) analytical device fabrication: procedures, materials, and applications. *Analytical chemistry*, 89(13):7053–7061, 2017.
- [66] J Moilanen and T Vadén. 3d printing community and emerging practices of peer production. *First Monday*, 2013.

- [67] H Kyriakou, JV Nickerson, and G Sabnis. Knowledge reuse for customization: Metamodels in an open design community for 3d printing. *arXiv preprint arXiv:1702.08072*, 2017.
- [68] AS Boeshaghi, E da Veiga Beltrame, D Bannon, J Gehring, and L Pachter. Principles of open source bioinstrumentation applied to the poseidon syringe pump system. *Scientific Reports*, 9(1):12385, 2019.
- [69] CJ Forman, H Tomes, B Mboobo, RJ Burman, M Jacobs, T Baden, and JV Raimondo. Openspritzer: an open hardware pressure ejection system for reliably delivering picolitre volumes. *Scientific Reports*, 7(1):2188, 2017.
- [70] EK Grasse, MH Torcasio, and AW Smith. Teaching uv-vis spectroscopy with a 3d-printable smartphone spectrophotometer. *Journal of Chemical Education*, 93(1):146–151, 2016.
- [71] BS Hosker. Demonstrating principles of spectrophotometry by constructing a simple, low-cost, functional spectrophotometer utilizing the light sensor on a smartphone. *Journal of Chemical Education*, 95(1):178–181, 2018.
- [72] K Sasidharan, AS Martinez-Vernon, J Chen, T Fu, and OS Soyer. A low-cost diy device for high resolution, continuous measurement of microbial growth dynamics. *bioRxiv*, page 407742, 2018.
- [73] Z Kleinman. Coronavirus: 3d printers save hospital with valves. 2020.
- [74] IO Bankole, OI Sikiru, DA Temitope, BO David, and Z Mohsen. Review on 3d printing: Fight against covid-19. *Materials Chemistry and Physics*, 258: 123943, 2021.
- [75] J Sarkis, MJ Cohen, P Dewick, and P Schröder. A brave new world: Lessons from the covid-19 pandemic for transitioning to sustainable supply and production. *Resources, conservation, and recycling*, 159:104894, 2020.
- [76] T Mueller, A Elkaseer, A Charles, J Fauth, D Rabsch, A Scholz, C Marquardt, K Nau, and SG Scholz. Eight weeks later—the unprecedented rise of 3d printing during the covid-19 pandemic—a case study, lessons learned, and implications on the future of global decentralized manufacturing. *Applied Sciences*, 10(12):4135, 2020.
- [77] M Goudswaard, J Gopsill, A Ma, A Nassehi, and B Hicks. Responding to rapidly changing product demand through a coordinated additive manufacturing production system: a covid-19 case study. In *IOP Conference Series: Materials Science and Engineering*, volume 1193, page 012119. IOP Publishing, 2021.
- [78] P Yager, GJ Domingo, and J Gerdes. Point-of-care diagnostics for global health. *Annu. Rev. Biomed. Eng.*, 10:107–144, 2008.
- [79] A St John and CP Price. Existing and emerging technologies for point-of-care testing. *The Clinical Biochemist Reviews*, 35(3):155, 2014.

-
- [80] V Gubala, LF Harris, AJ Ricco, MX Tan, and DE Williams. Point of care diagnostics: status and future. *Anal Chem*, 84(2):487–515, 2012.
- [81] A Turner, I Karube, and GS Wilson. *Biosensors : Fundamentals and applications*, 1987.
- [82] IR Lauks. Microfabricated biosensors and microanalytical systems for blood analysis. *Accounts of Chemical Research*, 31(5):317–324, 1998.
- [83] K Murata, L Glaser, M Nardiello, S Richardson, LV Ramanathan, and DC Carlow. Analytical performance of the abaxis piccolo xpress® point of care analyzer in whole blood, serum, and plasma. *Clinical Biochemistry*, 48(18):1344–1346, 2015.
- [84] CP Price. Point of care testing. *Bmj*, 322(7297):1285–8, 2001.
- [85] CO Laurence, JR Moss, NE Briggs, and JJ Beilby. The cost-effectiveness of point of care testing in a general practice setting: results from a randomised controlled trial. *BMC Health Serv Res*, 10:165, 2010.
- [86] T Hyötyläinen. Critical evaluation of sample pretreatment techniques. *Analytical and bioanalytical chemistry*, 394(3):743–758, 2009.
- [87] M Zarei. Portable biosensing devices for point-of-care diagnostics: Recent developments and applications. *TrAC Trends in Analytical Chemistry*, 91: 26–41, 2017.
- [88] Sammer-ul H, AM Nightingale, and X Niu. Micromachined optical flow cell for sensitive measurement of droplets in tubing. *Biomedical microdevices*, 20(4):1–7, 2018.
- [89] EJ Rastelli, D Yue, C Millard, and P Wipf. 3d-printed cartridge system for in-flow photo-oxygenation of 7-aminothienopyridinones. *Tetrahedron*, 79: 131875, 2021.
- [90] K Plevniak, M Campbell, T Myers, A Hodges, and M He. 3d printed auto-mixing chip enables rapid smartphone diagnosis of anemia. *Biomicrofluidics*, 10(5):054113, 2016.
- [91] W H Polonsky and D Hessler. What are the quality of life-related benefits and losses associated with real-time continuous glucose monitoring? a survey of current users. *Diabetes technology & therapeutics*, 15(4):295–301, 2013.
- [92] W H Polonsky, D Hessler, KJ Ruedy, and RW Beck. The impact of continuous glucose monitoring on markers of quality of life in adults with type 1 diabetes: further findings from the diamond randomized clinical trial. *Diabetes Care*, 40(6):736–741, 2017.
- [93] SF Clarke and JR Foster. A history of blood glucose meters and their role in self-monitoring of diabetes mellitus. *British journal of biomedical science*, 69(2):83–93, 2012.
- [94] JA Rock and LJ Gerende. Dextrostix method for determination of blood glucose levels: A statistical evaluation. *JAMA*, 198(3):231–236, 1966.

- [95] DM Nathan, S Genuth, J Lachin, P Cleary, O Crofford, M Davis, L Rand, and C Siebert. Diabetes control and complications trial research group the effect of intensive treatment of diabetes on the development and progression of long-term complications in insulin-dependent diabetes mellitus. *N Engl J Med*, 329(14):977–986, 1993.
- [96] O Didyuk, N Econom, A Guardia, K Livingston, and U Klueh. Continuous glucose monitoring devices: past, present, and future focus on the history and evolution of technological innovation. *Journal of diabetes science and technology*, 15(3):676–683, 2021.
- [97] GA Bonwick and CJ Smith. Immunoassays: their history, development and current place in food science and technology. *International journal of food science & technology*, 39(8):817–827, 2004.
- [98] JP Gosling. Immunoassays. *Reviews in Cell Biology and Molecular Medicine*, 2006.
- [99] A Wu. A selected history and future of immunoassay development and applications in clinical chemistry. *Clinica chimica acta*, 369(2):119–124, 2006.
- [100] JD Stekler, LR Violette, HA Clark, SJ McDougal, LA Niemann, DA Katz, PR Chavez, LG Wesolowski, SF Ethridge, and VM McMahan. Prospective evaluation of hiv testing technologies in a clinical setting: protocol for project detect. *JMIR research protocols*, 9(1):e16332, 2020.
- [101] J Parrot. From self-diagnosis to self-medication: inherent dangers, and impact on pharmacist-patient relationship. *Bulletin de L'Academie Nationale de Medecine*, 191(8):1509–14, 2007.
- [102] D Huckle. Point-of-care diagnostics: an advancing sector with nontechnical issues. *Expert Review of Molecular Diagnostics*, 8(6):679–688, 2008.
- [103] C H Chau, J D Strobe, and WD Figg. Covid-19 clinical diagnostics and testing technology. *Pharmacotherapy: The Journal of Human Pharmacology and Drug Therapy*, 40(8):857–868, 2020.
- [104] L Li, T Shim, and PE Zapanta. Optimization of covid-19 testing accuracy with nasal anatomy education. *American journal of otolaryngology*, 42(1):102777, 2021.
- [105] M Shephard. Point-of-care testing in australia: the status, practical advantages, and benefits of community resiliency. *Point of Care*, 12(1):41–45, 2013.
- [106] VV Menshikov. The point-of-care testing and security of patient: advantages and risks. *Klinicheskaja Laboratornaia Diagnostika*, (7):11–14, 2013.
- [107] M Viviano, P Vassilakos, U Meyer-Hamme, L Grangier, SL Emery, MU Malinverno, and P Petignat. Hpv self-sampling in the follow-up of women after treatment of cervical intra-epithelial neoplasia: A prospective

-
- study in a high-income country. *Preventive Medicine Reports*, 24:101564, 2021.
- [108] NP Pai, C Vadnais, C Denkinger, N Engel, and M Pai. Point-of-care testing for infectious diseases: diversity, complexity, and barriers in low- and middle-income countries. 2012.
- [109] K Haney, P Tandon, R Divi, MR Ossandon, H Baker, and PC Pearlman. The role of affordable, point-of-care technologies for cancer care in low- and middle-income countries: A review and commentary. *IEEE journal of translational engineering in health and medicine*, 5:1–14, 2017.
- [110] RI Chima, CA Goodman, and A Mills.
- [111] A Alwan and DR MacLean. A review of non-communicable disease in low- and middle-income countries. *International Health*, 1(1):3–9, 2009.
- [112] Y Balarajan, U Ramakrishnan, E Özalpin, AH Shankar, and SV Subramanian. Anaemia in low-income and middle-income countries. *The lancet*, 378(9809):2123–2135, 2011.
- [113] BFS Fernandes and P Caramelli. Ischemic stroke and infectious diseases in low-income and middle-income countries. *Current Opinion in Neurology*, 32(1):43–48, 2019.
- [114] K Martin, R Wenlock, T Roper, C Butler, and JH Vera. Facilitators and barriers to point-of-care testing for sexually transmitted infections in low- and middle-income countries: a scoping review. *BMC infectious diseases*, 22(1):1–41, 2022.
- [115] L Wallis, P Blessing, M Dalwai, and SD Shin. Integrating mhealth at point of care in low- and middle-income settings: the system perspective. *Global health action*, 10(sup3):1327686, 2017.
- [116] B Heidt, WF Siqueira, K Eersels, H Diliën, B van Grinsven, RT Fujiwara, and TJ Cleij. Point of care diagnostics in resource-limited settings: A review of the present and future of poc in its most needed environment. *Biosensors*, 10(10), 2020.
- [117] S Sayed, W Cherniak, M Lawler, SY Tan, W El Sadr, N Wolf, S Silkensen, N Brand, L Meng Looi, and SA Pai. Improving pathology and laboratory medicine in low-income and middle-income countries: roadmap to solutions. *The Lancet*, 391(10133):1939–1952, 2018.
- [118] R Rasti, D Nanjebe, J Karlström, C Muchunguzi, J Mwanga-Amumpaire, J Gantelius, A Mårtensson, L Rivas, F Galban, and P Reuterswärd. Health care workers’ perceptions of point-of-care testing in a low-income country—a qualitative study in southwestern uganda. *PLoS One*, 12(7): e0182005, 2017.
- [119] D Kuupiel, V Bawontuo, and TP Mashamba-Thompson. Improving the accessibility and efficiency of point-of-care diagnostics services in low-

- and middle-income countries: lean and agile supply chain management. *Diagnostics*, 7(4):58, 2017.
- [120] FR Ishengoma and AB Mtaho. 3d printing: developing countries perspectives. *arXiv preprint arXiv:1410.5349*, 2014.
- [121] CR Sagandira, M Siyawamwaya, and P Watts. 3d printing and continuous flow chemistry technology to advance pharmaceutical manufacturing in developing countries. *Arabian Journal of Chemistry*, 13(11):7886–7908, 2020.

2

The Liberalization of Microfluidics - Form2 Benchtop 3D Printing as an Affordable Alternative to Established Manufacturing Methods

Published: Heidt B*, Rogosic R*, Bonni, S, Passariello-Jansen J, Dimech D, Lowdon JW, Arreguin-Campos R, Steen Redeker E, Eersels K, Diliën H, van Grinsven B and Cleij TJ. (2020), *Phys. Status Solidi A*, 217
**authors contributed equally.*

Chapter preface

The market for 3D printing is valued at 15 billion US dollars (2021) with projected compound annual growth rate (CAGR) of 24% over the next 8 years. There are hundreds of 3D printers available on the market, with a broad range of prices and performances. From FDM printers to Stereolithography and Sintering, the market is able to satisfy the needs of hobbyists, small company engineers, and big manufacturers. Printable materials have as well developed over the years, with a great variety of choices in polymers, metals and ceramics. Despite this diversification, there are some players that consolidate themselves as sector leaders. Formlabs is one of these companies and the 3D printers they produce (SLA and Sintering) are known for their reliability, out-of-the-box operation, user-friendliness and neat design and engineering. The Form2, one of their most successful models, was one of the earliest affordable SLA printers, and it is still used today by countless engineers and researchers. While there is abundant review material regarding the general comparison between printers, literature does not provide an independent and systematic analysis of the printer performances for the design of microfluidic channels. The following chapter introduces a study, published in *Physica Status Solidii A*, in which the use of the Form2 3D printer for microfluidics fabrication, is evaluated.

Abstract

In laboratory environments, 3D printing can be used for fast prototyping of assays and devices. Stereo lithographic (SLA) 3D printers have been proven to be the best choice for most researchers due to their small feature size, which is achieved by selectively curing liquid resin using a laser with a small focal point and then forming consecutive layers out of cured polymer. However, in microfluidic applications, where the limits of these machines are reached, the final results are influenced by many factors. In this work, the Form2 SLA printer is tested to show how to achieve the best printing results for the creation of microfluidic channels. Several test structures were designed and printed with embedded and open channels in different orientations, sizes and resins. Embedded channels significantly under performed when compared to open surface channels in terms of accuracy. Under the best printing conditions, 500 μm is the limit for embedded channels, while the open surface channels showed good accuracy up to widths and depths of 250 μm .

2.1 Introduction

In the last two decades, 3D printing has revolutionized the world of prototyping and manufacturing. 3D printing in principle is a technology similar to classical 2D ink printing, but instead of ink on paper, it deposits multiple layers of a particular material one on top of each other, allowing for the creation of three-dimensional objects [1]. Multiple types of technology are used in 3D printing, everything that involves the creation of objects by multi layer deposition, falls under the definition of additive manufacturing (AM). The huge developments of the last decades enable the use a broad range of materials, each optimized for specific types of 3D printing [2, 3]. The most widely known and used techniques today are by far fused deposition modeling (FDM) and vat polymerization (VAT) also known as resin printing. These two types of AM technologies have experienced a huge commercial success: countless companies offer relatively cheap (available for private users) machines that have compact dimensions and are easily used to produce everyday objects. Thanks to the drive of the market, the advancements in technology allow these machines to reach high levels of precision today. Even in laboratory environments, researchers are more keen to use these devices in everyday activities, as 3D printing helps to develop custom-made and tailored assays [4] or laboratory devices [5]. FDM and VAT are based on very different technologies: in an FDM printer, a polymeric filament is extruded after being heated at an appropriate temperature. The extruded material is deposited in a thin layer on a building plate, and the following layers are stacked in order to form the final object (Figure 2.2). FDM technology is in principle very simple and allows for the use of a variety of thermoplastic materials that can be extruded through a heated nozzle. Thanks to its easy printing and reliability, the most commonly used material in FDM is poly lactic acid (PLA). Other materials, such as acrylonitrile butadiene styrene (ABS), poly-propylene (PP) and poly carbonate (PC) can be used as well [6]. The main advantages of FDM printing are the low cost of the material and the straightforward printing process.

Generally, spools of plastic filament are directly fed into the printer. No processing is needed once the print is done, and the printer itself needs very low maintenance as the modern designs are rugged. FDM

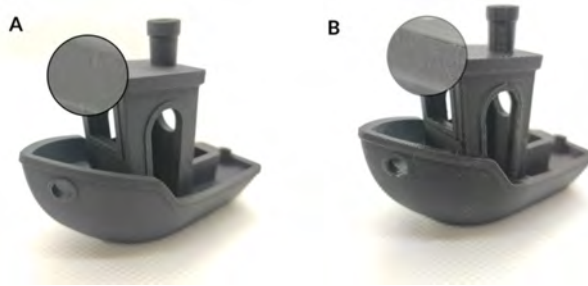


Figure 2.1: A. Object printed with the Form2 SLA printer (layer thickness $50\mu\text{m}$): the final part is much more detailed and the surface finish is smoother if compared to B. the same object printed with an FDM (Ultimaker 3, layer thickness $100\mu\text{m}$) printer. In the magnification, the stair-stepping lines are well visible.

might therefore seem the perfect printing process, however there is a main disadvantage: the surface smoothness of the final object is lower when compared to other AM techniques (Figure 2.1). This is intrinsic to the layer per layer melting, deposition and cooling process. While the discretization of an object introduces approximations such as stair-stepping for all AM techniques, this is particularly evident in FDM printers, due to the relatively high layer thickness. On the contrary, VAT techniques have layers with reduced thicknesses, limiting this effect. The material used for the creation of the object is a liquid resin, usually an acrylate [7, 8] and it is photo polymerized at near room temperature. The final result is a smoother and highly detailed object. VAT printers consist of a moving build platform that is immersed in the resin tank. The build platform is precisely positioned with respect to the bottom of the resin tank, in order to leave exactly the amount of resin necessary to cure a single layer. After the light source polymerizes one layer, the build platform is moved upwards by the same height of the layer, and then the next layer is cured (Figure 2.2). This process is repeated for each layer. As for FDM printing, commercially available modern resin printers are well optimized and allow for high accuracy prints in a range of materials with various properties [9]. VAT printers can be divided in two categories: stereo lithography (SLA) and digital light processing (DLP) printers. The difference lies in the light source used: SLA printers rely on a laser that,

through a series of mirrors, focuses the light at the appropriate planar coordinates on the build plate. DLP printers use a digital projector screen as the light source, projecting therefore the whole image of the layer and curing all the point simultaneously.

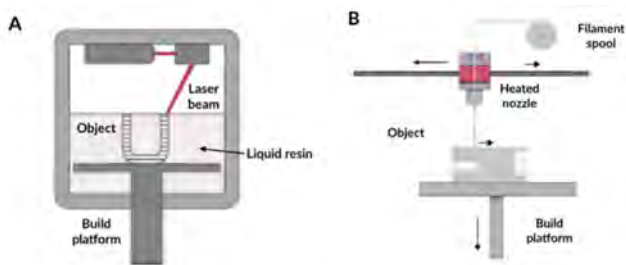


Figure 2.2: A. Vat polymerization (VAT) printing principle and B, fused deposition modeling (FDM) technology principle. Adapted from tractus3d.com/sla-vs-fdm/

3D printed Microfluidics. Thanks to the well known advantages of microfluidics in many laboratories applications [10], research in this field developed substantially in the last 10 years. The vast majority of microfluidic chips found in literature are fabricated by lithography techniques [11] however, in recent years, with the development of 3D printing, there are commercially available machines that allow for the fabrication of microfluidic devices with AM techniques [12]. The main advantage is the one-step process that reduces the time needed for fabrication [13]. A contribution to the recent development of 3D printed microfluidic devices, comes from the availability of bio compatible materials, which allow researchers to use their devices in biological applications [14, 15]. In this field, SLA is a commonly used technology: in 2014, researchers printed a 3D immuno-magnetic flow assay [6]. The device was used in combination with magnetic nanoparticles and antibodies, allowing for the separation of Salmonella bacteria. Similarly, another group, used SLA printers to fabricate a micro mixer, a gradient generator, a droplet extractor and a device for isotachopheresis [16]. This work showed how such structures can be obtained in a single fabrication step using SLA technology. In a later work, [17] researchers managed

to print in a single step designs with integrated valves, controlled by pneumatic actuation. All these examples illustrate the potential of SLA printers in the further development of 3D printed microfluidics. The higher accuracy and surface definition of this technique are the main advantages that made commercially available SLA printers the choice for the majority of researchers interested in 3D printing of microfluidic devices.

Accuracy in 3D printing. Comparing the accuracy of two resin printers only by looking at the technical specifications is a difficult task. Many factors such as materials, software settings and post processing contribute to the quality of the printed object. Resolution in the Z axis is often used as a selling point by manufacturer to attract attention, however, in resin printers, XY resolution is most of the times the limiting factor in achievable feature size. Z resolution is the minimum distance that the build plate can travel in the Z direction and corresponds to the layer thickness. The XY resolution depends on the light source used to cure the resin: in the Form2 printer the minimum feature size on the XY axis is 140 μm and corresponds to the size of the laser spot that is projected onto the build plate.

Benchmark of the Form2 SLA printer. The majority of literature on 3D printed microfluidics, use their own 3D printed setup or develop their own resin, optimized for the selected printer. This can result in difficulties when trying to replicate their work, limiting the knowledge transfer potential. In this work, we focus on a commercially well established SLA printer that has one of the best quality price ratios on the market: the Form2 from Formlabs. The Form2 printer can be used with a variety of different resins that are tuned for specific properties. In this work we characterize the printing quality of the Form2 printer in microfluidic applications, in terms of surface finish, accuracy (deviation from nominal size) and optical properties. We show how the printed objects are influenced by different printing orientations on the build plate as well as how the final result is affected by the different resin used (among three resins). We selected to test Clear resin, Tough resin and High Temperature resin as they are the ones most commonly used in lab environments thanks to their specific advantages (transparency,

resistance to temperature and good mechanical properties, respectively).

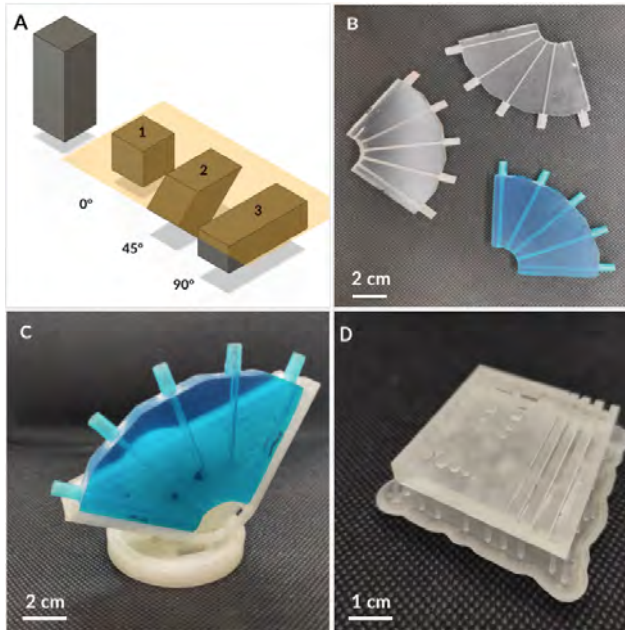


Figure 2.3: A. Printing object in different orientations has important effects on the end result. B. Test objects printed with different dimensions and orientations. C. Orientable stand for photo acquisition. D. Open channel features.

2.2 Materials and Methods

The resins used were: Clear resin V4(FLGPCL04), Tough resin V5, High Temperature resin V2. All the resins were purchased from Formlabs. Preform 3.0.1 (Formlabs) software was used as slicer and for every print was set to a layer thickness of 50 μm . The test objects were designed using Fusion 360 (AutoDesk).

Precision and repeatability. The goal is to highlight the influence of resin type and inclination of the printed object, on the final result.

The printer prints the object layer by layer: the planar projection, at a defined height, corresponds to the layer being printed at that height. The inclination of the object has different effects: as seen in Figure 2.3A, varying the inclination of an object on the build plate, will modify the surface area of each layer. A direct effect is the modification of the force acting on the object as this gets detached from the resin tank after the polymerization of each layer. A higher surface area will create higher stresses acting on the object. On the other hand, higher areas mean that the laser will be able to reproduce with higher accuracy a very small feature. For example, if we take into consideration the Form2 printer, with a laser spot size of 140 μm , and an object with a minimum feature size (in the XY axis) of 85 μm , if the object is printed vertically, the laser will not be able to reproduce accurately the feature, while if the object is tilted, the XY projection will increase, allowing the 140 μm spot size to reproduce the same features with more accuracy. In objects with specific irregular and small features, this technique can be exploited to obtain higher quality details. A Leica S6E optical microscope with a 40X times magnification, equipped with a Leica DFC290 HD digital camera, was used for all the photos and the prints were aligned to account for the viewing angle. The images were analysed with the software ImageJ, each channel/feature was measured 3 times to obtain an average. Accuracy (in %) is defined as the ratio between the nominal size and the measured size multiplied by 100.

Embedded channel accuracy. A test object (Figure 2.3A) was printed, featuring a single squared embedded channel oriented at five different angles, equally distanced between 0° and 90° with regard to the build plate. The test object, as seen in Figure 2.3, is a quarter disk. For each resin we printed 4 quarter disks with channel size of 0.5 mm, 1 mm, 1.5 mm and 2 mm. In total, we printed and tested 12 test objects. Open feature accuracy In order to test the accuracy of features printed on the outer part of an object, a test object featuring various geometrical shapes was printed. As seen in Figure 2.3D, the test object includes open channels, circular shapes as well as squares in different size and height configurations.

Optical properties. Optical transparency is important in microfluidics

as it allows observing the correct function of the device, discovery of disturbances like bubbles and eventually for the use of optical readout elements. In order to evaluate the optical properties of the three different resins, a simple 3 mm thick window adapted to be compatible with a Shimadzu UV1800 uv spectrophotometer was printed. The complete visible spectrum from 380 to 740 nm was measured in 1 nm increments. To improve the optical properties, the part was wet sanded in increasingly fine grain size (400, 600, 1000, 2000) and coated with Motip effect clear varnish and the spectrum measurement repeated.

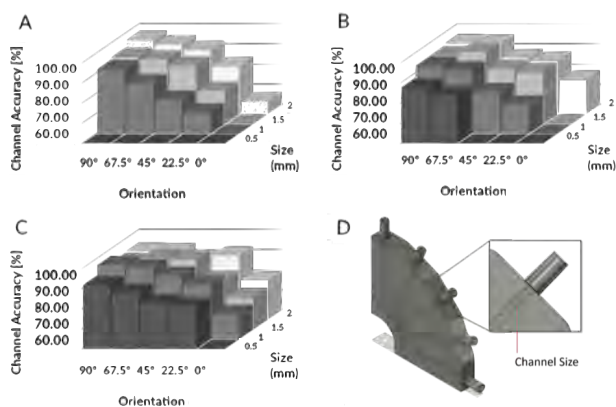


Figure 2.4: Accuracy of 3D test prints with internal channels in four different channel sizes and five different angles. A. Clear resin, B. High Temperature resin, C. Tough resin, D. Rendering of the test model.

2.3 Results

Open channels proved to be less difficult to produce than closed channels, as shown in Figure 2.5. The width of channels for the High Temperature resin and the Clear resin were over 90% accurate down to a channel size of 0.5 mm. The Tough resin however only managed over 90% width accuracy down to 1.5 mm and then slowly declined further until reaching an accuracy of 73.19% at 0.25 mm channel size. The lowest channel accuracy however showed the clear resin at 0.25 mm with 58.97%. For depth accuracy, the Clear resin and High

Temperature resin achieved even better results, retaining over 90% accuracy within all testes channel depth. The tough resin proved to be less accurate in depth as well, showing over 90% accuracy only at 2 mm, however 1,5 and 1 mm trailing close to 90% with 89.22% and 88.56% respectively. Only then follows a strong decline to 71.93% at 0.5 mm, before it ends with the lowest open channel value of 21.12% . The Clear resin and High Temperature resin could still produce open channels without much trouble at half the size of their closed channels lowest point.

The feature size accuracy was good throughout each resin and feature size as seen in 5. Every sample reached over 90% accuracy except the square with a length of 0.5 mm printed with High Temperature resin, which closely failed the 90% mark with 89.08% . Interestingly, the highest accuracy was achieved by the Clear resin at the smallest feature (0.5 mm). In general, a feature size of 1.5 mm showed to be most accurate with most resins. While the performance of the Clear resin and Heat-Resistant resin in the depth accuracy was satisfactory, reaching over 90% in every size increment, the tough resin showed to have troubles, reaching the best mark at 1 mm with only 73% and the lowest at 0.25% with only 55.2% accuracy.

When printing **closed channels**, as Figure 2.4 shows, there was a clear slope in performance visible in all resins for the production of internal laying channels. In general, the best performance was observed with larger channel size as well as higher degree of angle. This tendency is especially visible in the clear resin, where the largest vertical channel (2 mm at 90°) showed the highest accuracy (96.45%) while the smallest channel and the smallest angles (0.5 mm and 0°) could either not be printed at all, or had the lowest accuracy. This effect was less pronounced with the better performing High Temperature resin and Tough resin. 2 mm wide channels could be developed with every resin in every angle. While on the other hand, only the Tough resin was able to print the smallest channel (0.5 mm) down to 22.5° and only failed at a horizontal print of the smallest channel (0.5 mm at 0°). The Clear resin reached over 90% accuracy at an angle of 90° with 2 mm, 1.5 mm and 1 mm large channels. At 67.5° it achieved over 90% accuracy with only 2 and 1.5 mm and at 45° only with 2 mm channel size. At 0° it was only able to

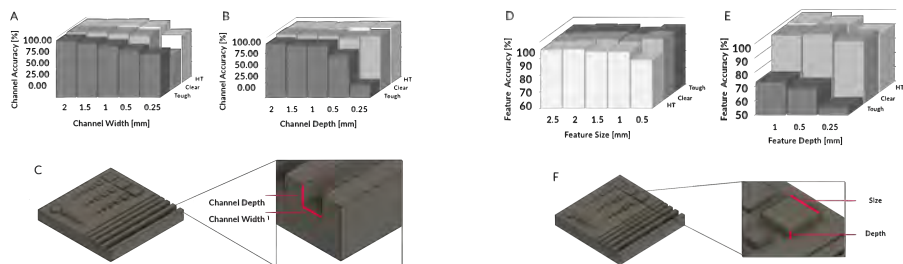


Figure 2.5: Accuracy of open channel prints. A.Width accuracy of the three different resins for five channel width. B. Depth accuracy of the three resins in five different depths. C.Rendering of the printed part with indicated measuring area. D.Size accuracy of five different square sizes with the three different resin types. E.Depth accuracy of the squares for three different height types. F.Rendering of the test structure with marked areas of measurement.

print channels of 2 mm size. Channels with a size of 0.5 mm could not be printed at all by the Clear resin, independently of angle. The high Temperature resin performed better reaching over 90% accuracy at 90° with 2 mm, 1.5 mm and 1 mm channel size and at 67.5° with 2, 2.5 and 1 mm channel size. It failed to produce channels at 0° from 0.5 to 1.5 mm. And channels with size of 0.5 mm to a slope with 46°. The tough resin performed best with over 90% accuracy at 90° and channel sizes 0.5 – 2; 67.5° with channel sizes of 1-2 mm, 45° and channel sizes of 1-2 mm, as well as 22.5° and 2 mm channel size. It only failed to produce channels at 0° and 0.5 mm channel size.

Optical Characteristics. As seen in Figure 2.6A, In the visible light range the High Temperature resin started with the largest transmission of light at 30.9%, followed by the Clear resin with 16.93% and the Tough resin with 12.36%. After the surface treatment process, The Clear resin showed the best properties with 73.18% transmission, followed by the High Temperature resin with 71.33% transmission. The Tough resin performed the poorest with only 38.8% transmission. This is due to two absorption maxima at 616 and 710 nm (Figure S1) leading to the resins intensive blue color. Since the surface treatment only decreases light scattering, the Tough resin does not profit from this effect as much as the

High Temperature and Clear resin, whose low initial transmission is mainly due to scattering. However, as seen in Figure 2.6B, the surface treatment shows the same effect in diminishing the light scattering from the surface.

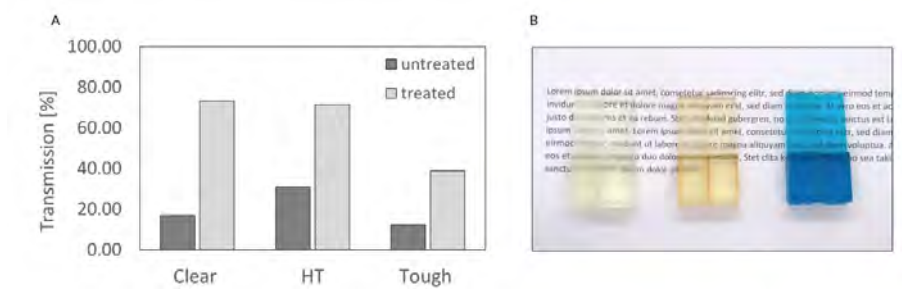


Figure 2.6: A. Transmission values for the three different resins before and after the surface modification process. B. Comparison of transparency for the three different resin types before (left) and after (right) the surface modification, from left to right : Clear, High Temperature and Tough resin.

2.4 Discussion

Performance of different resin types. The Clear resin did perform the worst of the three resin types for internal channels. This is surprising as it was assumed that the more specialized High Temperature and Tough resins would perform worse as they are fine-tuned for different purposes compared to the Clear resin which is used more as an all-rounder. As expected, larger channels, printed at more vertical angles, show the best accuracy. The reason for this effect is most likely the entrapment of uncured resin in the closed channels. With lower channel size and angle, the entrapped resin has less opportunity to flow out of the channel, and thus stays inside and is partially cured by stray light of subsequent layer formation. This in turn leads to a reduced accuracy and in extreme cases, as with small dimensions and angles, to complete clogging. This hypothesis is also supported by the observation that channels usually become clogged from the middle (Figure 2.7 A). As described above, this can be attributed to the trapped resin that manages to escape on

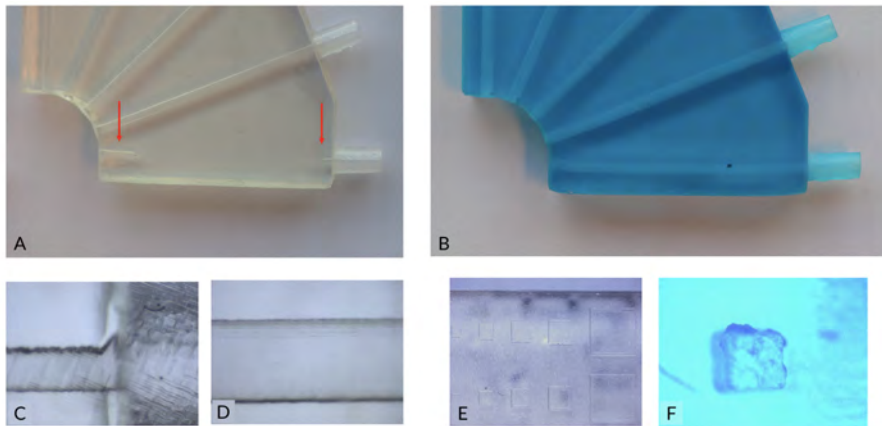


Figure 2.7: Channel clogging seemed to start from the inside, as it was observed that only partially clogged channels were always free at both ends (A). Warping was evident at the surface horizontal to the build platform and most pronounced with the Tough resin (B). The beginning and end of channels showed a higher chance of misprinting (C), as did smaller features (E and F). The middle part of the channels, where the measurements were conducted, was usually well-developed (D).

the sides but not in the middle. This also shows in the construction of open channels which was more accurate and worked very well for most resin types. Interestingly, the Tough resin was here under performing. A possible explanation might be the different curing properties of the Tough resin which seems to have problems with surfaces that are flat to the build plate, the direction this model was printed. On the underside of those prints, malformed parts of cured resin can often be observed, which is not the case for High Temperature and Clear resin (Figure 2.7 F). Regarding the open features, interestingly, the largest features did not perform best. However, the regularity of the shape was more accurate in the larger features and did tend to lose the perfect squared shape in the smaller samples (Figure 2.7 E).

Regarding the optical properties of the printed parts, the refined surface treatment method to improve the light transparency, worked very well and is consistent with former experiments conducted by Formlabs (Figure

2.8) [18].

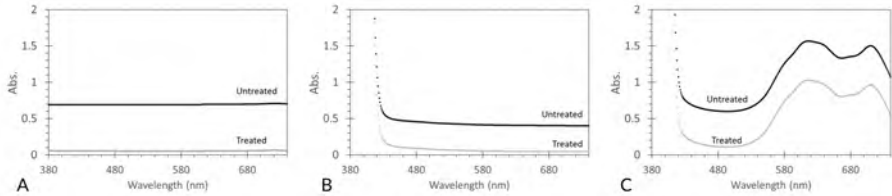


Figure 2.8: The visible light spectrum of Clear (A) High Temperature (B) and Tough (C) resin from 380-740 nm before and after the treatment process. The decrease in signal is due to decreased light scattering at the sample surface. The Tough resin shows a higher absorbance even after the treatment process, this is due to light scattering having only a minor role with the deep blue coloured Tough resin, compared to the absorption at its two maxima at 616 and 710 nm.

2.5 Conclusion

In this study, we demonstrated the capabilities of the Form2 SLA 3D printer, highlighting the relation between accuracy and channel size. In comparison to techniques such as 2-photon polymerization or photo lithography, which allow for boosting precision of the micro fabrication process, the 3D printers do not offer the same performance. However, they require very expensive equipment, limiting their use in everyday lab activity [19]. The results in this chapter highlight that it is possible to use the Form2 printer to fabricate microfluidic support devices in a fast and cost-effective manner. This illustrates that there is a wide array of researchers that can benefit from the utilization of an SLA printer such as the Form2 [20, 21].

Bibliography

- [1] JP Kruth. Material increment manufacturing by rapid prototyping techniques. *CIRP Annals - Manufacturing Technology*, 40(2):603–614, 1991.
- [2] JY Lee, J An, and CK Chua. Fundamentals and applications of 3d printing for novel materials. *Applied Materials Today*, 7:120–133, 2017.
- [3] RA Buswell, WR Leal de Silva, SZ Jones, and J Dirrenberger. 3D printing using concrete extrusion: A roadmap for research. *Cement and Concrete Research*, 112(October 2017):37–49, 2018.
- [4] A Roda, M Guardigli, D Calabria, MM Calabretta, L Cevenini, and E Michelini. A 3D-printed device for a smartphone-based chemiluminescence biosensor for lactate in oral fluid and sweat. *Analyst*, 139(24):6494–6501, 2014.
- [5] F Rengier, A Mehndiratta, H Tengg-Koblogk von, CM Zechmann, R Unterhinninghofen, and HU Kauczor. 3D printing based on imaging data: Review of medical applications. *International Journal of Computer Assisted Radiology and Surgery*, 5(4):335–341, 2010.
- [6] G Comina, A Suska, and D Filippini. Low cost lab-on-a-chip prototyping with a consumer grade 3d printer. *Lab Chip*, 14:2978–2982, 2014.
- [7] R Ding, Y Du, RB Goncalves, LF Francis, and TM Reineke. Sustainable near uv-curable acrylates based on natural phenolics for stereolithography 3d printing. *Polym. Chem.*, 10:1067–1077, 2019.
- [8] S Badilescu and M Packirisamy. *Microfluidics-nano-integration for synthesis and sensing*, volume 4. 2012.
- [9] XL Ma. Research on application of sla technology in the 3d printing technology. 401:938–941, 12 2013.
- [10] AA Yazdi, AW Popma, T Nguyen, Y Pan, and J Xu. 3d printing: an emerging tool for novel microfluidics and lab-on-a-chip applications. *Microfluidics and Nanofluidics*, 20(3):50, 2016.

- [11] AK Au, W Huynh, LF Horowitz, and A Folch. 3d-printed microfluidics. *Angewandte Chemie (International ed. in English)*, 55(12):3862–3881, 2016.
- [12] Y Xia and GM Whitesides. Soft lithography. *Annual Review of Materials Science*, 28(1):153–184, 1998.
- [13] CM Ho, SH Ng, KH Li, and JY Yoon. 3d printed microfluidics for biological applications. *Lab on a Chip*, 15(18):3627–3637, 2015.
- [14] SV Murphy and A Atala. 3d bioprinting of tissues and organs. *Nature Biotechnology*, 32(8):773–785, 2014.
- [15] W Lee, D Kwon, B Chung, GY Jung, A Au, A Folch, and S Jeon. Ultrarapid detection of pathogenic bacteria using a 3D immunomagnetic flow assay. *Analytical Chemistry*, 86(13):6683–6688, 2014.
- [16] N Sundararajan, D Kim, and AA Berlin. Microfluidic operations using deformable polymer membranes fabricated by single layer soft lithography. *Lab on a Chip*, 5(3):350–354, 2005.
- [17] CI Rogers, K Qaderi, AT Woolley, and GP Nordin. 3D printed microfluidic devices with integrated valves. *Biomicrofluidics*, 9(1), 2015.
- [18] Formlabs. Guide to transparent 3d printing with clear resin. 2018.
- [19] BH Cumpston, SP Ananthavel, S Barlow, DL Dyer, JE Ehrlich, LL Erskine, AA Heikal, SM Kuebler, IYS Lee, D McCord-Maughon, J Qin, H Rockel, M Rumi, XL Wu, SR Marder, and JW Perry. Two-photon polymerization initiators for three-dimensional optical data storage and microfabrication. *Nature*, 398:51–54, 1999.
- [20] R Rogosic, JW Lowdon, B Heidt, H Diliën, K Eersels, B Van Grinsven, and TJ Cleij. Studying the effect of adhesive layer composition on mip-based thermal biosensing. *Physica Status Solidi A-applications and Materials Science*, 216, 2019.
- [21] B Heidt, R Rogosic, Lowdon JW, F Crijns, H Diliën, E Steen Redeker, K Eersels, B van Grinsven, and TJ Cleij. Biomimetic bacterial identification platform based on thermal transport analysis through surface imprinted polymers: From proof of principle to proof of application. *physica status solidi (a)*, 216(12):1800688, 2019.

Chapter postface

Our department (Sensor Engineering Group, FSE-UM) is focused on the development of biomimetic sensors for the detection of a variety of targets, different in nature and characteristics. We saw, in 3D printing, a potential tool to adapt and optimize our sensors, around our sensing cores, for all the different applications needed. An example is the fabrication of flow cells used for sampling and transport. A possible way to fabricate those flow cell would have been to outsource production to laboratories equipped with soft lithography techniques. Despite the high resolutions achievable, costs and prolonged design cycle times, make this solution not ideal. 3D printing, on the other hand, gives us the flexibility and freedom to design, fabricate, test and iterate the process multiple times, in a cost-efficient manner. The benchmarking of the Form2 SLA 3D printer, allowed our research group to find an alternative to more costly solution for the production of flow cells.

In the following chapter, the capabilities of the Form2 are used in combination with molecularly imprinted polymers and the heat transfer method, for the optimization of a sensor for new psychoactive substances.

3

Studying the effect of Adhesive Layer Composition on MIP-based Thermal Biosensing

Published: Rogosic R, Lowdon JW, Heidt B, Diliën H, Eersels K, van Grinsven B and Cleij TJ. (2019), *Phys. Status Solidi A*, 216.

Chapter preface

Commercial biosensors for application in PoC diagnostics have been developed in selected fields (see 1.3.1). However, due to several bottlenecks in the design and manufacturing process, their full commercial potential is yet to be unlocked. The fast and low-cost development and large scale production of sampling devices is often overlooked in this process, and could therefore be regarded as one of the bottlenecks in the commercialization of PoC biosensor devices. Rapid prototyping techniques (e.g. 3D printing, rapid milling) could help in the development of new PoC devices. In the following Chapter, the findings of chapter 2, are exploited to create a 3D printed flow cell that was integrated into a thermal biosensor for the detection of designer drugs, using molecularly imprinted polymers (MIPs) as the receptor. The resulting sensor is used in a proof-of-principle study that illustrates the impact of the adhesive layer, used to immobilize MIPs on the sensor surface, on the performance of the biosensor. This study, published in *Physica Status Solidi A*, illustrates how a simple 3D printed device could be used in biosensor research to bring the technology closer to the market.

Abstract

Molecularly imprinted polymer (MIP)-based thermal sensing has proven to be a very interesting tool for diagnostic purposes. However, many fundamental phenomena are not yet fully understood. In the following study, MIPs were imprinted with the new psychoactive substance methoxphenidine (2-MXP). Thermal detection of this compound in water was demonstrated for the very first time, and the effect of varying the adhesive layer composition on the performance of the sensor was analysed. Three different polymers were used to create a uniform adhesive layer. The surface coverage of MIPs on each of the layers as well as the heat-transfer properties were studied. The results of the study indicate that the chips coated with Poly(vinyl butyral-co-vinyl alcohol-co-vinyl acetate) displayed a higher surface coverage and a lower thermal resistance value. This resulted in an improved effect size and therefore improved dynamic range of the sensor.

3.1 Introduction

Molecularly imprinted polymers (MIPs) are synthetic receptors that are designed to mimic the binding affinity natural receptors have for their target [1, 2]. The wide applicability of imprinting technology, ranging from separation and purification to point-of-care-diagnostics, can be attributed to the generic nature of the technology and the ability to mimic the affinity natural receptors have for their target. Other benefits include their low-cost and straightforward synthesis procedure and their thermal, chemical and long-term stability [3, 4, 5, 6], MIP-based biosensors have been made for small molecules as well as large macromolecular entities such as cells and pathogens [7, 8, 9, 10, 11]. The commercial potential of these sensors depends on the quality of the receptor layer, but also on the readout method used for analyzing rebinding. In recent years, a novel sensing technique, based on analyzing thermal transport over a liquid interface, was developed at the Sensor Engineering Department. This low-cost and fast readout method, coined the heat-transfer method (HTM) has proven to be particularly useful in combination with synthetic receptors [12, 13, 14]. Traditionally, aluminum chips are coated with a polymeric layer, as illustrated in Figure 3.1. Larger entities such as mammalian cells get imprinted directly into this layer, creating a homogenous receptor layer directly onto the surface of the measurement chip [15].

MIP particles for small molecules are often made in an external reaction vessel and need to be deposited onto the planar measurement electrode using an immobilization layer made by e.g. spin coating or dip coating. In the latter case, it was recently demonstrated that it is possible to dip coat thermocouples with DNA and roll coat them with polymeric particles for the direct detection of molecules in aqueous media without the need of planar electrodes [16]. Although, this approach is promising, the smaller contact area of the thermocouple limits the sensitivity of the methodology. Therefore, in most cases MIP particles are immobilized onto planar electrodes by means of an immobilization layer, often poly-vinyl-chloride (PVC) due to its wide-spread availability and low cost price [17]. This straightforward approach allows stamping the particles into the adhesive layer or sink them into the layer by sedimentation. However, little is known about the effect of the adhesive

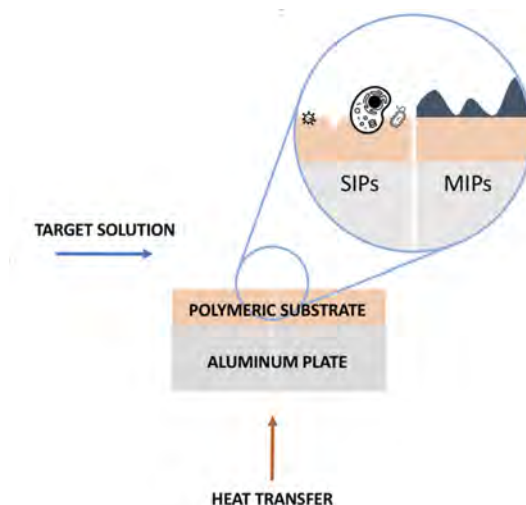


Figure 3.1: Concept of heat transfer method (HTM) combined with surface imprinted polymers (SIPs) and molecularly imprinted polymers (MIPs). The polymeric substrate has a crucial role in both applications, serving as functionalized surface in the SIPs and as adhesive in the MIPs, while in both cases being the active layer that vehicles the heat transfer across the sensor.

layer on thermal transport properties, which might play a role in the effect size of observed phenomena and the limit-of-detection of the methodology. In this study, the authors compared the effect of using three different polymers; poly(vinyl butyral-co-vinyl alcohol-co-vinyl acetate) (Polymer 1), poly-vinyl-chloride (Polymer 2) and polystyrene-block-poly(ethylene-ran-butylene)-block-polystyrene (Polymer 3) on the effect size in a thermal measurement experiment. The different polymers were selected based on their good adhesive properties, transparency to allow visual examination and glass transition temperature for MIP adhesion. The effectiveness of the deposition method was examined by optical analysis, after which the effect on thermal transfer measurements was studied. MIPs were made for the new psychoactive substance methoxphenidine (2-MXP) and their performance was assessed by comparing the response of a MIP to a non-imprinted reference (non-imprinted polymer or NIP). Thermal

detection of this compound by bulk MIPs was demonstrated for the first time and the measurements indicate that the optimal deposition of MIP particles observed using poly(vinyl butyral-co-vinyl alcohol-co-vinyl acetate) co-polymer as an immobilization layer, also resulted in an improved effect size and linear range of the resulting biomimetic sensor.

3.2 Experimental Section

Sample Preparation. Poly(vinyl butyral-co-vinyl alcohol-co-vinyl acetate), MW 90K-120K (Sigma Aldrich) was dissolved in THF at 6% (w/w). Poly-vinyl-chloride, MW 90K (Sigma Aldrich) was dissolved in tetrahydrofuran (THF) (Sigma Aldrich) at 4% (w/w). Polystyrene-block-poly(ethylene-ran-butylene)-block-polystyrene, MW 118K (Sigma Aldrich) was dissolved in toluene (Sigma Aldrich) at 2% (w/w). Flat, polished 10x10 (mm) aluminum plates with 0.3mm thickness were cleaned in acetone and air-dried. 1 mL of each solution was spin-coated on the aluminum plates at 3000 RPM for 1 minute.

Experimental set-up. A similar experimental setup to the one used in the work by Grinsven et al. was used for the experimental measurements [12]. Briefly, polymer-coated aluminum chips were placed on top of a copper block (thin polymer layer facing up), that was heated by a 22 Ohm power resistor (Vishay, Farnell), soldered onto the bottom part of the copper heat provider. The temperature of the copper block was carefully monitored using a type K thermocouple (TC Direct), inserted into the copper via a 0.6 mm wide hole on one of the lateral sides, reaching to the middle of the block (Figure 3.2). A software-driven proportional–integral–derivative (PID) controller keeps the block at 37 degrees Celsius, controlling a 9V supply to the power resistor. The whole set-up is contained in a 3D printed plastic casing. The setup is characterized by a custom-made lid that uses a rubber O-ring to create a cylindrical, sealed chamber on top of the treated aluminum. The lid features three channels that reach to the cylindrical chamber: two are used as inlet and outlet for the sample injection, while the third allows for a precise placement of a type K thermocouple. The thermocouple is

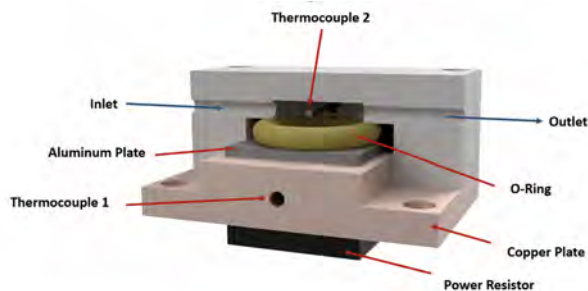


Figure 3.2: Section view of experimental setup: two thermocouples are used to control the temperature of the copper plate and monitor the temperature in the chamber, respectively.

glued in place, thus allowing monitoring the temperature inside the chamber (Figure 3.2).

MIP synthesis. MIP and NIP particles were obtained using the same method described by Lowdon et al [18, 19]. Briefly, MIPs were synthesized using methacrylic acid (MAA) as monomer and 2-MXP as template. A mixture of 1.82 mmol MAA and 0.17 mmol 2-MXP was dissolved in 3 mL of dimethylsulfoxide (DMSO). Following, Ethylene glycol dimethacrylate (EGDM, cross linker molecule, 3.64 mmol), 4,4-azobis (4-cyanovaleric acid) (initiator, 50 mg) were added. After five minutes of sonication, the mixture was purged with N₂ to remove any oxygen from the mixture and polymerization was initiated by heating the mixture to 65 °C for 12 h. The obtained polymer was ground and sieved to obtain microparticles with sizes between 25-50 μm . The template 2-MXP was then removed from the powders by continuous Soxhlet extraction with 50/50 mixtures of acetic acid and methanol and a 50/50 mixtures of methanol and water. Non-Imprinted Polymers (NIPs) were synthesized similarly, but without the presence of the template molecule. Finally, MIP and NIP powders were dried overnight in an oven at 100 °C.

MIP/NIP immobilization. The deposition method was adapted from the work of other authors and adapted to be used with the new polymers

[17]. Aluminum chips were coated with polymer by spin coating, following, 10 mg of the MIP/NIP powder was deposited on the polymer. The polymers were heated for 120 seconds to a temperature above their glass transition temperature to allow the MIPs to sink into the adhesive layer. Following, a polydimethylsiloxane (PDMS) cylindrical stamp was used to gently push the imprinted powder in the heated polymer layer. The plates were left at room temperature for 5 minutes for cooling, after which excess MIP particles were removed by rinsing the chips with deionized (Milliq or MQ) water and blow-drying them using a steady nitrogen flow.

Coverage Analysis. After MIP/NIP particle deposition, optical microscope images were acquired in order to evaluate the area covered by the polymer powder. 10 × magnification was used in order to evaluate an area of 0.54 mm² for each image. Three different images were taken for each sample. The free software ImageJ was used to compute the covered area. First, the images were translated to 8-bit format, then a threshold analysis was done in order to differentiate the darker substrate from the particles, matching the original image (Figure 3.3). Differences in surface coverage were analyzed using one way ANOVA to establish statistical relevance.

2-MXP detection experiment. After preparing the coated samples and assembling the experimental setup as shown in figure 3.3, a solution of 2-MXP in MQ water at a concentration of 200nM was prepared. After stabilization of the signal in MQ water, injections of 3 mL of the spiked solution were performed at a rate of 0.250 mL per minute to gradually increase the concentration of 2-MXP in the measurement chamber. After each injection the system was left to stabilize for 20 minutes. The thermal resistance was calculated using following formula:

$$R_{th} = (T_{heater} - T_{chamber}) / PowerOutput$$

The data were normalized by dividing the response at a certain target concentration by the baseline response when no target is present in the measuring chamber. The effect size at a certain concentration was

calculated as the normalized response of the MIP minus the normalized response of the NIP.

3.3 Results

3.3.1 MIP/NIP surface coverage

The particle distribution was analyzed using an optical microscope in reflection mode. The results are shown in Figure 3.3 and were transformed for analysis of the surface coverage using Image J.

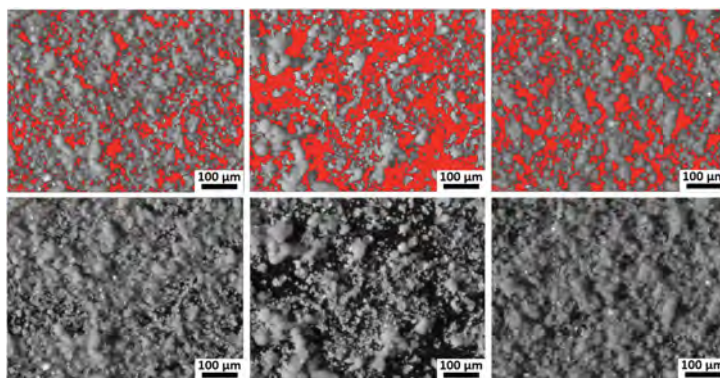


Figure 3.3: Coverage analysis of MIP/NIP particles: from left to right, samples coated with poly(vinyl butyral-co-vinyl alcohol-co-vinyl acetate) (Polymer 1), poly-vinyl-chloride (Polymer 2) and polystyrene-block-poly(ethylene-ran-butylene)-block-polystyrene (Polymer 3) as adhesive layer are shown respectively. In the bottom row the original images are shown while a threshold has been applied on the same images in the upper row to differentiate the substrate from the deposited particles.

Samples were coated with an adhesive layer composed of poly(vinyl butyral-co-vinyl alcohol-co-vinyl acetate), poly-vinyl-chloride and polystyrene-block-poly(ethylene-ran-butylene)-block-polystyrene, which from now on will be denoted Polymer 1, 2 and 3 respectively, for reasons of simplicity. The average surface coverage and standard deviation were calculated for each of the polymers under study and plotted in Figure 3.4. A significant difference in particle deposition coverage was

found among the three differently coated samples. The highest surface coverage was observed on the sample coated with Polymer 1, with a value of $(80.07 \pm 2.14 \%)$ in comparison to Polymer 3 ($70.83 \pm 1.37 \%$) and Polymer 2 with a value of $(63.71 \pm 3.64 \%)$.

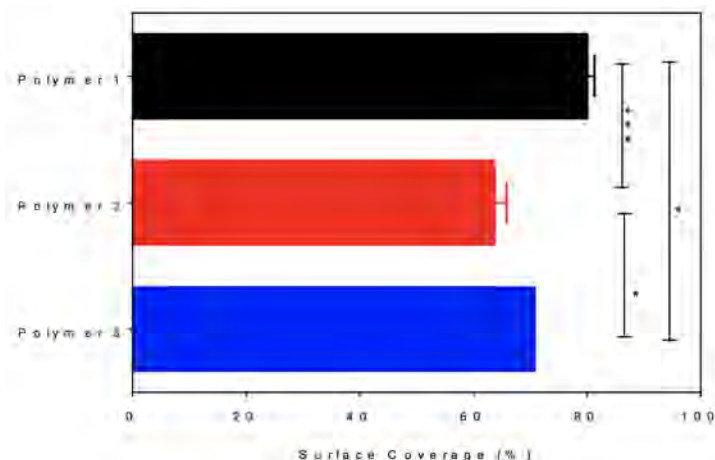


Figure 3.4: Percentage of covered area in function of the polymer used as adhesive layer. Differences in surface coverage were analyzed using one-way analysis of variance (ANOVA) illustrating that the observed differences are significant (* = $p \leq 0.05$ and *** = $p \leq 0.01$).

3.3.2 Effect of Adhesive Layer Composition on Thermal Properties of Solid-Liquid Interface

In order to have a better insight into the effect of using different adhesive layers on thermal transfer characteristics, background measurements (prior to MIP/NIP deposition) were performed for each of the polymers under study (Figure 3.5) on three identically prepared samples. After a stabilization period of 700 seconds with the measurement chamber filled with PBS (MQ water), the interfacial thermal resistance was measured for each sample across a 100 seconds period as described in the experimental section. As shown in figure 3.5, the lowest value of R_{th} was shown for Polymer 1, with a value of $2.59 \pm 0.12 \text{ } ^\circ\text{C/W}$ while

the highest reading was measured for Polymer 2, with a value of 3.26 ± 0.16 °C/W. In addition, a kinetic study on temperature stabilization on the same samples was performed, evaluating, starting from the temperature of 28 °C for all three polymers, the percentages of increase in the curves at 15, 30, 60 and 90 seconds with respect to the mean stabilized temperature calculated in the 100 interval seconds reached after 700 seconds of stabilization (Figure 3.5). All samples show a similar pattern, although the samples using polymer 1 and 2 as coating appear to heat up a little slower, reaching 95.7 ± 0.17 % and 95.8 ± 1.2 % of the final temperature after 90 seconds. The dynamic thermal resistance of the Polymer 3-coated is a little lower and reaches 99.3 ± 1.5 % of the final stabilized temperature after 90 seconds.

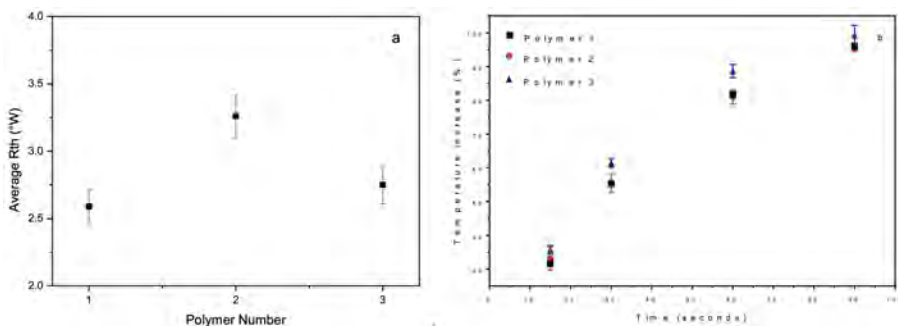


Figure 3.5: Thermal characterization of the substrates: a) Temperatures reached in the measurement chamber and the respective R_{th} of the three different polymers. b) Temperature dynamic curves of the differently coated samples.

3.3.3 Effect on 2-MXP detection

The samples coated with different adhesive layers were used in an experiment to detect 2-MXP in aqueous media. MIPs were immobilized onto the three different polymers as described in the experimental section. After a 20-minute stabilization time, the concentration of 2-MXP was gradually increased. For each addition, the thermal resistance was calculated over a period of 400 seconds. The response of a MIP-coated chip was compared to a non-imprinted reference chip. The effect

size was determined by subtracting the NIP signal from the MIP signal and normalizing the value to the baseline. This measurement was repeated three times for each of the polymers under study. The results, summarized in Figure 3.6, demonstrate that using Polymer 1 and Polymer 3 lead to an increase in the effect size over most of the concentration range in comparison to the polymer used in previous work [17]. In addition, the sensitivity seems to be improved, which in turn leads to a more pronounced dynamic range and a more clear relationship between concentration and effect size.

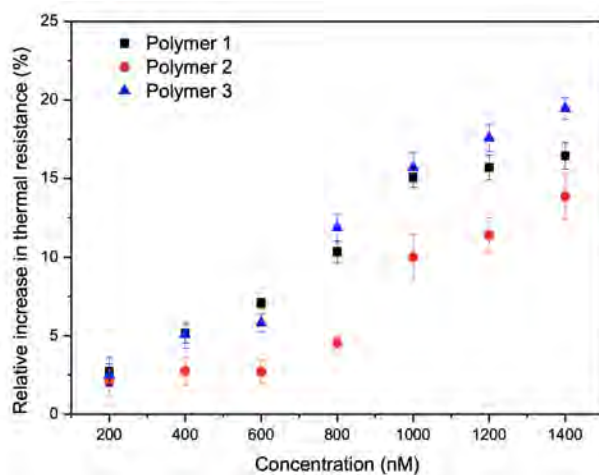


Figure 3.6: Effect size of the R_{th} of samples characterized by different substrates: R_{th} is measured as $R_{thMIP} - R_{thNIP}$ where R_{th} is calculated as $(T_{Heater} - T_{Chamber})/P$, with P being the power delivered by the power resistor in order to stabilize the system. For each addition of 200 nM 2MXP solution, the system is left to stabilize for 20 minutes and the mean value of R_{th} is calculated over the last 400 seconds. All data were normalized on the baseline.

3.4 Discussion

The results shown in this paper confirm that the adhesive layer composition can have a significant effect on the performance of the resulting MIP-based sensor. The surface coverage is highly influenced

by the type of polymer used for immobilizing the MIP particles onto a planar electrode. The data in Figure 3.3 provide a very first empirical confirmation that layer composition can influence MIP immobilization efficiency. Analyzing the data with ImageJ and the statistical analysis in Figure 3.4 confirmed that the observed differences in surface coverage were indeed significant. These findings are in line with a previous study performed by Petri et al. in 2002 [20]. Their study analyzed the morphology of different polymer films spin coated onto polar silica surfaces with atomic force microscopy and demonstrated that PVC in THF, polymer 2 in our study and the standard material used in previous studies, produces inhomogeneous layers. Polyvinyl butyral in THF on the other hand resulted in smooth, homogenous layers of polymer. The findings made by Petri et al. provide a potential explanation as Polymer 1, the polymer that gave the highest surface coverage, is actually a co-polymer of polyvinyl butyral dissolved in toluene, which offers a more homogenous immobilization platform for the MIP particles. The thermodynamic properties of Polymer 1 and Polymer 3 also seem to be beneficial in comparison to the previous standard, Polymer 2. Both polymers show a much lower static thermal resistance in comparison to Polymer 2. Surprisingly, this effect is absent in the dynamic thermal analysis, where only Polymer 3 seems to heat up a bit faster in comparison to the other polymers. However, the effect is only small, and the setups limited sensitivity requires further study to draw any meaningful conclusions. More importantly, the increased MIP surface coverage and lower baseline thermal resistance seem to be the most important parameters when actually analysing the different samples in an analytical setting. The data in Figure 3.6 do not only demonstrate that it is possible to use bulk 2-MXP MIPs for thermal detection purposes, a finding that to our knowledge have never been demonstrated before, but also confirm that the composition of the adhesive layer influences the performance of the sensor. The average effect size over the entire concentration range is higher for the samples coated with Polymer 1 and Polymer 3 and, more importantly, the sensitivity of the resulting sensor is improved, thereby increasing the linear relationship between concentration and effect size over a wider concentration range.

3.5 Conclusion

The results indicate that it is possible to detect the new psychoactive substance 2-MXP in a quantitative manner using the previously successful combination of bulk MIPs with a thermal readout unit. The easy synthesis process of the receptor particles and the fast, user-friendly readout open the door for low-cost detection platforms that enable law enforcement to identify new psychoactive substances in an easier and faster manner. The findings in this paper also illustrate the effect of the composition of the adhesive layer used for MIP immobilization on the surface coverage, with significant differences observed between the different polymeric adhesive layers under study. The composition also influences the static thermal resistance, an essential parameter of the thermal detection methodology. Optimal results were achieved using Poly(vinyl butyral-co-vinyl alcohol-co-vinyl acetate), allowing for a higher degree of MIP immobilization which in turns positively influences the correlation between effect size and target concentration and the binding capacity of the sensor chip by improving the limit-of-detection of the resulting sensor. The lower thermal resistance values further improve the dynamic range of the resulting MIP-based biosensor as the relative effect size increases. In this way, the results demonstrated in this paper, open up the possibility for further follow-up studies that examine these phenomena in more detail to come up with an optimal adhesive layer composition tailor-made for the envisioned analytical applications.

Bibliography

- [1] AA Malik, C Nantasenamat, and T Piacham. Molecularly imprinted polymer for human viral pathogen detection. *Materials Science and Engineering: C*, 77:1341–1348, 2017.
- [2] K Haupt and K Mosbach. Molecularly imprinted polymers and their use in biomimetic sensors. *Chemical Reviews*, 100(7):2495–2504, 2000.
- [3] M Hussain, J Wackerlig, and PA Lieberzeit. Biomimetic strategies for sensing biological species. *Biosensors*, 3(1), 2013.
- [4] A Molinelli, M Janotta, and B Mizaikoff. Molecularly imprinted polymers for biomolecular recognition. *Methods Mol Biol*, 300:243–54, 2005.
- [5] Y Hoshino, T Urakami, T Kodama, H Koide, N Oku, Y Okahata, and KJ Shea. Design of synthetic polymer nanoparticles that capture and neutralize a toxic peptide. *Small*, 5(13):1562–1568, 2009.
- [6] K Lettau, A Warsinke, M Katterle, B Danielsson, and FW Scheller. A bifunctional molecularly imprinted polymer (mip): Analysis of binding and catalysis by a thermistor. *Angewandte Chemie International Edition*, 45(42): 6986–6990, 2006.
- [7] Q Wang, D Zhang, S Tian, and P Ning. Simultaneous adsorptive removal of methylene blue and copper ions from aqueous solution by ferrocene-modified cation exchange resin. *Journal of Applied Polymer Science*, 131(21), 2014.
- [8] O Hayden and FL Dickert. Selective microorganism detection with cell surface imprinted polymers. *Advanced Materials*, 13(19):1480–1483, 2001.
- [9] CR Lowe. An introduction to the concepts and technology of biosensors. *Biosensors*, 1(1):3–16, 1985.
- [10] H Alftan, C Haglund, J Dabek, and UH Stenman. Concentrations of human choriogonadotropin, its beta-subunit, and the core fragment of the beta-subunit in serum and urine of men and nonpregnant women. *Clin Chem*, 38(10):1981–7, 1992.

- [11] O Hayden, K Mann, S Krassnig, and FL Dickert. Biomimetic abo blood-group typing. *Angewandte Chemie International Edition*, 45(16):2626–2629, 2006.
- [12] B van Grinsven, K Eersels, O Akkermans, S Ellermann, A Kordek, M Peeters, O Deschaume, C Bartic, H Diliën, E Steen Redeker, P Wagner, and TJ Cleij. Label-free detection of escherichia coli based on thermal transport through surface imprinted polymers. *ACS Sensors*, 1(9):1140–1147, 2016.
- [13] K Eersels, P Lieberzeit, and P Wagner. A review on synthetic receptors for bioparticle detection created by surface-imprinting techniques—from principles to applications. *ACS Sensors*, 1(10):1171–1187, 2016.
- [14] K Eersels, B van Grinsven, T Vandenryt, KL Jiménez-Monroy, M Peeters, V Somers, C Püttmann, C Stein, S Barth, GMJ Bos, WTV Germeraad, H Diliën, TJ Cleij, R Thoelen, WD Ceuninck, and P Wagner. Improving the sensitivity of the heat-transfer method (htm) for cancer cell detection with optimized sensor chips. *physica status solidi (a)*, 212(6):1320–1326, 2015.
- [15] Diliën H, M Peeters, J Royakkers, J Harings, P Cornelis, P Wagner, E Steen Redeker, CE Banks, K Eersels, and B van Grinsven. Label-free detection of small organic molecules by molecularly imprinted polymer functionalized thermocouples: toward in vivo applications. *ACS sensors*, 2(4):583–589, 2017.
- [16] TM Scholtens, F Schreuder, ST Ligthart, JF Swennenhuis, Arjan GJ T, J Greve, and LW Terstappen. Celltracks tdi: An image cytometer for cell characterization. *Cytometry Part A*, 79A(3):203–213, 2011.
- [17] T Vandenryt, B Van Grinsven, K Eersels, P Cornelis, S Kholwadia, TJ Cleij, R Thoelen, W De Ceuninck, M Peeters, and P Wagner. Single-shot detection of neurotransmitters in whole-blood samples by means of the heat-transfer method in combination with synthetic receptors. *Sensors*, 17(12), 2017.
- [18] JW Lowdon, SMO Alkirk, RE Mewis, D Fulton, CE Banks, OB Sutcliffe, and M Peeters. Engineering molecularly imprinted polymers (mips) for the selective extraction and quantification of the novel psychoactive substance (nps) methoxphenidine and its regioisomers. *Analyst*, 143(9):2002–2007, 2018.
- [19] JW Lowdon, K Eersels, R Rogosic, B Heidt, H Diliën, E Redeker Steen, M Peeters, B van Grinsven, and Thomas CJ Cleij. Substrate displacement colorimetry for the detection of diarylethylamines. *Sensors and Actuators B: Chemical*, 282:137–144, 2019.
- [20] DFS Petri. Characterization of spin-coated polymer films. *JOURNAL OF THE BRAZILIAN CHEMICAL SOCIETY*, 13(5):695–699, 2002.

Chapter postface

In this chapter, an engineering approach is used to study the influence of the adhesion layer used to immobilize the MIPs to the readout part of the sensor. To do so, a 3D printed flow cell is fabricated and integrated in a heat transfer method based sensors [14]. The work of the chapter shows that the adhesive layer has a significant effect, due to the different thermal and topographical properties of the polymer layer. It also offers two alternatives to the traditional system used, opening possibilities for future optimisations. The effectiveness of a 3D printed flow cell, manufactured at a fraction of the original cost price, is demonstrated. The next chapter, continues exploring the possibilities of integration of rapid prototyping in research, focusing on a cost efficient pumping system.

4

Cost-effective, Scalable and Smartphone-controlled 3D-Printed Syringe Pump - From Lab Bench to Point of Care Biosensing Applications

Published: Rogosic R, Poloni M, Marroquin Garcia R, Dimech D, Passariello-Jansen J, Cleij TJ, Eersels K, van Grinsven B and Diliën H. (2022), *Physics in Medicine*,12.

Chapter preface

In line with the rationale of the previous chapter, the study presented in this chapter aims at exploring the opportunities that 3D printing, combined with other rapid prototyping techniques (e.g. rapid and modular PCB fabrication), could offer in terms of scientific research. While low-cost self-test kits typically employ handheld passive fluid transport samplers, some of the more performant integrated biosensor devices, require a pumping system to transport liquids to the receptor layer. This is often a bottleneck that inflicts with commercialization of the final product. In this study, we demonstrate how rapid prototyping (and in the future rapid manufacturing) techniques could be used to design a pump in a much faster and cost-effective manner. The pump was benchmarked in a scientific study, published in *Physics in Medicine*, to illustrate its potential impact on scientific research. Furthermore, the use of the pump has also been evaluated in educational settings, as it was used during the laboratories of the Business Engineering course at Maastricht University (bachelor degree, Laboratory and Research Skills). The benefits of the pump, in particular its cost efficiency and easiness of usage, lowered expenditure for the course managers, maintaining high quality standards. The tutors, and students that used the syringe-pump, were asked to compile a questionnaire based on their experience. Results of this questionnaire are presented in the article postface section of the chapter and illustrate that low-cost devices made via rapid prototyping could also impact science in an educational sense.

Abstract

Laboratories around the world use syringe pumps every day for a multitude of purposes. The market of syringe pumps is limited, as it does not consider the broad range of specifications required by different researchers. In this work, we present a 3D printed syringe pump designed to be affordable, customizable, and extremely user-friendly while still maintaining reliability and precision. The pump, thanks to its flexible design and smartphone-controlled interface, can be used in educational settings as well as in biological and chemical laboratories. The presented syringe-pump is used in this work to run a light catalysed polymerization of butyl methacrylate using visible light, in a continuous flow setup.

4.1 Introduction

Healthcare laboratories, as well as research centers for biology, tissue engineering and chemistry, use small volume pumps every day for a variety of applications. Some of the example studies in which low flow-rate pumping systems are used are cell-conditioning experiments [1, 2] or cell-related biosensors [3, 4]. More and more researchers want to conduct high throughput experiments maximizing efficiency [5, 6]. In this regard, commercially available pumping systems often fail to address their needs. Commercially available pumps are often complex, bulky and expensive. The dominant types of pumps used in such systems are the syringe pump, the peristaltic pump and the pressure pump [7]. Syringe pumps are commonly used in applications where a defined flow rate is needed, but can also be adapted to provide constant pressure if required. The main advantage of commercially available pumps is that they can enable highly precise flow control. However, highly precise flow control is often coupled to other high-end specifications (e.g. extremely low flow rates, high end materials) which are not required for a wide range of research activities [8, 9]. As a result, the pumps are too big and too expensive for incorporation into simple lab test facilities or commercial devices for e.g. low-cost sample analysis [10]. Additionally, there is a strong drive worldwide to take into account sustainability [11, 12]. From this perspective, flexibility and affordability are specifications that today must be considered when designing an experimental setup. With the rise of desktop 3D printing and DIY machining, it has become easier for researchers around the world to develop custom devices that have specifications exactly tuned to what the needs of the individual are [13, 14, 15]. Low resource laboratories could especially benefit from these recent developments. Thanks to additive manufacturing (AM), many research groups developed their own solutions, focusing for example on integrating cost-effective microscope imaging and pumping systems [16] or designing administration systems for microfluidic applications [17, 18, 19]. Similarly, some groups focused on minimizing costs [20, 21, 22], or on flexibility and ease of use by relying on Arduino boards to control the pumping systems [23], and building wireless solutions [24]. In this work, we describe the fabrication of a low-cost (100 Euros) syringe pump that combines the above-mentioned benefits and that

further improves on the employability of the pump by making it fully portable (integrated battery and reduced size) and controllable by a smartphone with an intuitive user interface. The pump can be easily fabricated and assembled with the use of two common 3D printers, off-the-shelf electronics and easily available components. The pump described in this work is a reliable tool designed to minimize the loss of resources in terms of costs and time needed to build an experimental setup [25]. With its intuitive design, customizable and low-cost nature, it has the potential to improve processes in a variety of applications, inside and outside the laboratory.

4.2 Materials and Methods

The body of the pump can be divided into three sections: the pump head, the main body and the moving elements. To guarantee better mechanical properties and durability, the production of the pump-head has been outsourced to a company that could provide Nylon 3D printing. While this can be done with low-end FDM printers, for user-friendliness and production efficiency, it has been deemed more appropriate to outsource the part. The rest of the parts have been printed with Poly-lactic acid (PLA) using an Ender 3-Pro printer. The “Snail” component, as well as the connector parts that allow to connect the syringe to different tubing sizes, have been printed with an SLA resin printer, a Form2 from Formlabs, using the Clear Resin V4 (Figure S1). The “Snail” part is the connecting element between the Syringe and the tubing, and thus it comes in contact with the fluid dispensed by the pump. The market offers a large variety of resins that the user can chose from, including biocompatible resins (Formlabs Biomed Resin). The pump head is a completely enclosed section that holds the electronic board and the motor. It connects to the main body through two M3×12 mm and one M3×6 mm square-head screws (Figure 4.1.A). This solution guarantees the isolation of the electronic components from the rest of the pump. The main body holds the syringe in place and allows the linear movements of the syringe plunger thanks to 4 enclosed linear bearings (Figure 1.B). The last macro-section of the pump are the moving parts: these are a set of parts that control the correct positioning of the syringe pump and allow for the generation of a precise and controlled flow (Figure

4.2.C). The electronics controlling the Pump consist of two PCBs that

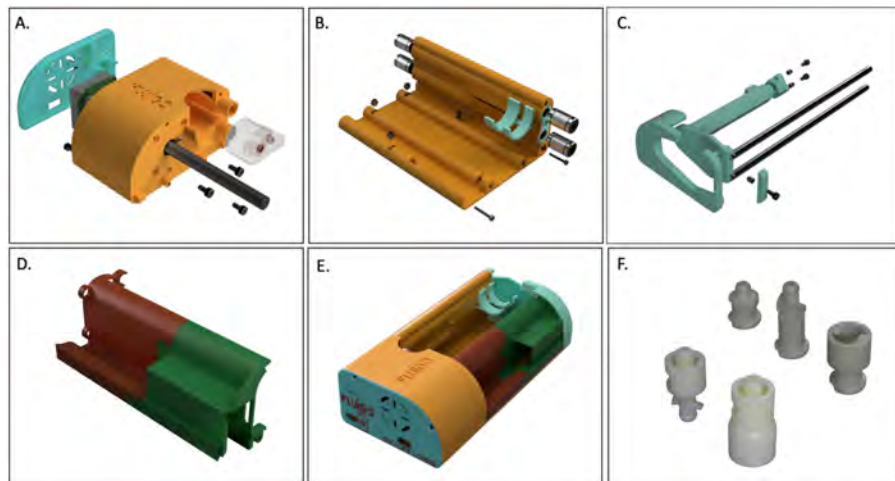


Figure 4.1: Main components of the syringe-pump. A) Pumphead where the motor and the electronics are located . B) Pump body with syringe holder and linear bearings. C) Moving parts that translate horizontally, allowing to fill and empty the syringe. D) Cover body, battery holder and sensor holder. E) Full assembly, and F) connectors for tubing and adapters.

are connected to maximize the user experience. The choice was made to design the PCBs to work with off-the-shelf modules to minimize costs, avoid problems with chip shortages and most of all to give the possibility of rapid and cost-effective repairs in case a single module fails [26]. The main board (50×90 mm) (Figure 4.2.A) features a CH340 Chip, compatible with an Arduino Nano, as the brain of the system. The module is connected to the motor through an A4988 stepper driver module. Communication is allowed by a HC-10 BLE BT module, while the power management system is made of a 8.4 V rechargeable Li-Ion battery with a capacity of 600 mAh combined with a TP5100 module for the battery charging. Lastly, a MT3608 boost converter module is used to convert 5V input from a USB-C port to the 12V needed to power the battery module and provide appropriate power to charge the battery. The main board features also a 2-pin, 2mm JST connectors that allows to connect a magnetic sensor use to stop the pump when it reaches the

complete opening of the plunger. The second board (20×20 mm) (4.2.B) is provided with a push button that functions as a safe switch for the end of run of the syringe pump closing and with 3 LEDs that are used to provide information on the functioning of the pump and on the battery status (Green LED: mode ON-OFF, Blue LED: Battery Charged, Red LED: battery needs charging). The CH340 has been programmed so that the green LED blinks in case the battery needs to be recharged. In this case, the user can switch the pump to the charging mode (4.5.A) and a red LED will light up until the battery reaches complete charge. Once the battery is charged, the LED will turn to blue and the pump will be ready to be operated again. The syringe-pump described in this



Figure 4.2: Electronic boards. A) Main board. B) Top layer of secondary board, C) bottom layer of secondary board

work is designed to be controlled through the Flui.Go Kit Experiments App, an IOS/Android compatible app, downloadable for free from the Apple Store and Play Store. The app features a user-friendly interface that allows the user to connect and control easily one or more pumps simultaneously (Figure 4.3). The app allows as well to select two administration modes: a scientific mode in which the amount of ml/min administered is visualized, and a basic mode in which the flow-rate can be varied between a value of 1 and 10. The basic mode is helpful for example in educational settings where inexperienced users might be confused by experimental details such as the unit of measurement. Figure 4.4 shows the syringe pump assembled: the total dimensions of the pumps are (198 L×98 W×52 H) mm for a total weight, all components included, of 800 g. The syringe pump is powered by an 8.4 V Li-ion rechargeable battery with a capacity of 600 mAh that guarantees up to 1.5 h of continuous pumping. The stepper driver A4988, combined with the AccelStepper™ library, allows driving the stepper motor in 5 different

modes: from full step down to 1/16 of a step. Best performances, however, in terms of smoothness of operation were achieved with a quarter stepping mode. The assembled pump features a quick release mechanism for the syringe and a set of adaptors that allow the user to connect a tubing or Luer-lock connectors (4.1.F).

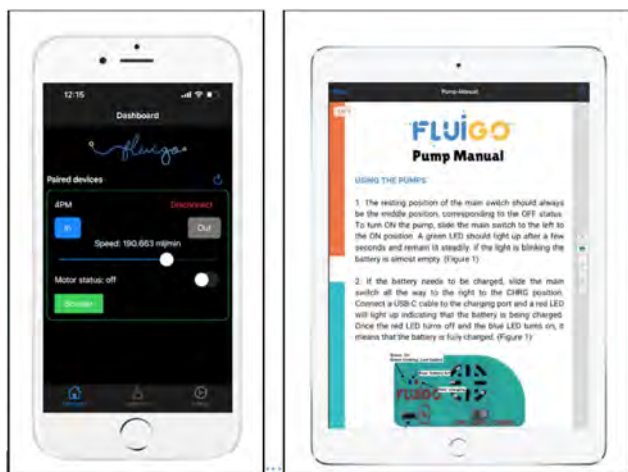


Figure 4.3: The Flui.Go App allows controlling multiple pumps simultaneously. The interface is intuitive and easy to use and can be customized based on the needs of the user. Simple UI can be used for educational purposes, while more complex options that allow to control more parameters are better suited for laboratory environments.

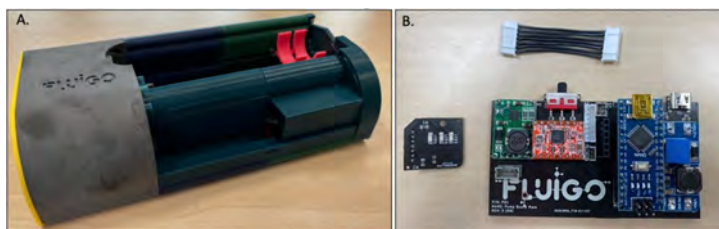


Figure 4.4: Assembled components. A) The Flui.Go Pump assembled, B) and the electronics used in the setup.

4.3 Validation and Characterization

A detail explanation of the pump functioning is shown in the Supplementary.Video1, available at <http://doi.org/10.17605/OSF.IO/QKW42>. Continuous smooth delivery of fluid and consistency in volumes is demonstrated. The current configuration of the pump featuring a 30 ml syringe, allows to have a considerably high volume at disposition while still achieving smooth delivery of low flow rates (200 $\mu\text{l}/\text{min}$). While much lower flow rates can be achieved changing the syringe (lower volumes) or reprogramming the driving software, for many applications in the lab, such flow rates are not required [27, 28, 29]. Thus, the current configuration has been found to be optimal for everyday use in the lab. Table 4.1 and Table 4.2 show the technical specifications of the pump in its current configuration and the comparison with other syringe pumps, commercial ones, and DIY ones. In particular, 4.5 shows how the developed pump could be a cost-effective alternative to commercial devices in applications where high portability is needed. Finally, to validate the capabilities of the device in a laboratory environment, a light-catalyzed polymerization of butyl methacrylate was performed under continuous flow, provided by the syringe-pump.

Volume delivered	Syringe (ml)	Flow rate ($\mu\text{l}/\text{min}$)	Random Error (n = 5)	
			μl	%
1 ml	30	200	18	1.8
1 ml	30	2000	23	2.3
10 ml	30	2000	137	1.37
10 ml	30	20000	210	2.1

Table 4.1: Technical performance of the DIY pump.

Reagents and characterization. N,N-dimethylformamide (DMF, Biosolve BV, 99.5%) and Methanol (MeOH, Biosolve BV, 99%), Butyl methacrylate (BMA, Sigma Aldrich, 99%) was purified one

Pump	Type and Cost	Min flow rate ($\mu\text{l}/\text{min}$)	Max flow rate (ml/min)	Max Force (N)	Max Pressure (kPa)	Wireless / Control
Flui.Go Pump	DIY - 100 €	1.829	45	80	100	yes/smartphone
Ender 3 Kit [16]	DIY - 170 €	< 5	1-10	-	-	no/software
HK-400VET	Commercial - 800 €	0.002	50	-	40-160	yes/direct
Dual pump [18]	DIY - 350-600 €	100	100	-	-	no/direct
Open Source Pump [25]	DIY - 85 €	-	130	90 - 200	-	no/software
CETONI Nemesys S	Commercial - >2000 €	0.02	150	400	1000	no/software
NE-1000	Commercial - 750 €	0.25	18.6	150	-	no/software
T60-CME	Commercial - 2000 €	0.002	1.6	-	50-110	yes/direct

Table 4.2: Pump performance in comparison with literature and commercial syringe pumps.

time through a column filled with basic alumina oxide and stored at 2°C prior the polymerization. Ethyl 2-bromoisobutyrate (EBiB, Sigma Aldrich, 98%), N,N -diisopropylethylamine (iPr2Net, Sigma Aldrich, 98%), tris(bipyridine)ruthenium(II) dichloride hexahydrate ($\text{Ru}(\text{bpy})_3\text{Cl}_2 \cdot 6\text{H}_2\text{O}$) were used as received unless indicated otherwise. The polymers obtained in this work were characterized via gel permeation chromatography (GPC) using HFIP as eluent (equipment info) Continuous flow reactor and photo-polymerization As a proof of concept for application in a laboratory environment, a continuous flow photo-reactor, driven by the pump, was designed for the polymerization of butyl methacrylate using visible light (Figure 4.6). Butyl methacrylate is commonly used in the synthesis of molecularly imprinted polymers (MIPs) a promising technology for biosensing applications [30, 31]. The use of continuous flow systems in the photo-induced synthesis of polymers has gained major attention in the past years due to its resource-efficiency. The polymerization reaction was based and adapted from batch reactions taken from literature [32, 33]. In short, 1.5 mg (2 μmol) of $\text{Ru}(\text{bpy})_3\text{Cl}_2 \cdot 6\text{H}_2\text{O}$ were weighed and dissolved in a 5 mL flask using 2 mL of DMF under dark conditions. A second flask was prepared containing BMA 2.8 g (20 mmol), 130 mg (1 mmol) of iPr2Net, and 98

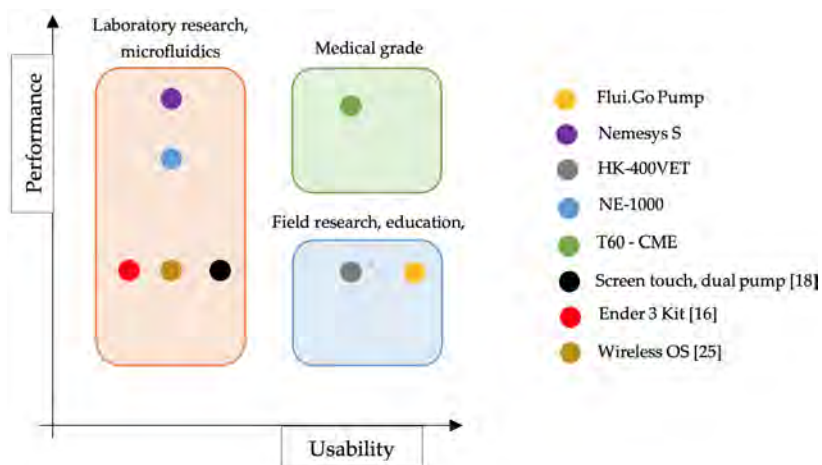


Figure 4.5: Usability VS performance in existing syringe pumps (commercial and DIY) and areas of application. Data is taken from Table 2: performance is evaluated by comparing minimum and maximum flow rates, deviations in volumes administered and maximum force the pump can achieve. Usability is evaluated as tradeoff between certification (medical, veterinary or research), type of interface (direct control, computer software, smartphone application) and portability (dimensions, sturdiness, power source). The graph is intended as a qualitative comparison between pumps and its purpose is to illustrate the different areas of application of commercial and DIY syringe pumps.

mg (0.5 mmol) of EBiB. Both flasks were seal-capped and de-gassed by bubbling argon for 20 minutes under dark conditions. At the same time, 30 mL of DMF was loaded into an air-tight syringe and placed in the pump (Figure 4.6, a). After degassing of the solutions, the content of both flasks was mixed under argon protection and then transferred to a new syringe. The content of this syringe was injected into the reactor tubing using a three-way valve (Figure 4.6, b and c). Once the reaction mixture was loaded, the pump maintained a continuous flow of 0.2 mL/min for 60 minutes. The reaction was initiated by irradiating the reactor coil (Figure 4.6, f) with a 12 V led-light strip (Figure 4.6, e). The final solution was precipitated in an excess of cold MeOH (Figure 4.6, g) and the polymer was then characterized via GPC (Figure 4.7).

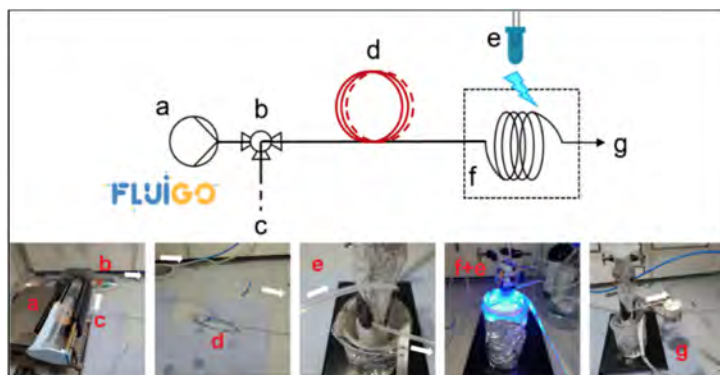


Figure 4.6: Continuous flow photo-reactor set-up where: a) represents the Flui.Go pump, b) a three-way valve, c) syringe entry, d) pre-reactor coil, e) 12 V led-light strip (1 m), f) reactor coil (distance from the light was 9 mm) and, g) product collection flask.

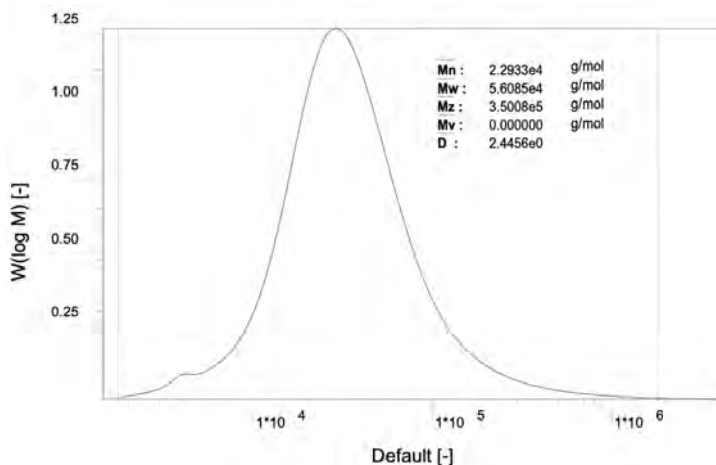


Figure 4.7: Continuous flow photo-reactor set-up where: a) represents the Flui.Go pump, b) a three-way valve, c) syringe entry, d) pre-reactor coil, e) 12 V led-light strip (1 m), f) reactor coil (distance from the light was 9 mm) and, g) product collection flask.

4.4 Discussion and Conclusion

The pump described in this work is a robust and flexible tool for everyday applications in research and academic environments. The added value of being highly portable and controllable with a smartphone, makes the pump potentially available to a larger pool of people. As demonstrated, researchers can use the pumps for laboratory experiments in which precise continuous flow needs to be maintained. Potential application for the developed system are experiments of flow chemistry [34], biosensor development [35], point of care applications [36] and drug delivery [37]. Similarly, thanks to the intuitive design and robustness, inexperienced users, such as pupils or educators, can use the pump for educational purposes. Another interesting potential application for the developed pump could be its use in low-resource environments in which flexibility and usability are crucial.

Additional resources

All design files are provided with the GNU General Public License V3 and are available (.STL, PDF schematics of the PCBs) at the online repository: <http://doi.org/10.17605/OSF.IO/QKW42>. A **Bill of materials** and **Build instructions and operation instructions**, are also provided at the same location. A detailed **explanatory video** of the pump assembly is provided in (Supplementary Video Assembly.mp4), and of the pump operation (Supplementary Video Pump.mp4), both available at the same link.

Bibliography

- [1] P Abgrall and AM Gue. Lab-on-chip technologies: making a microfluidic network and coupling it into a complete microsystem—a review. *Journal of micromechanics and microengineering*, 17(5):R15, 2007.
- [2] P Almada, PM Pereira, S Culley, G Caillol, F Boroni-Rueda, CL Dix, G Charras, B Baum, RF Laine, C Leterrier, and R Henriques. Automating multimodal microscopy with nanofluidics. *Nature Communications*, 10(1):1223, 2019.
- [3] R Arreguin-Campos, KL Jiménez-Monroy, H Diliën, TJ Cleij, B van Grinsven, and K Eersels. Imprinted polymers as synthetic receptors in sensors for food safety. *Biosensors*, 11(2):46, 2021.
- [4] S Baas and V Saggiomo. Ender3 3d printer kit transformed into open, programmable syringe pump set. *HardwareX*, 10:e00219, 2021.
- [5] MR Behrens, HC Fuller, ER Swist, J Wu, MM Islam, Z Long, WC Ruder, and R Steward. Open-source, 3d-printed peristaltic pumps for small volume point-of-care liquid handling. *Scientific Reports*, 10(1):1543, 2020.
- [6] AS Boeshaghi, EDV Beltrame, D Bannon, J Gehring, and L Pachter. Principles of open source bioinstrumentation applied to the poseidon syringe pump system. *Sci Rep*, 9(1):12385, 2019.
- [7] CK Byun, K Abi-Samra, YK Cho, and S Takayama. Pumps for microfluidic cell culture. *Electrophoresis*, 35(2-3):245–257, 2014.
- [8] MC Carvalho and RH Murray. Osmar, the open-source microsyringe autosampler. *HardwareX*, 3:10–38, 2018.
- [9] HN Chan, Y Shu, B Xiong, Y Chen, Y Chen, Q Tian, SA Michael, B Shen, and H Wu. Simple, cost-effective 3d printed microfluidic components for disposable, point-of-care colorimetric analysis. *ACS Sensors*, 1(3):227–234, 2016.

- [10] M Coakley and DE Hurt. 3d printing in the laboratory: maximize time and funds with customized and open-source labware. *Journal of Laboratory Automation*, 21(4):489–495, 2016.
- [11] P Cormack and AZ Elorza. Molecularly imprinted polymers: synthesis and characterisation. *Journal of chromatography B*, 804(1):173–182, 2004.
- [12] M Cubberley and W Hess. An inexpensive programmable dual-syringe pump for the chemistry laboratory. *Journal of Chemical Education*, 94, 2016.
- [13] JJ Davis, M Padalino, AS Kaplitz, G Murray, SW Foster, J Maturano, and JP Grinias. Utility of low-cost, miniaturized peristaltic and venturi pumps in droplet microfluidics. *Analytica Chimica Acta*, 1151:338230, 2021.
- [14] VE Garcia, J Liu, and JL DeRisi. Low-cost touchscreen driven programmable dual syringe pump for life science applications. *HardwareX*, 4:e00027, 2018.
- [15] VE Garcia, J Liu, and JL DeRisi. Low-cost touchscreen driven programmable dual syringe pump for life science applications. *HardwareX*, 4:e00027, 2018.
- [16] A Gervasi, P Cardol, and PE Meyer. Open-hardware wireless controller and 3d-printed pumps for efficient liquid manipulation. *HardwareX*, 9:e00199, 2021.
- [17] P Gravesen, J Branebjerg, and OS Jensen. Microfluidics-a review. *Journal of Micromechanics and Microengineering*, 3(4):168–182, 1993.
- [18] S Gupta, K Ramesh, S Ahmed, and V Kakkar. Lab-on-chip technology: A review on design trends and future scope in biomedical applications. *Int. J. Bio-Sci. Bio-Technol*, 8:311–322, 2016.
- [19] J Gutierrez, A Santaolalla, A Tercjak, N Rojo, D Encinas, Z Gomez-de Balugera, and G Gallastegui. Creating a green chemistry lab: Towards sustainable resource management and responsible purchasing. *Sustainability*, 12(21):8934, 2020.
- [20] N Hamidah, SY Prabawati, I Fajriati, and I Eilks. Incorporating sustainability in higher chemistry education in indonesia through green chemistry: inspirations by inquiring the practice in a german university. *International Journal of Physics & Chemistry Education*, 9(1):1–7, 2017.
- [21] T Kassis, PM Perez, CJW Yang, LR Soenksen, DL Trumper, and LG Griffith. Piflow: A biocompatible low-cost programmable dynamic flow pumping system utilizing a raspberry pi zero and commercial piezoelectric pumps. *HardwareX*, 4:e00034, 2018.
- [22] JR Lake, KC Heyde, and WC Ruder. Low-cost feedback-controlled syringe pressure pumps for microfluidics applications. *PLOS ONE*, 12(4):e0175089, 2017.
- [23] DJ Laser and JG Santiago. A review of micropumps. *Journal of Micromechanics and Microengineering*, 14(6):R35–R64, 2004.

-
- [24] Z Li, SY Mak, A Sauret, and HC Shum. Syringe-pump-induced fluctuation in all-aqueous microfluidic system implications for flow rate accuracy. *Lab on a Chip*, 14(4):744–749, 2014.
- [25] P Losada-Pérez, KL Jiménez-Monroy, B Van Grinsven, J Leys, SD Janssens, M Peeters, C Glorieux, J Thoen, K Haenen, and W De Ceuninck. Phase transitions in lipid vesicles detected by a complementary set of methods: heat-transfer measurements, adiabatic scanning calorimetry, and dissipation-mode quartz crystal microbalance. *physica status solidi (a)*, 211(6):1377–1388, 2014.
- [26] R Marroquin-Garcia, J Royakkers, M Gagliardi, R Arreguin-Campos, TJ Cleij, K Eersels, NMS van den Akker, DGM Molin, B van Grinsven, and H Diliën. Polyphosphate-based hydrogels as drug-loaded wound dressing: An in vitro study. *ACS Applied Polymer Materials*, 4(4):2871–2879, 2022.
- [27] T Nguyen, S Zoëga Andreassen, A Wolff, and D Duong Bang. From lab on a chip to point of care devices: The role of open source microcontrollers. *Micromachines*, 9(8):403, 2018.
- [28] JM Pearce, NC Anzalone, and CL Heldt. Open-source wax rewrap 3-d printer for rapid prototyping paper-based microfluidics. *Journal of laboratory automation*, 21(4):510–516, 2016.
- [29] MH Reis, FA Leibfarth, and LM Pitet. Polymerizations in continuous flow: Recent advances in the synthesis of diverse polymeric materials. *ACS Macro Letters*, 9(1):123–133, 2020.
- [30] R Rogosic, B Heidt, J Passariello-Jansen, S Björnör, S Bonni, D Dimech, R Arreguin-Campos, JW Lowdon, KL Jiménez Monroy, M Caldara, K Eersels, B van Grinsven, TJ Cleij, and H Diliën. Modular science kit as a support platform for stem learning in primary and secondary school. *Journal of Chemical Education*, 98(2):439–444, 2021.
- [31] Y Saylan, S Akgönüllü, H Yavuz, S Ünal, and A Denizli. Molecularly imprinted polymer based sensors for medical applications. *Sensors*, 19(6):1279, 2019.
- [32] R Schirhagl. Bioapplications for molecularly imprinted polymers. *Analytical chemistry*, 86(1):250–261, 2014.
- [33] A Sivo, R Galaverna, GR Gomes, JC Pastre, and G Vilé. From circular synthesis to material manufacturing: advances, challenges, and future steps for using flow chemistry in novel application area. *Reaction Chemistry & Engineering*, 6(5):756–786, 2021.
- [34] Just infusion syringe pump. <https://www.syringepump.eu/product/ne-300-just-infusion-syringe-pump/>.
- [35] B van Grinsven, N Vanden Bon, L Grieten, M Murib, SD Janssens, K Haenen, E Schneider, S Ingebrandt, MJ Schöning, V Vermeeren, M Ameloot, L Michiels, R Thoelen, W De Ceuninck, and P Wagner. Rapid

- assessment of the stability of dna duplexes by impedimetric real-time monitoring of chemically induced denaturation. *Lab on a Chip*, 11(9):1656–1663, 2011.
- [36] T Vandenryt, B Van Grinsven, K Eersels, P Cornelis, S Kholwadia, TJ Cleij, R Thoelen, W De Ceuninck, M Peeters, and P Wagner. Single-shot detection of neurotransmitters in whole-blood samples by means of the heat-transfer method in combination with synthetic receptors. *Sensors*, 17(12):2701, 2017.
- [37] J Voas, N Kshetri, and JF DeFranco. Scarcity and global insecurity: The semiconductor shortage. *IT Professional*, 23(5):78–82, 2021.

Supplementary Manuals

ASSEMBLY INSTRUCTIONS

1. [Figure S1] Slide the NEMA 14 motor in the pump-head and fix it in place with 4 M3x6mm screws. Insert the 9V standard battery clip in the dedicated hole, crimp the terminals and plug the JST PH 2pin Male connector. Insert the O-rings in place in the Snail part and slide it in place. Insert 2 M3X14mm + 1 M3X8mm screws from the inside of the head-pump (these screws will be tightened later to connect the rest of the parts of the pump).

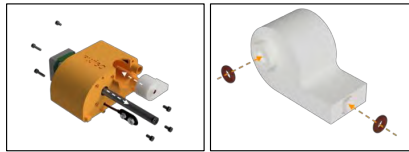


Figure S1

2. [FigureS2] Join Body 1 and Body 2, slide the 4 LM006 linear bearings in place. Insert 4 M3 nuts in the designed pockets and use 2 M3x14 mm screws to secure Body 1 and Body 2 together.

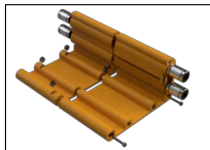


Figure S2

3. [Figure S3] Insert the brass threaded M3 insert in upper left corner of Body 1, join the Pump-head with Body 1 and secure the parts with the M3 screws previously inserted in the Head-pump. Following, Slide Board 1 in the Head-pump part, using the designed guides.



Figure S3

4. [Figure S4] Clip the mini-fan in place, insert Board 2 in the guides on the Head cover and secure with the brass insert and the M3x6mm screw. Use the 7 pin connector cable to connect Board 1 and Board 2 and then clip the Head cover in the Head-pump, completing the first part of the assembly.

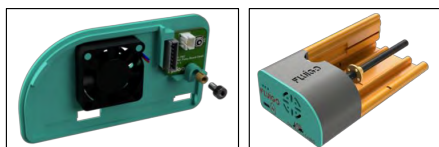


Figure S4

5. [Figure S5] Position the brass rods in the dedicated slots in the Plunger part, put in place the threaded insert, close with the Plunger side body and secure with the M3x6mm screw. Take the Joint part and insert two threaded inserts in the holes. Then slide the Joint part on the brass component provided with the motor (the cylindrical threaded component) and secure with two M3x6mm screws.



Figure S5

6. [Figure S6] Slide the battery in place clipping it to the Battery clip and pushing it flush to the Pump-head. Screw the assembled Joint onto the Plunger part, slide the Plunger in place making the brass rods enter the linear bearings and screwing the motor screw inside the Joint part. Slide in place the Box part paying attention to clip correctly the part in place around the screws fixing the motor.

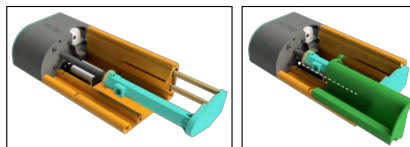
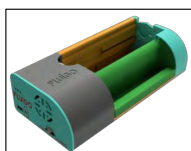


Figure S6

7. [Figure S7] Lastly, clip in place the Back cover part and slide the Syringe holder in place. The assembly is finished.



FigureS7

Important notes

To provide the most complete guide possible to the building of the pumps, the authors include some detail on the assembly of the parts that will help reproduce the work.

1. The assembly of the Brass Rods-Plunger-Plunger Side Body parts require some simple machining working on the brass rods as shown in Figure S8.



Figure S8. Brass rods used to guide the moving parts of the pump.

2. To assemble the boards used in the Flui.Go Pump, a minimum knowledge and skills in soldering is required. Furthermore, two of the components used in Board 1 need to be tuned before being mounted onto the Board:
 - a. MT3608: the step-up module needs to be tuned to step up the 5V voltage to the required 10-12 V. This is done by connecting a fixed 5 V source at the input, monitoring the voltage at the output, and turning the screw of the potentiometer until the desired voltage is reached (Figure S9A).
 - b. TP5100: as shown in Figure S 9B, the open contact on the board (red circle) should be soldered to set the module to the 8.4 V recharge setting. Furthermore, the two factory-mounted current resistors on the board, limit the charging current to 2A which is too much. To lower this value the two parallel resistor (green circle) should be de-soldered and substituted with two 0.47 Ohm resistor that will limit the recharging current to a safer 0.3 A.

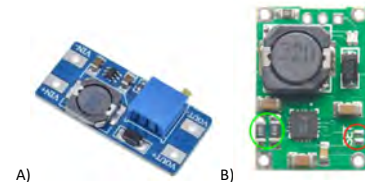





Figure S9. Details on the modules mounted on the custom-made PCB.

3. Some applications might require longer utilization of the pumps that can't be guaranteed with the integrated battery provided. For this reason, the authors provide an alternative pump setup that relies on a power plug. The portability and simplicity of the setup is compromised to gain the possibility of conducting longer experiments. In this configuration, the TP5100 module as well as the MT3608 module are not needed and thus can be neglected. Instead, a 2.1 mm Jack

port is added to the Cover part of the Pump-head and the power is provided with a 9V transformer.

Head Cover V2	Alternative configuration	1	0.5	Printed with Ender V2 Pro	
2.1 mm Jack	Used to secure the Plunger side body	1	0.5	https://nl.aliexpress.com/item/4000053061272.html?spm=a2g00.9042311.o.0.4d326c371OUaM6	
9V transformer	9V general purpose transformer	1	0.5	https://nl.aliexpress.com/item/329219363.html?spm=a2g00.9042311.o.0.4d326c371OUaM6	

SYRINGE PUMP MANUAL

I. Using the pumps

1. The resting position of the main switch should always be the middle position, corresponding to the OFF status. To turn ON the pump, slide the main switch to the left to the ON position. A green LED should light up after few seconds and remain lit steadily. If the light is blinking the battery is almost empty. (Figure S10)
2. If the battery needs to be charged, slide the main switch all the way to the right to the CHRG position. Connect a USB-C cable to the charging port and a red LED will light up indicating that the battery is being charged. Once the red LED turns off and the blue LED turns on, it means that the battery is fully charged. (Figure S10)

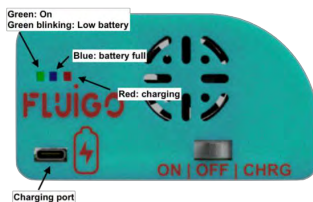


Figure S10: main switch and operation modes of the pump.

3. Make sure that the Bluetooth is turned on your device. Open the Flui.Go Experiments App on your Android or iOS device. Under the settings tab, toggle between Scientific mode and basic mode and in case of the former, insert in the input box the internal diameter of the syringe used. (Figure S11)

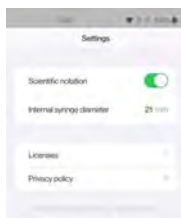


Figure S11

4. Select the Dashboard tab. All the available pumps will be listed here. Connect the pump/pumps that need to be driven by clicking the CONNECT button (Figure 12A). A slider window and control buttons will appear (Figure 12B). Use the slider to select the flow rate of the pump, the IN/OUT buttons to select the direction of the pump. Finally click on the toggle status motor selector to turn the motor on. To momentary pause the pump,

deselect the direction while maintaining the motor status ON. This will keep the motor in a fixed position but will keep consuming current.
IMPORTANT: to STOP the pump between experiments or for a longer period, toggle the motor status to OFF. This will prevent the draining of the battery.



Figure S12

5. The setup described in this work uses 30ml luer-lock syringes. The Flui.Go-to-luer adapter has to be fit on the tip of the syringe. To ensure leak-proof sealing, use two O-rings in between the syringe and the adapter and screw clockwise. To minimize dead volume, pre-fill the syringe manually with the desired amount of liquid and clip the tip of the syringe in the snail part. With the app, open the pump until the moving part of the syringe can fit in the plunger part. Clip the syringe in place, slowly purge the air inside the snail part and stop the pump as soon as you see liquid coming out of the snail. The pump is now ready to be connected and used.



Figure S13

Chapter postface

The results in Chapter 4 illustrate that a pump with tailored characteristics could be developed in a low-cost and fast manner. The use of the pump in research settings is illustrated using a simple chemical synthesis experiment, but it is easy to conceive that it can also have a large impact on biosensor research. In Chapter 3 we used a commercial device that is a lot more expensive than our pump and offers limited flexibility in terms of device handling. In the future, the pump introduced in this chapter will be used in biosensor experiments.

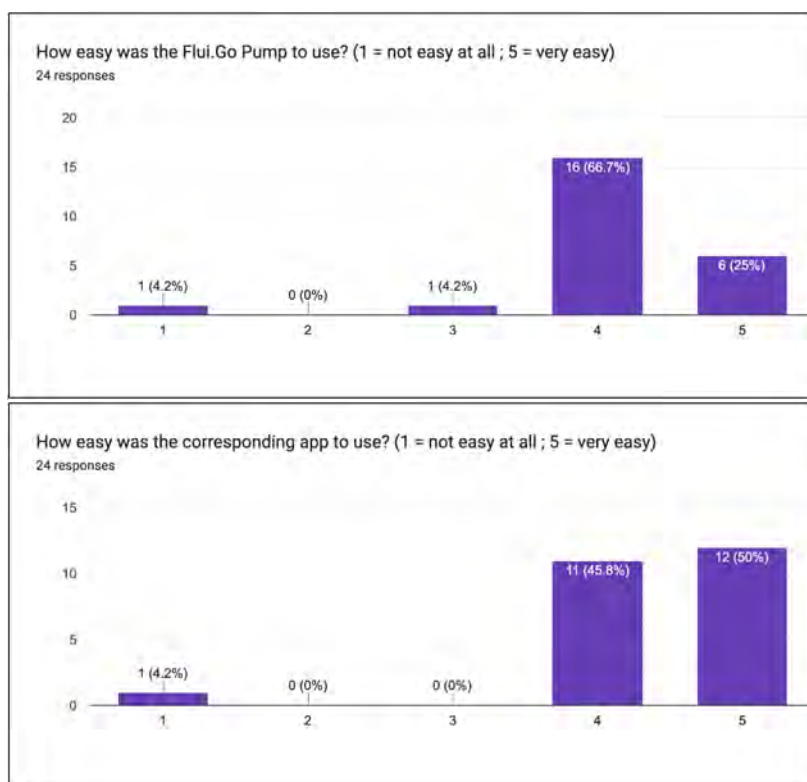


Figure 4.8: Simple questions to assess the user-friendliness of the pump and application used to control the pumps.

As mentioned in the preface section at page 76, the syringe pump could also be used for educational purposes and has therefore been used during the laboratories of a bachelor course at Maastricht University. The students and tutors involved, were asked to compile a Google form questionnaire at the end of the course. A total of 24 people answered the questions (2 tutors and 22 students). The goal was to have an overview of the pumps performance, and an indication on whether the benefits described in the chapter were confirmed by the on-field test. It is important to highlight that the students participating in the course had no laboratory experience. Being their first time in a chemistry laboratory, and coming in contact for the first time with laboratory equipment, they were the perfect test subjects to assess the pumps qualities.

As seen in Figure 4.8, on a scale from 1 to 5 (1 being low score and 5 high score), 89% and 95% of the interviewed gave a score between 4 and 5 to the operation of the pumps and smartphone app, respectively. The experiment, performed during the classes, had the goal of performing a free radical polymerization in flow-chemistry regime.

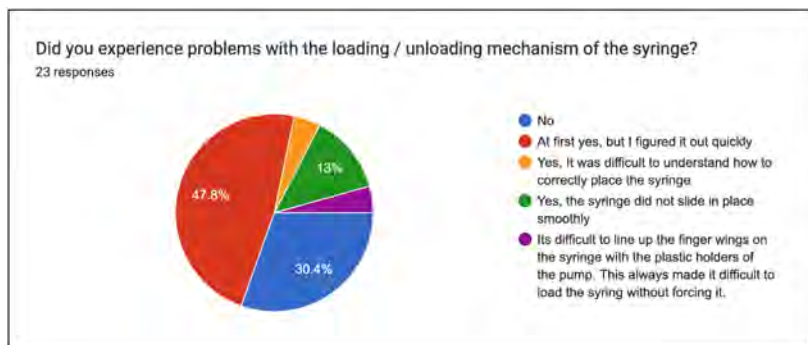


Figure 4.9: The inserting and removing process of the syringe in the dedicated seating, was not completely straightforward for some of the students.

A potential improvement that can be done in future iterations, consists in the loading/unloading procedure of the syringe in the pump. As seen in Figure 4.9, 22% of the students had problems understanding and executing this process.

The smartphone application scored very high, showing stability (no

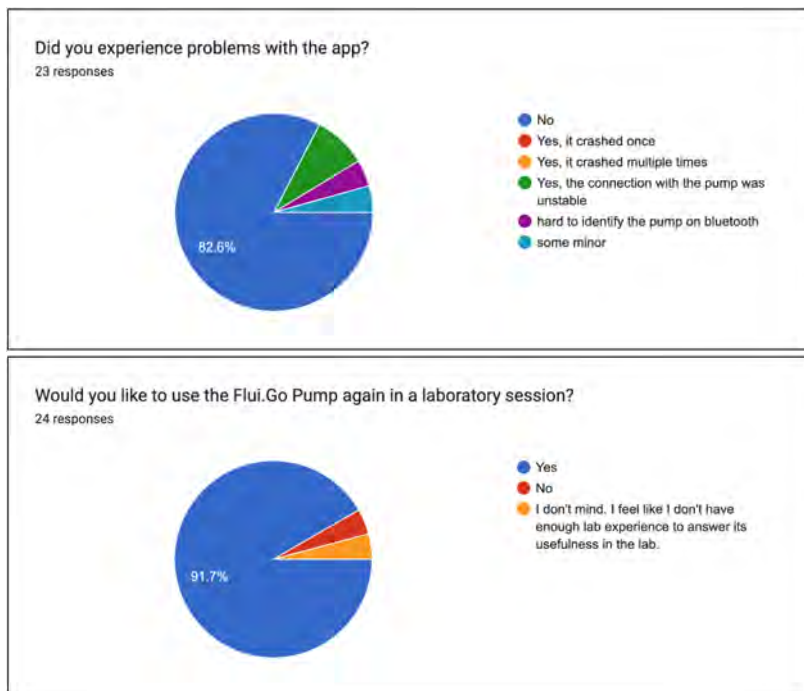


Figure 4.10: Representation of the answers concerning the usability of the smartphone application, used to control the pumps, and the overall laboratory experience.

crashing events) and only isolated minor problems (mainly pump Bluetooth identification). The overall experience of using the Flui.Go Pump in a laboratory session, for untrained personnel with no experience, was very positive, with more than 90% of interviewed willing to use this syringe pumps in future laboratory experiments (Figure 4.10). These positive findings need to be addressed on a larger scale to get significant insights into the full potential of these type of tools on STEM education, but these preliminary results are highly encouraging and provide a rationale for the work presented in Chapter 5 and the outlook discussed in the conclusion of the thesis.

5

Modular Science Kit as a support platform for STEM learning in primary and secondary school

Published: Rogosic R, Heidt B, Passariello-Jansen J, Björnör S, Bonni S, Dimech D, Arreguin-Campos R, Lowdon JW, Jiménez Monroy KL, Caldara M, Eersels K, van Grinsven B, Cleij TJ and Diliën H. (2021), *Journal of Chemical Education*, 439-444.

Chapter preface

This study, which was published in the *Journal of Chemical Education*, illustrates how to build and use a 3D printed, science kit to perform experiments in STEM classes. As the kit also implements the pump developed in Chapter 4, this chapter serves as a final assessment of the overarching research question, namely the potential positive impact of 3D printing in designing tools for educational and research purposes. In doing so, 5 will tie all the results presented in the previous chapters together. The rationale for this chapter is based on literature studies on visual and hands-on approaches in education and the results of the previous chapter. The authors wanted to investigate whether it is possible to make a scientific tool kit using the previously described approaches. In addition, the authors wanted to investigate if the kit could be used to improve the classroom experience of children in primary education. Despite the will to field test the science kit presented in this chapter in a real classroom, due to COVID-19 regulations active at the time of the development of the work, this was not possible, and is therefore not part of this Chapter.

It should be noted that such a study has been done at a later stage. However, once the COVID-19 restrictions had been lifted, the startup Flui.Go Science (see the Valorization chapter for more info) was already founded. As a result, a study investigating the positive impact of the commercial kit on education would create a commercial conflict of interests. Therefore, the study was done by an external researcher, Dr. Nardie Fanchamps, a professor of educational sciences at the Open University of the Netherlands. Dr. Fanchamps, used the kit for an on-field study in a local primary school. The findings have been published at the *INTED2022* Proceedings conference. As they are not the work of the author of the thesis, the study is not included in Chapter 5, but its results are presented at the end of the chapter, in the article postface section (5.5) because the results and conclusions drawn from this study are essential for assessing the impact of the work in this thesis.

Abstract

The need to develop interest in STEM (science, technology, engineering, and mathematics) skills in young pupils has driven many educational systems to include STEM as a subject in primary schools. In this work, a science kit aimed at children from 8 to 14 years old is presented as a support platform for an innovative and stimulating approach to STEM learning. The peculiar design of the kit, based on modular components, is aimed to help develop a multitude of skills in the young students, dividing the learning process into two phases. During phase 1 the pupils build the experimental setup and visualize the scientific phenomena, while in phase 2, they are introduced and challenged to understand the principles on which these phenomena are based, guided by a handbook, which is added as supplementary information at the end of the Chapter. This approach aims at making the experience more inclusive, stimulating the interest and passion of the pupils for scientific subjects.

5.1 Introduction

Our society is more and more dependent on technology and engineering, however there is a profound lack of understanding of the basic principles of most of these technologies by a majority of the population [1]. In the early 2000s, scientists started noticing that in the USA there was an incongruence between the job market demands and the distribution of college graduates across different fields of studies [2]. This phenomenon was not a problem in the USA alone. Many reports in the 2000s and 2010s, showed that science and mathematics education in post-compulsory years of schooling was dramatically declining also in Australia [3, 4] and Europe [5], while the demand for the application of STEM skills was rapidly increasing [6]. In the same period, the term STEM subject was introduced: an acronym for science, technology, engineering and mathematics. The idea behind STEM was to create a subject that would give the students an integrated course, focused on skills that are required in today's job market, rather than letting them learn fragmented bits of knowledge. The development of high-level STEM skills is reliant on an early age onset of interest and passion for scientific subjects. Primary education has a crucial role in this regard. In 2012, the PISA survey (Programme for International Student Assessment, promoted by OCSE) showed that in the European Union, 18% of the pupils had low-level science skills, in line with the USA but much higher in comparison with 7% for Korea and 8% for Japan. To address these problems, many different initiatives have been launched, both nationally and internationally. One branch of such initiatives included the development of new pedagogical approaches to STEM, focusing especially on the link between experience and classroom [7, 8, 9]. The idea is that young students should be engaged in the learning process, making STEM lessons more enjoyable. Hand in hand with this evolution of the teaching methods, a multitude of supporting materials were developed. In the last decade, many scientific kits appeared on the market: affordable platforms focused on a scientific subject that allow pupils to learn in a fun and entertaining way. These kits are mainly focused on children with an age between 8 and 14, in order to be usable both in primary and secondary school classrooms [10], as well as at home as entertaining tools. The STEM kits are generally focused on one of the following subjects: chemistry, simple electronics and coding, physics

and engineering, biology and life sciences. While these kits provide a valid platform to engage the pupils and stimulate in an early phase their interest and passion for science, they are focused on one specific subject. To address this issue, we designed an educational toy made up of modular blocks that allow to create a multitude of different scientific experiments, in various STEM fields. As shown in literature, 3D printing is playing an important role also in the field of education, providing new tools for novel teaching methods [11, 12, 13]. In these examples, the authors exploit the advantages that 3D printing offers, mainly versatility and cost-efficiency, to develop all kinds of ideas that could have a benefit on the learning process of students [14]. One of the fields where such tools are employed is chemistry, with examples ranging from simple visualization of concepts (3D printed models of molecules and proteins) [15, 16] to more complex examples such as the fabrication of Ag/AgCl reference electrodes [17]. Also developed thanks to 3D printing, our scientific kit features individual building blocks that have internal fluidic channels, making it possible to create a connected system by combining different blocks. This allows a kid to flush liquids through the system: we designed scientific experiments that can be performed inside such created connected structures. Thanks to the modular approach, it is possible to develop many experiments, exploring a broad range of scientific phenomena. Our aim is to let kids play in the first place and, along the way, get passionate about science and ultimately discover properties and procedures of scientific experiments.

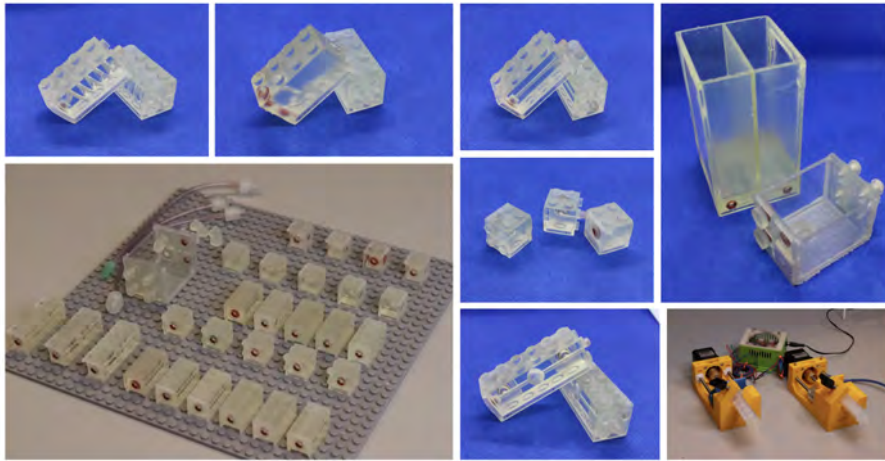


Figure 5.1: A. The science toy kit. Coiled channels, droplet generator, straight channels, 90° turn and T-junction, mixing and visualization chamber. In the lower left corner all the blocks together, while in the right corner a picture of the Poseidon pumps used.

5.2 Materials and Hazards

The kit is composed of modular transparent building blocks, inspired by Lego bricks. The classic design with the circular features was replicated, allowing for vertical interconnection of the blocks. In addition, to allow the creation of a “fluidic circuit”, a second type of connection has been developed: an axial link (Figure 5.1) between two adjacent blocks that allow to connect the outlet of one block to the inlet of the second one. In such way, the blocks can be combined to create a fluidic channel. Furthermore, standard Lego bricks can be used in combination with the kit, to build supporting structures (Figure 5.2).

The kit is made out of 8 different types of blocks, divided in functionalized and non-functionalized parts. Functionalized parts are those that feature geometries and design features which allow creating and visualize a specific scientific phenomenon. Functionalizes parts are mixing chambers, droplet generators and reservoirs. Non-functionalized parts are blocks that are used to complete the fluidic circuit: straight



Figure 5.2: "Fruit Caviar" experiment. From left to right: layout of the experiment with the modular blocks assembled and placed on the supporting mat; schematic of the assembly that the children have to build in order to perform the experiment; final results of the experiment, with the colored alginate droplets created in the reservoir section.

channels, coiled channels, 90 degree turns, T-junctions and connectors for tubing. Each kit is also provided with a set of pumps that allow to control the flow rates inside the fluidic circuit (Figure 5.2). The pumps are based on an open access model [18]. A simple software (Supplementary) is used to control the pumps through an intuitive user interface. The bricks are designed with Fusion 360 (Autodesk) and printed with a commercially available desktop 3D printer (Form2, Formlabs). Based on previous studies [19], we selected Clear resin V5 (Formlabs) as material, thanks to its transparency characteristics and reliability in printing. For the current study, three examples of experiments have been developed and tested. All the experiments can be performed with non-toxic, non-harmful and easily available materials. For the set of experiments presented in this study, on top of the supplied science kit, the following items are necessary: fruit juice (any type), food coloring, sodium alginate, calcium chloride, water, lemons, red cabbage, baking soda and vegetable oil.

5.3 The experiencing phase

5.3.1 Fruit Caviar

The goal of the experiment is to create colored spherical droplets (fruit caviar) with a solution of sodium alginate and calcium chloride. The experiment starts by building the fluidic circuit as shown in the schematic in Figure 5.2. There are two inlets, both of which are connected to non-functional blocks. These parts terminate in a functional droplet generator block. The outlet of the droplet generator is linked to a mixing block, which ends in a reservoir. For this experiment, we use two simple syringe pumps (see Figure 5.1): pump 1 is filled with air, while pump 2 is filled with a solution of sodium alginate (1.8% w/w) in water and fruit juice. Once the pumps are turned on, the fluids from the pumps meet at the droplet generator block: here the two streams are conveyed in one stream, where droplets of the sodium alginate solution are created. The size and frequency of the droplets can be adjusted, varying the flow rate of the pumps. The reservoir was previously filled with a solution of calcium chloride (0.25 M). The inlet at the reservoir is functionalized with an appendix that guides the flow created by the bubble generator inside the reservoir. The solution of sodium alginate, once in contact with the calcium chloride solution, starts to gel. The goal of the experiment is to tune the pumps to an appropriate flow rate that allows the creation of a steady flow of sodium alginate droplets with a diameter of approximately 3 mm. The stream is gently guided in the static solution of calcium chloride, where it forms beautiful spherical particles, the so-called “fruit caviar”.

5.3.2 Veggie Alchemy

In this experiment, the goal is to visualize a chemical reaction obtained with natural ingredients that can be found in a normal kitchen. As seen in the schematic of Figure 5.3, in this experiment the students will assemble a fluidic circuit with three inlets and one outlet. Two pumps are used: water saturated with baking soda is distributed by pump 1, while freshly squeezed lemon juice will be dispensed by pump 2. A third solution, the “indicator solution” is obtained by chopping a fresh red cabbage and mixing the cut leaves in warm water. Once the water cools



Figure 5.3: “Veggie Alchemy” experiment. From left to right: layout of the experiment with the modular blocks assembled and placed on the supporting mat; schematic of the assembly that the children have to build in order to perform the experiment; final results of the experiment, with the chromatic change achieved inside the circuit built, obtained with the modulation of the pH of the flowing solution.

down and shows a strong purple color, the cabbage is filtered out, and the solution is collected in a syringe (syringe number 3 in the schematic of figure 5.3) that is actuated manually. The functionalized parts used are three mixing chambers, sequentially connected in the middle of the circuit, each alternated with a coiled channel. The mixing blocks feature a spherical, hollow chamber that allows to clearly observe the liquid that flows through the circuit. Furthermore, each mixing chamber has 3 inlets and one outlet. Once the circuit is built, the pumps are turned on and tuned to the specified flow rate. Simultaneously, the third pump is manually actuated to push the indicator solution in the circuit. The user will be able to observe the fluids fill the blocks: after a short transitory phase, each of the chambers on the three functionalized blocks will have a different colour. The first chamber will have the purple color of the cabbage solution, the second chamber will turn to a dark blue, while the third one will show a bright pink colour. This experiment exploits the presence in red cabbage of anthocyanin, a pigment that is sensible to pH and changes its colour accordingly. In the first chamber, the solution has a pH close to 7, thus maintaining the purple colour. However, in the second chamber, pump 1 is pumping a basic solution of baking soda, increasing the pH and turning the solution to a dark blue. In the third step, the acidic lemon juice decreases the pH, resulting in another

chromatic change: the solution turns to a bright pink (Figure 5.3).

5.3.3 Space Juice

In this simple experiment, a reservoir with two chambers is used. Two identical submarine-like parts that can be filled with fluid, have been designed, 3D-printed and are used in combination with the modular kit (Figure 5.4).

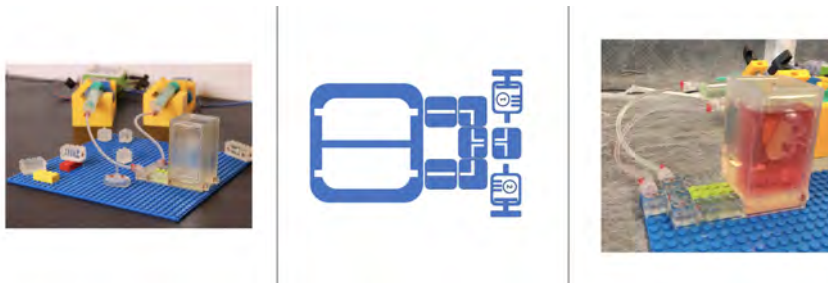


Figure 5.4: “Space Juice” experiment. From left to right: layout of the experiment with the modular blocks assembled and placed on the supporting mat together with the “Space Submarine”; schematic of the assembly that the children have to build in order to perform the experiment; final results of the experiment, where it is possible to see two phenomena: the different behavior of the two submarines and the spatial separation between oil and water due to their different specific weight.

They are filled with 2.5 ml of sunflower oil and positioned in each of the empty compartments of the reservoir. Following, the two syringe pumps are filled with sunflower oil and colored water respectively and connected via two tubes to the reservoir. Once the pumps are turned on, the two chambers start to fill: in the section with water, the submarine will float, while in the oil section it will stay on the bottom of the reservoir. This happens because the volume of oil injected in the subs, is calculated in order to achieve a density higher than sunflower oil but lower than water. Once the reservoir has been filled almost to the top, the pumps are paused, the connections to the reservoir are switched (the oil syringe goes to the water section and vice-versa) and the pumps are turned on again. The fluids entering from the bottom of the reservoir will act differently:

the oil will create bubbles, and it will rise to the top; the water will stay on the bottom, creating a big colored bubble on the bottom of the reservoir. Again, this phenomenon is due to the different density of the fluids.

5.4 The learning phase

During the experiments, multiple physical and chemical processes are happening. After experiencing “hands-on” the scientific phenomena, the pupils can be introduced to these concepts. The first phase of experiencing ends and the second phase of learning starts. Thanks to the handbook provided, (Appendix 1) the students will be guided in this second phase with intuitive explanations of the basic principles underlying the experiments. They will also be challenged to test their understanding of the phenomena observed by a short questionnaire provided at the end of each experiment. In this way, the teacher can have a first insight on the efficacy of the method. The complexity of the concepts explained in the handbook and of the questionnaire provided can be easily tuned based on the age and the background knowledge of the students.

5.4.1 Fruit Caviar

For the “fruit caviar” experiment, the handbook (Supplementary) provided introduces some basic concepts that help to put into context the experiment. Furthermore, the teacher can introduce specific concepts based on the skill level of the students. The concept of polymeric chains can be introduced together with the concept of polysaccharides, such as sodium alginate. At this point, the students will be confronted with the fact that both compounds (sodium alginate and calcium chloride) are in liquid form when they are in a water solution, but specific bonds are created when the solutions are mixed together. An introduction on different types of bonds will be made, followed by an explanation of the creation of the specific bond between the alginate and the calcium ions, seen in the experiment. For the most advanced users, the learning process will be taken one step further, introducing not only the chemistry concepts mentioned, but focusing also on the physical process behind

the creation of the droplets. The droplet generator works by exploiting the shear forces between two immiscible phases. The students will be introduced to the concept of viscosity, surface tension, shear force, laminar and turbulent flow and how these factors affect the formation of the droplets in the fruit caviar experiment. Finally, the questionnaire in the handbook will assess at which extent these concepts have been assimilated.

5.4.2 Veggi Alchemy

This experiment is intended to introduce the students to the concept of pH. Referring to their everyday experience, the handbook (Appendix 1) explains what are acids and bases. The pH scale is introduced and the concept of pH indicator explored. Students can then be introduced to pH sensitive molecules, especially to anthocyanin, the pigment present in red cabbage responsible for the pH sensitiveness of the solution. The structure of the molecule will be shown, focusing on the presence of the functional groups that get protonated or de-protonated, causing a shift in the absorbance spectrum. In the handbook, the questionnaire has the goal of assessing if the students understood the idea of pH and how it is measured. For the higher-level students, the experiment can be further used to challenge their analytical skills. By knowing the flow rates selected for lemon juice and baking soda solution syringes, and measuring the flow rate of the manually-actuated syringe (reading the volume on the syringe and measuring the injection time with a stop-watch), the students will be challenged to calculate (approximately) the volume ratios of the three solutions in each mixing chamber where the color is observed. Starting from the volumes and by knowing the pH of each solution, they will calculate the pH of the mixed liquid in each chamber, comparing the obtained value with the pH-color scale of anthocyanin.

5.4.3 Space Juice

The space juice experiment wants to introduce the concepts of density and buoyancy. Despite the two printed submarines being completely identical and filled with the same amount of the same fluid, they behave

differently due to the different fluid that surrounds them. Through the handbook (Supplementary), the students are introduced to the concepts of density, weight and buoyancy. In the experiment they will see how density is a property of an object as well as of a substance and that it has a direct influence on its dynamical behavior. Finally, buoyancy can be introduced, completing the explanation of the balance of forces acting on a body immersed in a fluid: the floating submarine is floating because of the equilibrium of forces created between gravity and buoyancy, while the submerged one, met his equilibrium of forces at the bottom of the reservoir. The questionnaire provided (Supplementary) includes a series of questions that stimulate the critical thinking of the kids, challenging them to explain the phenomena observed based on the information acquired from the handbook.

5.5 Conclusion

While the work presented in this manuscript only describes three experiments, many more applications can be developed and performed due to the modular nature of the kit and the ease-of-production of its building block. In the same way, it is possible to expand on the explanatory part, introducing new concepts and phenomena that are involved in the experiments, as well as the handbook. Even the pumps offer the possibility for the students to explore principles of coding: the Arduino board that controls the pumps through the dedicated module, can be accessed through a USB cable and easily reprogrammed to perform specific tasks. The effects of introducing new teaching methods, more engaging and fun for primary school students, has been shown to improve not only the desired learning results¹⁹, but also increase the collaboration and engagement [20, 21] of classes where such methods have been implemented. This kit presented in this work is an extremely flexible platform that, rather than focusing on one specific type of skill, leaves room to the imagination of its user. Children can learn while playing, allowing them to get passionate and more confident about their capabilities.

Bibliography

- [1] RW Bybee. Achieving technological literacy: A national imperative. *Technology and Engineering Teacher*, 60(1):23, 2000. ISSN 2158-0502.
- [2] WE Dugger. Evolution of stem in the united states. In *6th biennial international conference on technology education research*, volume 10.
- [3] J Hogan and B Down. A steam school using the big picture education (bpe) design for learning and school—what an innovative stem education might look like. *International Journal of Innovation in Science and Mathematics Education*, 23(3), 2016. ISSN 2200-4270.
- [4] K Bissaker. Transforming stem education in an innovative australian school: The role of teachers' and academics' professional partnerships. *Theory into Practice*, 53(1):55–63, 2014. ISSN 0040-5841.
- [5] A Joyce. Stimulating interest in stem careers among students in europe: Supporting career choice and giving a more realistic view of stem at work. In *Educ. Employers Taskforce Res. Conf.*
- [6] M Humburg, R van der Velden, and A Verhagen. Cedefop.(2014). *Employability and skills of higher education graduates. Analytical Highlight. Luxembourg: Publications Office of the European Union.*
- [7] F Tuluri. Using robotics educational module as an interactive stem learning platform. In *2015 IEEE Integrated STEM Education Conference*, pages 16–20. ISBN 1479918296.
- [8] RH Rizzardini and C Gütl. A cloud-based learning platform. 2016.
- [9] CW Pinger, A Castiaux, S Speed, and DM Spence. Plate reader compatible 3d-printed device for teaching equilibrium dialysis binding assays, 2018.
- [10] JJ Wietsma, JT Van Der Veen, W Buesink, A Van Den Berg, and M Odijk. Lab-on-a-chip: Frontier science in the classroom. *Journal of chemical education*, 95(2):267–275, 2018. ISSN 0021-9584.

- [11] K C Bhargava, B Thompson, and N Malmstadt. Discrete elements for 3d microfluidics. *Proceedings of the National Academy of Sciences*, 111(42):15013–15018, 2014.
- [12] LM Veltri and LA Holland. Microfluidics for personalized reactions to demonstrate stoichiometry. *Journal of Chemical Education*, 97(4):1035–1040, 2020. ISSN 0021-9584.
- [13] MT Vangunten, UJ Walker, HG Do, and KN Knust. 3d-printed microfluidics for hands-on undergraduate laboratory experiments. *Journal of Chemical Education*, 97(1):178–183, 2019. ISSN 0021-9584.
- [14] T Tabassum, M Iloska, D Scuereb, N Taira, C Jin, V Zaitsev, F Afshar, and T Kim. Development and application of 3d printed mesoreactors in chemical engineering education. *Journal of Chemical Education*, 95(5):783–790, 2018. ISSN 0021-9584.
- [15] CW Pinger, MK Geiger, and DM Spence. Applications of 3d-printing for improving chemistry education. *Journal of Chemical Education*, 97(1):112–117, 2019. ISSN 0021-9584.
- [16] VF Scalfani and TP Vaid. 3d printed molecules and extended solid models for teaching symmetry and point groups. *Journal of Chemical Education*, 91(8):1174–1180, 2014. ISSN 0021-9584.
- [17] SC Meyer. 3d printing of protein models in an undergraduate laboratory: leucine zippers. *Journal of Chemical Education*, 92(12):2120–2125, 2015. ISSN 0021-9584.
- [18] B Schmidt, D King, and J Kariuki. Designing and using 3d-printed components that allow students to fabricate low-cost, adaptable, disposable, and reliable ag/agcl reference electrodes. *Journal of Chemical Education*, 95(11):2076–2080, 2018. ISSN 0021-9584.
- [19] A Boeshaghi, E Beltrame, D Bannon, J Gehring, and L Pachter. Principles of open source bioinstrumentation applied to the poseidon syringe pump system. *Scientific reports*, 9(1):1–8, 2019. ISSN 2045-2322.
- [20] B Heidt, R Rogosic, S Bonni, J Passariello-Jansen, D Dimech, JW Lowdon, R Arreguin-Campos, E Steen Redeker, K Eersels, and H Diliën. The liberalization of microfluidics: Form 2 benchtop 3d printing as an affordable alternative to established manufacturing methods. *physica status solidi (a)*, 217(13):1900935, 2020. ISSN 1862-6300.
- [21] A Raja, ES Lavin, T Gali, and K Donovan. Science alive!: Connecting with elementary students through science exploration. *Journal of microbiology & biology education*, 17(2):275–281, 2016. ISSN 1935-7885.
- [22] N Fanchamps and K Kreijns. Stem learning in primary education by means of highly visualised digital applications. In *INTED2022 Proceedings*, pages 3050–3058. IATED, 2022.

-
- [23] CG Frantom, KE Green, and ER Hoffman. Measure development: The children's attitudes toward technology scale (cats). *Journal of Educational Computing Research*, 26(3):249–263, 2002.

Supplementary

Handbook and Software codes

THE HANDBOOK

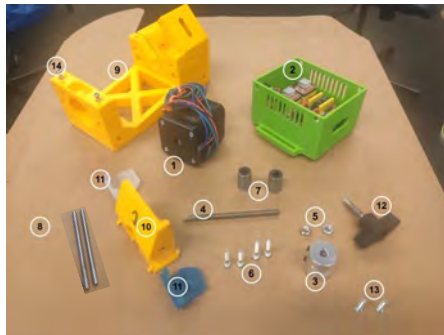
In order to facilitate the experimental replication, we provide a handbook that will guide the reader in the design, fabrication and usage of the material. The handbook is also a useful tool for the students: it will guide them through the experiments and in the learning phase by explaining the scientific phenomena addressed. Finally, for each experiment the handbook provides a set of questions aimed at giving an insight on the learning achievements.

BUILDING THE PUMPS:

The pumps used in the experiments are based on the design of the Poseidon pump, an open source syringe pump available online (<https://github.com/pachterlab/poseidon>). At this address it is possible to find a very detailed explanation of the pump assembly procedure, with a detailed video explanation and list of materials. Because in the present work we slightly modified the hardware in order to make it more practical for the purpose of the work, here we provide our own list of materials and a brief explanation on the build of the pumps.

List of materials: (Corresponding numbers in the assembly schematics)

- 1) NEMA 17 Stepper Motor ([LINK](#))
- 2) Stepper Motor Driving Board + controller ([LINK](#))
- 3) Shaft connector ([LINK](#))
- 4) M5 threaded shaft
- 5) 2x M5 Nuts
- 6) 4x M3 15mm screws
- 7) 2x linear bearings ([LINK](#))
- 8) 2x smooth steel shafts 100mm
- 12) Fixer for syringe
- 13) 2x M3 10mm screws
- 14) 2x M3 25mm screws



List of .STL files:

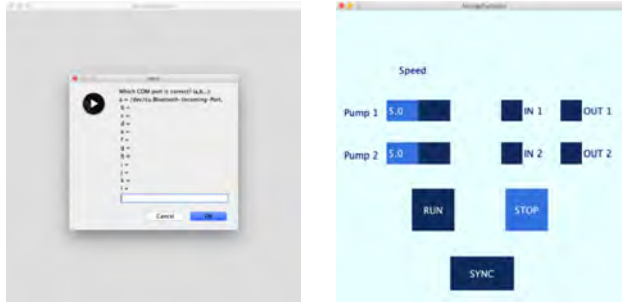
- 9) Main body
- 10) Moving Platform
- 11) Side inserts

Assembly:



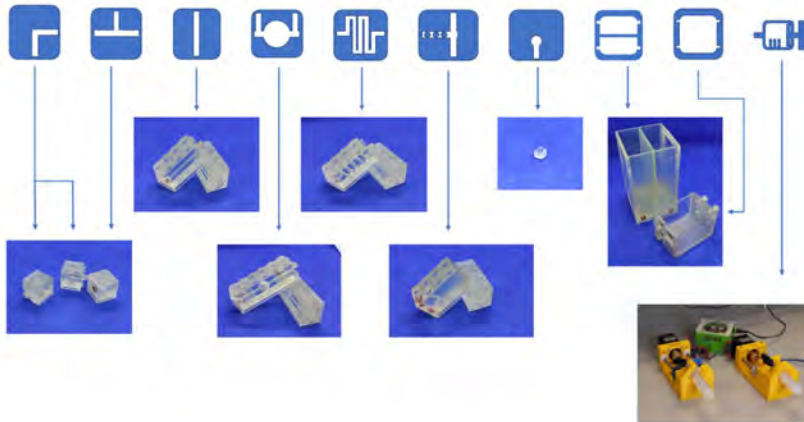
Using the pumps

While the hardware is almost identical, the software has been developed by the team using Processing (www.processing.org) and the Arduino IDE (www.arduino.cc) together with an Arduino Uno board with a stepper motor driver shield based on the A4988 driver (Longrunner GRBL CNC Sign Expansion Board V3.0), with the goal of developing a software intuitive and easy to use even for primary school pupils (code attached in Appendix 2).



In the figure above, the software for the control of the pumps is shown. Once the Processing code is launched, the software checks the serial connections and allows the user to select the desired port (the user will select the port to which the pump is connected). After the selection of the port, the user is presented with a simple interface with 2 sliders, 4 checkboxes and 3 buttons. The software controls two pumps and allows the user to select the speed of each pump (from 1 to 10, AUM), the direction of the pumps and to enter run mode or to stop the pumps. The sync button is used every time one of the parameters is changed and allows to send the new parameters to the Arduino controlling the pumps.

THE MODULAR BLOCKS:

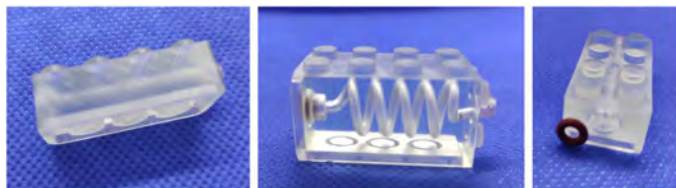


List of materials:

- .STL Files (Appendix)
- Sandpaper (grain 600 – 1000 – 2000)
- O-rings 2.9 mm Bore ([LINK](#))

The kit is made out of 10 different modular blocks. In the figure above, each of the 9 blocks is associated to a schematic representation that is used in the explanation of each experiment. By using this mapping, it is possible to uniquely link each experimental schematic to the corresponding parts and to their arrangement. All the .STL files for the blocks are provided in as Appendix.

The blocks can be fabricated with SLA/DLP 3D printing. In order to make the parts more transparent and thus improve the visibility of the experiments, the parts are treated after the print. The post processing of the modular blocks consists in the sanding of each part with different grain paper until a smooth surface is obtained. Once the surface is smooth, a common acryl spray is applied to further increase the transparency. When the parts are dried, in each of the female connections of the modular blocks, a silicon o-ring is inserted. The o-ring slides without effort inside the groove of the connection (see figure below). Wetting the o-ring can be useful before insertion. The parts are now ready to be used!



In the photo above, on the left can be seen an example of a printed block and the opaque finish obtained immediately after printing. In the middle photo, the increased transparency can be observed, thanks to the sanding and spray coating post processing process. In the last photo on the right a detail of the o-ring next to the female connection groove of an example block.

THE EXPERIMENTS

FRUIT CAVIAR

You will need:



Calcium Chloride



Food Coloring



Sodium Alginate



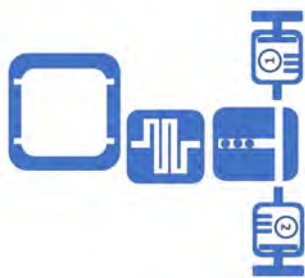
Water

Before diving into the experiment, here are the concepts you will put in practice:

- **Molecular gastronomy:** a field of science that seeks to understand how cooking can be explained through science, focusing on how the food tastes, feels, and smells and how it transforms.
- **Sodium alginate:** alginate is a long chain of sugars that comes from brown seaweed. It is what makes seaweed so flexible! Alginate is used to thicken liquids in foods like ice cream and sauces.
- **Spherification:** spherification uses calcium ions to activate the hardening of an alginate droplet. When you add calcium ions to the solution of alginate, something special happens: as you see in the image below, calcium interacts with the alginate (brown “spaghetti” or chains) and new bonds are formed. These bonds prevent the different alginate chains from freely moving, forming the gel.



The first step in an experiment is building the right set up! The picture below shows you how to put the blocks together to work.



Once the set-up is ready you must make the solutions used in the set up.

1. Calcium chloride mixing

The reservoir needs to be filled with water that has calcium in it.

- Measure 1.38 grams of calcium chloride powder
- Fill a beaker with 50 ml of distilled water
- Pour the calcium chloride powder into a cup and mix with a stirring stick until all the powder is gone!

This will make a 0.25 molar solution of calcium water perfect for the reservoir!

2. Sodium alginate mixing

Sodium alginate dissolves in water but beware, it needs lots of mixing and heat!

- Measure 0.90 grams of powder sodium alginate
- Measure out 50 ml of distilled water in a cup
- Pour in a single drop of dye
- Carefully pour a tiny bit of sodium alginate into the cup with water, heat up in a microwave (do not let it boil!) and stir until the sodium alginate has dissolved

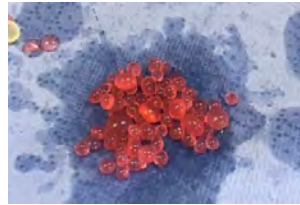
This will make a 1.8% sodium alginate solution in the color you like!

With the blocks set up and all the solutions created it is time for you to start the experiment!

1. Fill syringe #1 with air
2. Fill syringe #2 with sodium alginate

3. Turn the pumps on and find the optimal rates to create bubbles in the blocks
4. Add the Calcium Chloride to the container once the pumps are up and going

RESULTS



Questions

Why do you think we heat up the water when dissolving sodium alginate?

[1 point]

What is a molecular bond? Can you guess what elements are linked with molecular bonds in the solution?

[1.5 points]

What is the process that allowed for the formation of the small 'candy like' particles? Do you think they are soft or hard on the inside? (look at the drawings in the explanatory part)

[2 + 1 points]

Why are we using air in one of the syringes? What happens if you stop the syringe with air? How would changing the speed of the pumps affect the final result?

[1.5 points]

Tot: .../7

VEGGIE ALCHEMY

You will need:



Red Cabbage



Lemons



Baking Soda



Water

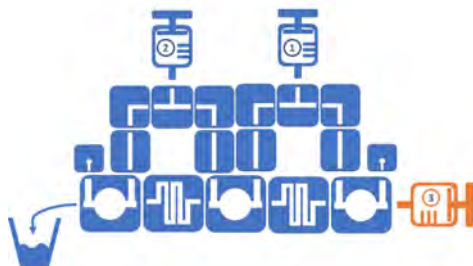
Before diving into the experiment, here are the concepts you will put in practice:

- **pH scale:** the pH scale allows to classify the acidity of liquids. The scale goes from 0 to 14 and the substances are organized by the level of concentration of hydronium ions in the liquid. Substances with a pH of 7 – right in the middle - are considered neutral.
- **Acids:** substances with a *low* number in the pH scale are categorized as acids. These substances in solution show a *high* concentration of hydronium.
- **Bases:** substances with a *high* number in the pH scale are categorized as bases. These substances in solution have a *low* concentration of hydronium.
- **Indicator:** an indicator is a chemical that changes color when it is in contact with an acid or a base. It is used to identify the hydronium concentration of a substance and therefore, its pH level.
- **Red cabbage as an indicator:** this vegetable contains a chemical called anthocyanin. This chemical is a pigment that dissolves in water and changes color according to the acidity of the substance. This means that its structure changes depending on the concentration of hydronium. Since the pH level of the substances affects the color of the pigment, it is said to be pH sensitive and therefore, can be used as an indicator.

Red cabbage color change due to different pH



Now that we are familiar with the topic, the first step of the experiment is to build the set up! Follow the schematic below to have a working mechanism:



The system is ready! The solutions for the experiments should be prepared next.

1. Preparation of indicator

- Peel the red cabbage
- Chop the leaves and place them in a cup
- Add water to the cup until it covers all the leaves, and mix
- Microwave for 2 minutes
- Let the water cool and observe the color change
- Filter out the cabbage and keep only the purple water



2. Preparation of basic component

- Place a full spoon of baking soda powder in a sealable container
- Add 50mL of water
- Shake and mix until the powder has dissolved in the water



3. Preparation of acidic component

- Cut 2 lemons
- Extract the juice from each



Once the materials and the system are set, the experiment can be put in practice!

1. Add the *indicator component* to syringe #3
2. Add the *basic component* to syringe #1
3. Add the *acidic component* to syringe #2
4. Prepare the pumps

Phase 1 – Base effect

1. Set the pump system to work with syringe #1 and use syringe #3 manually
2. Let the system run and observe the substance flowing through the system
3. What changes do you see? Record your observations

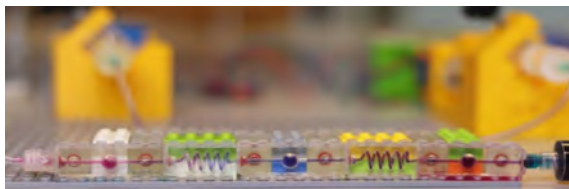
Phase 2 – Acid effect

1. Set the pump system to work with syringe #2 and use syringe #3 manually
2. Let the system run and observe the substance flowing through the system
3. What changes do you see? Record your observations

Phase 3 – Mixed effect

1. Set the pump system to work syringe #1 and #2, while using syringe #3 manually
2. Let the system run and observe the substance flowing through the system
3. What changes do you see? Record your observations

RESULTS



Questions

What did you extract from the red cabbage leaves?
[1 point]

What is the pH of the indicator solution?
[1 point]

What happens when the baking soda solution is added to the system and why? Hint: hydronium ions. This substance has a low concentration of hydronium.
[2.5 points]

What happens when the lemon juice is added to the system and why? Hint: hydronium ions/acidity. If you drink lemon juice, you can taste the acidity!
[2.5 points]

Tot: .../7

SPACE JUICE

You will need:



Before diving into the experiment, here are the concepts you will put in practice:

- **Density:** the ratio between the mass of an object and its volume. In practice it indicates how much space (volume) a certain amount of a material (mass) occupies.
- **Weight:** it is defined as the force that acts on a defined object. It is caused by gravity, which affects everything that you see around you.
- **Buoyancy:** is a force that acts on any object immersed in a fluid. When you go to the swimming pool and jump in the water, you feel much lighter in comparison to the feeling you have when you walk on land. This happens because the water is pushing you from below upwards, with a force that is called buoyancy.

Now that we are familiar with the topic, the first step of the experiment is to build the set up! Follow the schematic below to have a working mechanism:



The system is ready! For this experiment, only one solution needs to be prepared.

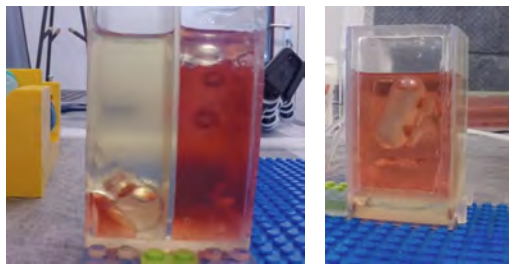
1. Preparation of colored water

- Add water in a cup and add some food coloring. Mix a bit and the solution is ready!

The Experiment:

1. Fill the submarines with oil and put one submarine in each of the two chambers
2. Fill syringe #1 with colored water
3. Fill syringe #2 with oil
4. Connect the pumps to the reservoir and fill each chamber halfway to the top
5. Use your hand to cover the top of the reservoir, then unplug the pumps from the reservoir and invert them (the oil pump will now be connected to the water chamber and the water pump will be connected to the oil chamber)
6. Start the pumps and observe what is happening in the reservoir!

RESULTS



Questions

Take the two submarines and use a scale to weight them while they are filled: register the weight of each of them. Do you think they have the same density?
[1.5 points]

What forces are acting on the submarines?
[2 points]

Why is one submarine floating while the other has sunk?
[2 points]

How could you make both submarines float in the respective chambers?
[1.5 points]

Tot: .../7

```
ProcessingCode
import controlP5.*;
import processing.serial.*;
import static javax.swing.JOptionPane.*;

#####SERIAL USER INTERFACE PART #####

Serial myPort;    // The serial port

ControlP5 control_cp5;

PFont Font1;

float syringeSpeedNoC[] = {0,0};
float syringeSpeedC[] = {0,0};
float syringeAcceleration[] = {1000,1000};
float PumpChoiceDir[] = {0,0,0,0};
String finalString;

void setup(){

    String COMx, COMlist = "";

    size(700,690);
    textSize(32);

    Font1 = createFont("Lato Regular.ttf", 22);

    textFont(Font1);

    //initiates the visual parts
    setControlPage();

    ##### COM SERIAL PART #####
    try {
        int i = Serial.list().length;
        if (i != 0) {
            if (i >= 2) {
                // need to check which port the inst uses -
                // for now we&apos;l just let the user decide
                for (int j = 0; j < i; ) {
                    COMlist += char(j+&apos;a&apos;) + " = " + Serial.list()[j];
                    if (++j < i) COMlist += ", \n ";
                }
                COMx = showInputDialog("Which COM port is correct? (a,b,..):\n"+COMlist);
            }
        }
    }
}
```

```

    if (COMx == null) exit();
    if (COMx.isEmpty()) exit();
    i = int(COMx.toLowerCase().charAt(0) - 'a') + 1;
}
String portName = Serial.list()[i-1];
//if(debug) println(portName);
myPort = new Serial(this, portName, 9600); // change baud rate to your liking
//myPort.bufferUntil('\n'); // buffer until CR/LF appears, but not
required..
}
else {
    showMessageDialog(frame,"Device is not connected to the PC");
    exit();
}
}
catch (Exception e)
{ //Print the type of error
    showMessageDialog(frame,"COM port is not available (may be in use by
another program)");
    println("Error:", e);
    exit();
}
}
}

void draw(){
    setControlPageTxt();
}

Computations
public float pitchVal = 1;

//Converts the speed from 1 to 10 into suitable speed for the AccelStepper
library
int mmpsToSteps(float speed){
    float a = speed;
    a = a * 40;
    return int(a);
}

void mmSpeedConversion(){
    for(int i=0; i<2; i++){
        syringeSpeedC[i] = mmpsToSteps(syringeSpeedNoC[i]);
    }
}
}

```

ControlPage

```
##### FUNCTIONS FOR THE Control PAGE  
#####
```

```
CheckBox Pump1SX;  
CheckBox Pump1DX;  
CheckBox Pump2SX;  
CheckBox Pump2DX;
```

```
int d = 350; //horizontal placement of some objects
```

```
void setControlPage(){  
control_cp5 = new ControlP5(this);
```

```
ControlFont font = new ControlFont(Font1);  
control_cp5.setFont(font);
```

```
control_cp5.addSlider("units1")  
    .setRange(0,10)  
    .setValue(5)  
    .setPosition(120,212)  
    .setSize(150,50)  
    .setDecimalPrecision(1);
```

```
control_cp5.addSlider("units2")  
    .setRange(0,10)  
    .setValue(5)  
    .setPosition(120,312)  
    .setSize(150,50)  
    .setDecimalPrecision(1);
```

```
control_cp5.addButton("Run")  
    .setPosition(180,420)  
    .setSize(100,100);
```

```
control_cp5.addButton("Stop")  
    .setPosition(400,420)  
    .setSize(100,100);
```

```
control_cp5.addButton("Sync")  
    .setPosition(270,580)  
    .setSize(150,80);
```

```
Pump1SX = control_cp5.addCheckBox("Pump1SX")  
    .setPosition(40+d,212)  
    .setColorForeground(color(120))
```

```

        .setColorActive(color(255, 255, 102))
        .setColorLabel(color(0, 0, 102))
        .setSize(50,50)
        .addItem("IN 1",1);

Pump1DX = control_cp5.addCheckBox("Pump1DX")
        .setPosition(180+d,212)
        .setColorForeground(color(120))
        .setColorActive(color(255, 255, 102))
        .setColorLabel(color(0, 0, 102))
        .setSize(50,50)
        .addItem("OUT 1",1);

Pump2SX = control_cp5.addCheckBox("Pump2SX")
        .setPosition(40+d,312)
        .setColorForeground(color(120))
        .setColorActive(color(255, 255, 102))
        .setColorLabel(color(0, 0, 102))
        .setSize(50,50)
        .addItem("IN 2",1);

Pump2DX = control_cp5.addCheckBox("Pump2DX")
        .setPosition(180+d,312)
        .setColorForeground(color(120))
        .setColorActive(color(255, 255, 102))
        .setColorLabel(color(0, 0, 102))
        .setSize(50,50)
        .addItem("OUT 2",1);
}

//This function generates the text parts of the control page
void setControlPageTxt() {
background(230, 255, 255);
fill(0, 0, 102);
text("Pump 1",20,250);
text("Pump 2",20,350);
text("Speed",150,150);
}

//#####
//##### Controller Functions #####
//#####

void Sync(){
finalString = "<"; //opener

```



```
mmSpeedConversion();

finalString += (str(syringeSpeedC[0])+",");
finalString += (str(syringeSpeedC[1])+",");
finalString += (str(syringeAcceleration[0])+",");
finalString += (str(syringeAcceleration[1])+",");
finalString += (str(PumpChoiceDir[0])+",");
finalString += (str(PumpChoiceDir[1])+",");
finalString += (str(PumpChoiceDir[2])+",");
finalString += (str(PumpChoiceDir[3]));

finalString += ">";

println(finalString);
myPort.write(finalString); //SENDS THE FINAL STRING TO ARDUINO
}

void Run(){
myPort.write("<R>");
//println("R");
}

void Stop(){
myPort.write("<S>");
//println("S");
}

void units1(float a){
syringeSpeedNoC[0] = a;
}

void units2(float a){
syringeSpeedNoC[1] = a;
}

void Pump1SX(float[] a) {
PumpChoiceDir[0] = a[0];
if (Pump1DX.getState(0)) {
Pump1DX.toggle(0);
PumpChoiceDir[1] = 0;
}
}

void Pump1DX(float[] a) {
PumpChoiceDir[1] = a[0];
if (Pump1SX.getState(0)) {
```

```
Pump1SX.toggle(0);
PumpChoiceDir[0] = 0;
}
}

void Pump2SX(float[] a) {
PumpChoiceDir[2] = a[0];
if (Pump2DX.getState(0)) {
Pump2DX.toggle(0);
PumpChoiceDir[3] = 0;
}
}

void Pump2DX(float[] a) {
PumpChoiceDir[3] = a[0];
if (Pump2SX.getState(0)) {
Pump2SX.toggle(0);
PumpChoiceDir[2] = 0;
}
}
```

```
ProcessingCode
import controlP5.*;
import processing.serial.*;
import static javax.swing.JOptionPane.*;

#####SERIAL USER INTERFACE PART #####

Serial myPort;    // The serial port

ControlP5 control_cp5;

PFont Font1;

float syringeSpeedNoC[] = {0,0};
float syringeSpeedC[] = {0,0};
float syringeAcceleration[] = {1000,1000};
float PumpChoiceDir[] = {0,0,0,0};
String finalString;

void setup(){

    String COMx, COMlist = "";

    size(700,690);
    textSize(32);

    Font1 = createFont("Lato Regular.ttf", 22);

    textFont(Font1);

    //initiates the visual parts
    setControlPage();

    ##### COM SERIAL PART #####
    try {
        int i = Serial.list().length;
        if (i != 0) {
            if (i >= 2) {
                // need to check which port the inst uses -
                // for now we&apos;l just let the user decide
                for (int j = 0; j < i; ) {
                    COMlist += char(j+&apos;a&apos;) + " = " + Serial.list()[j];
                    if (++j < i) COMlist += ", \n ";
                }
                COMx = showInputDialog("Which COM port is correct? (a,b,..):\n"+COMlist);
            }
        }
    }
}
```

```

    if (COMx == null) exit();
    if (COMx.isEmpty()) exit();
    i = int(COMx.toLowerCase().charAt(0) - 'a') + 1;
}
String portName = Serial.list()[i-1];
//if(debug) println(portName);
myPort = new Serial(this, portName, 9600); // change baud rate to your liking
//myPort.bufferUntil('n'); // buffer until CR/LF appears, but not
required..
}
else {
    showMessageDialog(frame,"Device is not connected to the PC");
    exit();
}
}
catch (Exception e)
{ //Print the type of error
    showMessageDialog(frame,"COM port is not available (may be in use by
another program)");
    println("Error:", e);
    exit();
}
}
}

void draw(){
    setControlPageTxt();
}

Computations
public float pitchVal = 1;

//Converts the speed from 1 to 10 into suitable speed for the AccelStepper
library
int mmptsToSteps(float speed){
    float a = speed;
    a = a * 40;
    return int(a);
}

void mmSpeedConversion(){
    for(int i=0; i<2; i++){
        syringeSpeedC[i] = mmptsToSteps(syringeSpeedNoC[i]);
    }
}
}

```

ControlPage

```
##### FUNCTIONS FOR THE Control PAGE  
#####
```

```
CheckBox Pump1SX;  
CheckBox Pump1DX;  
CheckBox Pump2SX;  
CheckBox Pump2DX;
```

```
int d = 350; //horizontal placement of some objects
```

```
void setControlPage(){  
control_cp5 = new ControlP5(this);
```

```
ControlFont font = new ControlFont(Font1);  
control_cp5.setFont(font);
```

```
control_cp5.addSlider("units1")  
    .setRange(0,10)  
    .setValue(5)  
    .setPosition(120,212)  
    .setSize(150,50)  
    .setDecimalPrecision(1);
```

```
control_cp5.addSlider("units2")  
    .setRange(0,10)  
    .setValue(5)  
    .setPosition(120,312)  
    .setSize(150,50)  
    .setDecimalPrecision(1);
```

```
control_cp5.addButton("Run")  
    .setPosition(180,420)  
    .setSize(100,100);
```

```
control_cp5.addButton("Stop")  
    .setPosition(400,420)  
    .setSize(100,100);
```

```
control_cp5.addButton("Sync")  
    .setPosition(270,580)  
    .setSize(150,80);
```

```
Pump1SX = control_cp5.addCheckBox("Pump1SX")  
    .setPosition(40+d,212)  
    .setColorForeground(color(120))
```

```

        .setColorActive(color(255, 255, 102))
        .setColorLabel(color(0, 0, 102))
        .setSize(50,50)
        .addItem("IN 1",1);

Pump1DX = control_cp5.addCheckBox("Pump1DX")
        .setPosition(180+d,212)
        .setColorForeground(color(120))
        .setColorActive(color(255, 255, 102))
        .setColorLabel(color(0, 0, 102))
        .setSize(50,50)
        .addItem("OUT 1",1);

Pump2SX = control_cp5.addCheckBox("Pump2SX")
        .setPosition(40+d,312)
        .setColorForeground(color(120))
        .setColorActive(color(255, 255, 102))
        .setColorLabel(color(0, 0, 102))
        .setSize(50,50)
        .addItem("IN 2",1);

Pump2DX = control_cp5.addCheckBox("Pump2DX")
        .setPosition(180+d,312)
        .setColorForeground(color(120))
        .setColorActive(color(255, 255, 102))
        .setColorLabel(color(0, 0, 102))
        .setSize(50,50)
        .addItem("OUT 2",1);
}

//This function generates the text parts of the control page
void setControlPageTxt() {
background(230, 255, 255);
fill(0, 0, 102);
text("Pump 1",20,250);
text("Pump 2",20,350);
text("Speed",150,150);
}

//#####
//##### Controller Functions #####
//#####

void Sync(){
finalString = "<"; //opener

```

```
mmSpeedConversion());

finalString += (str(syringeSpeedC[0])+",");
finalString += (str(syringeSpeedC[1])+",");
finalString += (str(syringeAcceleration[0])+",");
finalString += (str(syringeAcceleration[1])+",");
finalString += (str(PumpChoiceDir[0])+",");
finalString += (str(PumpChoiceDir[1])+",");
finalString += (str(PumpChoiceDir[2])+",");
finalString += (str(PumpChoiceDir[3]));

finalString += ">";

println(finalString);
myPort.write(finalString); //SENDS THE FINAL STRING TO ARDUINO
}

void Run(){
myPort.write("<R>");
//println("R");
}

void Stop(){
myPort.write("<S>");
//println("S");
}

void units1(float a){
syringeSpeedNoC[0] = a;
}

void units2(float a){
syringeSpeedNoC[1] = a;
}

void Pump1SX(float[] a) {
PumpChoiceDir[0] = a[0];
if (Pump1DX.getState(0)) {
Pump1DX.toggle(0);
PumpChoiceDir[1] = 0;
}
}

void Pump1DX(float[] a) {
PumpChoiceDir[1] = a[0];
if (Pump1SX.getState(0)) {
```

```
Pump1SX.toggle(0);
PumpChoiceDir[0] = 0;
}
}

void Pump2SX(float[] a) {
PumpChoiceDir[2] = a[0];
if (Pump2DX.getState(0)) {
Pump2DX.toggle(0);
PumpChoiceDir[3] = 0;
}
}

void Pump2DX(float[] a) {
PumpChoiceDir[3] = a[0];
if (Pump2SX.getState(0)) {
Pump2SX.toggle(0);
PumpChoiceDir[2] = 0;
}
}
```


Chapter postface

NB: the information described in this section (including graphs and tables) is the result of an independent study conducted by an external research group and was published [22]. The material included in the following pages can therefore not be regarded as the work of the author of this thesis, and constitutes a summary of the concepts illustrated in the above cited article. However, as the results of this study are instrumental to benchmarking the results demonstrated in this thesis, the data of the article have been extrapolated and modified with permission of the authors. The science kit described in chapter 5, is referred here as the Flui.go Kit. For more information, see page 104.

Introduction

The research question that the on-field study wanted to answer, was whether *"inquiry-based learning empowered by a visual STEM learning environment can provide meaningful added value when compared to other teaching settings"*. In order to answer to that question, the study wanted to find out if any of the following targets had been obtained by using the Flui.go kit:

- More positive attitude toward STEM subjects
- Increased scientific and systematic scientific thinking
- Improved linking between theory and practice

Methodology

One hundred primary school students aged 9 to 13 (grade five to eight) were selected from four different primary schools in the Netherlands. They were assigned to one of the following groups: group 1 (n = 32) attended STEM classes (inquiry-based learning) integrating the usage of the innovative science kit described in chapter 5. Group 2 (n = 32) attended STEM classes (inquiry-based learning) integrating the usage of a commercial science box. The control condition, group 3, (n = 36) attended the traditional form of STEM education, meaning



Figure 5.5: On-field testing setup of the educational STEM kit in a primary schools in the Netherlands.

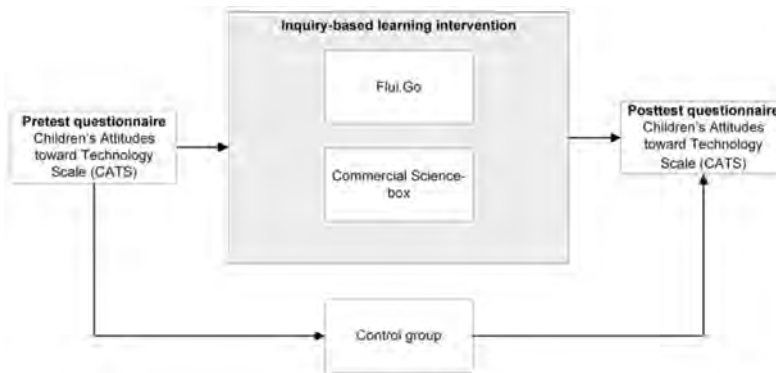


Figure 5.6: Research design.

that in this condition students had to follow the regular science and technology curriculum. Five different lessons, each 1 h-long, have been conducted with the three groups. A questionnaire was administered to the pupils before the start of the first class and at the end of the last class (5.6). The selected questionnaire was the *Children's Attitude Towards Science (CATS)* system [23]. This questionnaire is optimized to evaluate the students' attitude, fascination, and valuing towards science and technology. Additionally, qualitative data were collected by interviewing the students and by observation. All groups were offered the same assignments, task and difficulty level.

Results

The results, displayed in Table 1, show that both group 1 and group 2 registered a notable increase in score between pre- and post- test, while group 3 (control group), had a different trend. The mean scores for group 1 are the highest, however this difference was present also in the pre-test evaluation. In addition to the quantitative evaluation provided by the study, qualitatively insights were collected. Based on the observations in the classroom, interviews with the teachers and pupils, the usage of the Flui.Go Kit was associated with an increase in enthusiasm, excitement and curiosity towards the lesson. The utilization of highly visual supporting tools (both the Flui.Go Kit and the Commercial kit) contributed to maintain high levels of focus throughout the lessons, and a feeling of accomplishment when the experiments were successfully completed. When comparing group 1 with group 2, it has been noticed that how the Flui.Go Kit also stimulated the student's creativity, as the modular nature of the kit pushed some of the pupils to recombine the blocks and try to build "their own experiments". Last but not least, the group using the Flui.Go Kit, showed a higher level of cooperation in comparison to groups 2 and 3.

Variable	Pre-test CATS (26 items)				Post-test CATS (26 items)			
	M	SD	Range	Mdn	M	SD	Range	Mdn
Flui.Go (n = 32)	2.75	0.13	0.54-2.96	2.77	2.80	0.18	2.54-3.23	2.81
Science box (n = 32)	2.63	0.26	2.19-3.31	2.60	2.74	0.24	2.50-3.42	2.70
Control group (n = 36)	2.68	0.27	2.12-3.38	2.69	2.63	0.16	2.35-2.92	2.67

Note. M = average; SD = standard deviation; range = spread in measurement; Mdn = median.

Table 1. Results of the CATS test for the three different groups, based on the pre- and post- questionnaires.

Conclusion

This study confirms that highly visualised environments show potential in STEM education. Following exposure to such environments, the study

showed quantitatively and qualitatively improvements in the student's attitude towards science. This could be due to the entertaining nature of such tools, and to the simple but effective ICT control technology that ensures that pupils themselves are conducting the experiments. While the results are encouraging, further research should be conducted, especially focusing on the added value of highly visual ICT STEM learning environments, in terms of didactical knowledge acquired. In order to do so, similar studies will be repeated with larger groups of students, expanding the experiments performed and matching them to specific school curricula. In terms of the thesis, the results confirm that rapid prototyping and manufacturing have the potential to facilitate science at every level in coming decades. Not just, in scientific research and valorization of the resulting technologies, but also in STEM education.

6

General Discussion

The achievement of the thesis is to demonstrate, from an engineering point of view, how affordable, user-friendly, devices made with rapid prototyping can facilitate scientific research and education in coming years. The work presented in this thesis therefore covers different fields, ranging from biosensors development, engineering studies, to educational development and market valorization. Despite seemingly addressing different subjects, the chapters are connected by the common principle that user-specific requirements are more and more relevant and that customization, and thus demassification of production, will become an even more central argument in the future of additive manufacturing. In this way it can have a massive impact on various scientific fields, ranging from biosensor R&D to STEM education, where a more student centered approach seems to become increasingly dominant on a global scale.

The Liberalization of Microfluidics Form2 Benchtop 3D Printing as an Affordable Alternative to Established Manufacturing Methods

In Chapter 2 of the thesis, we investigated the potential of a well-known and used SLA 3D printer, the Form2. The developed testing protocol, allowed to highlight accuracy and dimensional limits of the printer and of the three different materials used. Particular attention has been dedicated to the testing of closed and open channel fabrication, given that such information can be used for the fabrication of microfluidic devices, which is the focus of the study. This parameter is of particular importance, as the main added value of 3D printing in biosensor research could lay in the design and rapid manufacturing of fluid transport samplers. The results show that accuracy achievable with this machine is not comparable with soft lithography, the traditional fabrication techniques of microfluidic devices. However, this process not only is time consuming, but very expensive as it relies on costly machines and a clean-room [1]. Soft lithography allows for great resolution, and it is the gold standard in fields such as cell-culture, where tight control of the environment on a cellular level is important, however for many applications in the lab, such resolution is not needed. 3D printing has been explored as a cost-effective alternative for the fabrication of flow cells, both through polydimethylsiloxane (PDMS) casting from 3D

printed molds [2], and direct printing [3]. Understanding the functioning parameters and limits of the Form2 3D printer, gives important insights on how to exploit the potential of such machine. Formlabs provides a variety of materials (resins) that can be used to fabricate objects, each of them with specific characteristics. In this study, it was chosen to analyze three different resins, considered as representative of three different classes of materials that are most used in laboratory environments. Respectively, the materials were a clear resin, a prototyping resin and a high temperature resin. A clear resin is important in application where transparency is crucial, such as spectroscopy [4], or applications in which fluid visualization or monitoring is important. The second material studied is the tough resin, a material with the best mechanical properties between the three, and thus ideal for prototyping mechanically functional parts. Lastly, the high temperature resin can be used in laboratory applications such as 3D printed PCR devices [5], in which thermal cycling is required. The main take-away of this study is that Clear resin can be used with the Form 2 printer to make flow cells for biosensor experiments, which was further explored in Chapter 3.

Studying the effect of Adhesive Layer Composition on MIP-based Thermal Biosensing

The findings in Chapter 2 were used to construct a flow cell for a biosensor experiment using molecularly imprinted polymers as receptors and the heat transfer method technology as a transducer [6], for the detection of 2-MXP. The study focuses on the recognition element of the sensor, analyzing the influence of the adhesive layer used to immobilize the MIPs onto the chip substrate. Traditionally, spin coated PVC is used as an adhesive layer, most likely thanks to its low-cost price, high availability and well3-studied properties. In order to improve the sensor performance, the study compared the behavior of 3 polymers: PVC, a copolymer of PVB, PVOH and PVA, and a copolymer of PS, PE and PB-1. The choice fell on these polymers, thanks to their comparable cost but different monomers and thus properties. The sensor used, relies on the heat transfer method as a readout technique, thus the thermal properties of the films created were studied. The results show that the PVB-PVOH-PVA copolymer has the lowest R_{th} , closely followed by

the PS-PE-PB/1 copolymer, and both have considerably lower R_{th} in comparison to PVC. This could be a consequence of the higher thermal conductivity of PVA (0.39 W/mK) and PVB (0.35 W/mK) present in the copolymers. Thermal properties are important for a sensor relying on thermal readout, however other factors might influence the overall sensor performance. Ultimately, the polymer film serves as an adhesive layer, therefore particle coverage of the polymer surface is of crucial importance. The two copolymers chosen as alternatives to PVC show a higher percentage of area covered by the MIPs particles. A possible explanation can be found in the mechanical properties of PVB and PVA that have higher elasticity and ductility in comparison to PVC. The polymer film created, seems to be better suited to retain the MIP particles, or to have better structural resistance. The resulting sensors analyzed, therefore show a better performance when the two copolymers selected are used, thus this work identifies two alternatives to PVC as adhesive layers for MIP deposition but on a more general scale demonstrates the effect an adhesive layer could have on biosensor performance and how a 3D printed flow cell can be used to study these types of parameters at a fraction of the cost price. In further studies, more complex polymers structures can be analyzed, such as PVA combined with graphene oxide [7, 8], in which the thermal conductivity of the film is considerably improved.

Cost-effective, scalable and smartphone-controlled 3D-Printed syringe pump - From lab bench to point of care biosensing applications

When we think of medical devices, we tend to imagine bulky and complex machines, well suited to be found in a hospital or clinic, but difficult to imagine as tools we use in our everyday lives without the assistance of trained personnel. PoC devices refute this common belief, giving the power to the user. Products nowadays are more and more compact, easy to use and safe, and with today's technology, we have the tools to design and manufacture better suited product for our needs. 3D printers have an important role in this transformation and have become nowadays an essential tool for any type of product development [9]. The syringe pump described in Chapter 4, is not a medical device in itself, however it explores the possibility of fabricating a low-cost laboratory

equipment that could easily be integrated into a benchtop biosensor application in the future. Syringe pumps are amongst the most used types of pumps in biology, tissue-engineering and chemistry labs and are part of several biosensor applications demonstrated in academic literature. Custom-made laboratory equipment has become common in research groups around the world, thanks to additive manufacturing [10]. The work presented in this chapter showed an example of such a device, with a focus on general usability, friendliness and reliability. The device developed has successfully been used by untrained personnel to perform a free radical polymerisation experiment in continuous flow. In this on-field application, the results confirmed that the syringe pump performed well, both experimentally, and from a user satisfaction perspective. This study demonstrates that fast prototyping techniques can be used to make low-cost devices with tailor-made specifications for the application at hand. This strategy can be extrapolated later in commercial biosensor design to create large batches of rapidly produced, low-cost components. As demonstrated in chapter 5, it can also be used to create low-cost modular tool kits for other purposes such as STEM education.

Modular Science Kit as a support platform for STEM learning in primary and secondary school

Finally, Chapter 5 combines the outcomes of Chapters 3 and 4, focusing on the advantages that 3D printing could bring in educational environments. In this particular study, 3D printing is used to fabricate a modular science kit. This kit is made of 3D printed transparent blocks with embedded fluidic channels. The kit includes a set of syringe pumps, which are made in the same way as the pump presented in Chapter 4. The science kit described in Chapter 5 is a tool designed to be used in science classes with pupils aged 9+. It takes inspiration for the most famous toy in the world, LEGO, and similarly, allows building different structures. These structures, however, allow to internally flush liquids that react and combine, visualizing scientific phenomena, in the field of chemistry and physics. Science, Technology, Engineering and Mathematics (STEM) education, has a central role in primary and secondary schools, and often teachers add engaging

activities to traditional classes in order to keep the pupils motivated and engaged [11]. The science kit developed in Chapter 5 falls under this category of integrative tools for education. From the proof of principle described in the published article, to the on-field application, the work describes the technical procedure to fabricate the kit and the results obtained when the kit has been used in STEM classes. Questionnaires have been used to evaluate and quantify the students' attitude towards technology, fascination and perception of science, before and after the class. The group using the science kit, showed higher motivation and ability to maintain focus and enthusiasm for a longer period of time, as well as an increased level of involvement and creativity. The study also highlighted for both experimental groups an increase on all dependent variables when compared with the control group. The external study done by researchers of the Open University confirm that the tool kit has a positive impact on the learning experience in children and stimulates their interests in STEM. Summarizing, the insights obtained in Chapter 5, together with the promising results from field testing, show the potential of the tool kit for future applications and further development in educational settings.

Bibliography

- [1] JA Rogers and RG Nuzzo. Recent progress in soft lithography. *Materials Today*, 8(2):50–56, 2005. ISSN 1369-7021.
- [2] A Bonyár, H Sántha, M Varga, B Ring, A Vitéz, and G Harsányi. Characterization of rapid pdms casting technique utilizing molding forms fabricated by 3d rapid prototyping technology (rpt). *International Journal of Material Forming*, 7(2):189–196, 2014.
- [3] G Weisgrab, A Ovsianikov, and PF Costa. Functional 3d printing for microfluidic chips. *Advanced Materials Technologies*, 4(10):1900275, 2019.
- [4] Berglund GD and TS Tkaczyk. Enabling consumer-grade 3d-printed optical instruments – a case study on design and fabrication of a spectrometer system using low-cost 3d printing technologies. *Opt. Continuum*, 1(3):516–526, Mar 2022.
- [5] RA Mendoza-Gallegos, A Rios, and JL Garcia-Cordero. An affordable and portable thermocycler for real-time pcr made of 3d-printed parts and off-the-shelf electronics. *Analytical Chemistry*, 90(9):5563–5568, 05 2018.
- [6] B van Grinsven, K Eersels, M Peeters, P Losada-Pérez, T Vandenryt, TJ Cleij, and P Wagner. The heat-transfer method: A versatile low-cost, label-free, fast, and user-friendly readout platform for biosensor applications. *ACS Applied Materials & Interfaces*, 6(16):13309–13318, 08 2014.
- [7] S Gahlot, V Kulshrestha, G Agarwal, and PK Jha. Synthesis and characterization of pva/go nanocomposite films. In *Macromolecular Symposia*, volume 357, pages 173–177. Wiley Online Library, 2015.
- [8] F Luo, M Zhang, S Chen, J Xu, C Ma, and G Chen. Sandwich-structured pva/rgo films from self-construction with high thermal conductivity and electrical insulation. *Composites Science and Technology*, 207:108707, 2021.
- [9] J Lettori, R Raffaelli, M Peruzzini, J Schmidt, and M Pellicciari. Additive manufacturing adoption in product design: an overview from literature

- and industry. *Procedia Manufacturing*, 51:655–662, 2020. ISSN 2351-9789. 30th International Conference on Flexible Automation and Intelligent Manufacturing (FAIM2021).
- [10] Y Zhou, C Duan, IJ Doh, and E Bae. Exploring the utility of 3-d-printed laboratory equipment. *Applied Sciences*, 9(5):937, 2019.
- [11] DTK Ng and SKW Chu. Motivating students to learn stem via engaging flight simulation activities. *Journal of Science Education and Technology*, 30(5): 608–629, 2021.

Summary

The work presented in this thesis, is made of heterogeneous but complementary parts. While rapid prototyping has been the greatest common factor between chapters, metaphorically we can say that the least common multiple, is the user. Each study conducted, includes user-end specification, and one of the common goals, has been to develop or optimize technologies, in order to make them more relevant for a larger pool of people. The thesis begins with a study on 3D printing applied to flow cell development, which gives the tools to develop the following chapters: an experimental biosensor optimization, and a DIY laboratory instrument. Finally, the findings of all the chapters are combined in the last part of the thesis, which presents a scientific kit for educational purposes, its validation and the derived valorization efforts.

The Form2 from FormLabs, is one of the most used desktop SLA resin printers on the market. In **Chapter 2**, this printer is bench-marked, focusing on fabrication of milli- to micro-sized fluidic channels. Different types of resin are analysed, investigating accuracy and limits of the printer. The goal of this study is to offer an insight on how to efficiently use this printer in laboratory environments, lowering costs, production time, and allowing researchers to custom-build tools for their projects. The findings of this chapter show how commercial 3D printers can be used to create microfluidic channels, at lower resolutions with respect to the golden standard, but with alternative advantages. Examples of applications in which the performances of commercial 3D printers are satisfactory, are flow cells used in small to medium volume liquid handling.

Chapter 3 uses such 3D printed flow cell, in combination with a Molecularly Imprinted Polymer-based (MIP) sensing core and a Heat Transfer Method (HTM) readout. The goal of this chapter is to optimize, from an engineering point of view, the adhesion layer used to immobilize the MIPs to the readout part of the sensor. Three different adhesive layer

are studied, showing their performance and behaviour. The results of the chapter are multiple: it is shown how the 3D printed flow cells performs well in comparison to older, more expensive models; the experiment also highlights that there is a significant effect due to the adhesive layer of choice, opening up possibilities for follow-up studies and in which similar technologies are used.

Chapter 4 describes a DIY syringe-pump, designed and fabricated with rapid prototyping techniques and optimized to be used by untrained personnel. Syringe pumps are amongst the most used types of pumps in biology, tissue-engineering and chemistry labs. The pump, described in this work, focuses on the maximization of the instrument usability, which would give it an edge over the currently available solution in literature, and on the market. The result is a compact, wireless, internally powered device, controlled by a custom-made app that can be downloaded on any type of smartphone. The technical performance of the pump is shown to be comparable with similar DIY instruments in literature. The user experience, has been evaluated during a class of bachelor-level students that have used and tested the pump. The qualitative investigation that followed showed that the majority of the users, despite having no laboratory experience, found the pump to be easy to use and had a good experimental experience, confirming that the initial goal of the study has been achieved.

Chapter 5 describes the design and fabrication, with 3D printing, of a modular science kit used for educational purposes. The kit is made of 3D printed, transparent, modular blocks, with embedded fluidic channels. The kit is equipped with two, 3D printed, syringe pumps (similar to the ones in Chapter 4). After building specific fluidic circuits with the modular blocks, liquids can be flushed through the system, creating and visualising scientific phenomena. The attention is caught by the visual effects created, and the curiosity of the pupils, stimulated. This chapter proposes an innovative educational tool for STEM classes, based on the principle of meaningful play: learning through the process of playing. The work in this chapter, focuses on the tools and the explanations on how to build and use the kit. However, to field-test its effectiveness, a study has been conducted in a primary school in Limburg. Because

of the commercial valorization efforts, that the project lead to, and thus conflict of interest, data collection and evaluation was done by Nardie Fanchamps, a professor of educational sciences at the Open University of the Netherlands. Thanks to this collaboration, an article has been published, and the results are shown as external corroborating information. In summary, the results are promising, showing how the kit developed, improved the involvement of students, their fascination with the subjects studied, and with science in general.

Valorization

Translating research topics to concrete applications for the commercial market, is always a challenge. Academic research is crucial thanks to its role in pushing boundaries, and exploring unknown grounds. Many times, these unknown grounds prove to be infertile from a commercial perspective, even more for medical devices, where new products have a particularly long development life. Nonetheless, during my PhD, I had the privilege to work on a project that tried to close the gap between academia and the market. During my second year as a researcher, I had the chance to found a start-up, active in the educational field. The company, called Flui.Go Science, was established in March 2020 and has since produced its first product: The Flui.Go Kit (Figure 1). Flui.Go's mission is to bring science to young people in a more entertaining and engaging way.



Figure 1: Flui.Go's first product, the Flui.Go Kit

The Flui.Go kit is an education(-toy)tool, composed of transparent modular blocks with integrated fluidic channels. Featuring also a pumping system (further development of the work in Chapter 5), the kit allows students and children to build fluidic circuits by combining the blocks together. Such system is studied to allow creating and displaying scientific phenomena, in an engaging way (Figure 2). Whether by visualising a colour change of the fluid due to Ph variation, or by creating colourful candy-like spheres, the young students are guided by a digital handbook including pre-made experiments that allow children to play with physics, chemistry, mathematics and much more.



Figure 2: Visual appeal is essential for the Flui.Go Kit. The goal is to attract the student's attention and curiosity for the phenomena underlying the effects visualized.

The idea to develop an educational tool was born during my tutoring duties as a PhD candidate. The courses I tutored were mainly multidisciplinary courses focused on science, particularly on theoretical and practical skills in the laboratory. The students joining this course often had various high-school backgrounds, resulting in different preparations. However, all of them liked the hands-on experiments conducted in the laboratory. From this experience, together with a colleague of mine, I decided to extend the concept that we used in our

classes, to basic, introductory science classes. Thanks to the support of my supervisors and to the possibility to combine my PhD research topics with some activities performed at Flui.Go Science, I managed to push the project forward. In September 2019 the concept won a prize at an internal UM competition, which allowed us to kick-start our idea and create the first prototypes. Another significant milestone was the SWOL Grant (University Fund Limburg) that we secured at the end of 2019. Thanks to the funding acquired and the enthusiastic reaction from the people that got involved in the project, we founded the company in March 2020.



A team of motivated students from various faculties of Maastricht University joined Flui.Go, helping us improve on our prototypes and release our first beta version of the Flui.Go Kit. In parallel, we developed a business plan, established the first contacts in local schools and started a collaboration with professional educators and researchers to field test our prototypes. The results of our study are published in the INTED2022 (<https://library.iated.org/view/FANCHAMPS2022STE>), demonstrating how our Flui.Go Kit helps young pupils to develop a positive attitude towards science.



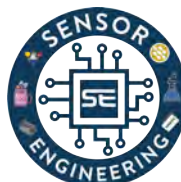
In late 2021 Flui.Go secured an agreement with 26 secondary schools in Limburg, with the goal of providing the Flui.Go Kit as an education support tool in STEM classes. This was an important milestone for Flui.Go and gave us the possibility to plan a large scale, commercial pilot-study. Today Flui.Go is collecting feedback from the schools that are using the kit and using this feedback to optimize our future strategy. In May 2022, Flui.Go Science, in Collaboration with the Open University of the Netherlands, secured the prestigious Comenius grant. The 50,000 euro funding will be spent to provide the Flui.Go Kit to educators across the Netherlands and evaluate the efficacy of the implementation of the Flui.Go Kit as a supporting tool in science classes.

At Flui.Go, we consider academic research a crucial part of our product development. Flui.Go Science was born as a research project, and we showed that research and valorization can not only coexist, but also thrive together. Our plans for the future are to continue improving our Flui.Go Kit, developing new experiments, but also to expand our range of products in order to provide educational tools to more and more young students. We want to give the best tools possible to the new generations, helping them learn more and become the game-changers of tomorrow.

Partners involved in the project:



Special acknowledgement:



Published work

R Rogosic, M Poloni, R Marroquin-Garcia, D Dimech, J Passariello-Jansen, TJ Cleij, K Eersels, B van Grinsven, H Diliën. (2022), Cost-effective, scalable and smartphone-controlled 3D-Printed syringe pump-From lab bench to point of care biosensing applications. *Physics in Medicine*, 14, 100051

SWL Lee, **R Rogosic**, C Venturi, MT Raimondi, A Pavesi, G Adriani. (2022), A Human Neurovascular Unit On-a-Chip. *Organ-on-a-Chip: Methods and Protocols*, 107-109

R Arreguin-Campos, K Eersels, **R Rogosic**, TJ Cleij, Thomas J, H Diliën, B van Grinsven. (2022), Imprinted Polydimethylsiloxane-Graphene oxide composite receptor for the biomimetic thermal sensing of Escherichia coli. *ACS sensors*, 7, 5, 1467-1475

R Arreguin-Campos, K Eersels, JW Lowdon, **R Rogosic**, B Heidt, M Caldara, K Jimenez-Monroy, H Diliën, TJ Cleij, B van Grinsven. (2021), Biomimetic sensing of Escherichia coli at the solid-liquid interface: From surface-imprinted polymer synthesis toward real sample sensing in food safety. *Microchemical Journal*, 169, 106554

M Caldara, JW Lowdon, **R Rogosic**, R Arreguin-Campos, K Jimenez-Monroy, B Heidt, K Tschulik, TJ Cleij, H Diliën, K Eersels, B van Grinsven. (2021). Thermal detection of glucose in urine using a molecularly imprinted polymer as a recognition element. *ACS Sensors*, 6, 12, 4515-4525

B Heidt, **R Rogosic**, N Leoné, E Brás, TJ Cleij, JAW Harings, H Diliën, K Eersels, B van Grinsven. (2021), Topographical vacuum sealing of 3d-printed multiplanar microfluidic structures. *Biosensors*, 11, 10, 395

R Rogosic, B Heidt, J Passariello-Jansen, S Björnör, S Bonni, D Dimech, R Arreguin-Campos, JW Lowdon, KL Jiménez Monroy, M Caldara, K Eersels, B van Grinsven, TJ Cleij, H Diliën. (2021),

Modular Science Kit as a support platform for STEM learning in primary and secondary school. *J. Chem. Educ.*, 98, 2, 439–444

B Heidt*, **R Rogosic***, S Bonni, J Passariello-Jansen, D Dimech, JW Lowdon, A Arreguin-Campos, E Steen Redeker, K Eersels, H Diliën. (2020), The Liberalization of Microfluidics: Form 2 Benchtop 3D Printing as an Affordable Alternative to Established Manufacturing Methods. *Phys. Status Solidi A*, 217: 1900935

*Authors contributed equally

JW Lowdon, H Ishikura, A Radchenko, R Arreguin-Campos, **R Rogosic**, B Heidt, K Jimenez Monroy, M Peeters, H Diliën, K Eersels, TJ Cleij. (2020), Rapid Colorimetric Screening of Elevated Phosphate in Urine: A Charge-Transfer Interaction. *ACS omega*, 5(33), pp.21054-21066.

JW Lowdon, K Eersels, **R Rogosic**, T Boonen, B Heidt, H Diliën, B van Grinsven, TJ Cleij. (2020) Surface grafted molecularly imprinted polymeric receptor layers for thermal detection of the New Psychoactive substance 2-methoxyphenidine. *Sensors and Actuators A: Physical*. 15;295:586-95.

JW Lowdon, H Ishikura, A Radchenko, R Arreguin-Campos, **R Rogosic**, B Heidt, K Jimenez Monroy, M Peeters, H Diliën, K Eersels.(2020), Rapid Colorimetric Screening of Elevated Phosphate in Urine: A Charge-Transfer Interaction. *ACS omega*, 5, 33, 21054–21066

JW Lowdon, K Eersels, R Arreguin-Campos, M Caldara, B Heidt, **R Rogosic** K Jimenez-Monroy, TJ Cleij, H Diliën, B van Grinsven. (2020), A molecularly imprinted polymer-based dye displacement assay for the rapid visual detection of amphetamine in urine. *Molecules*, 25, 22, 5222

R Rogosic, JW Lowdon, B Heidt, H Diliën, K Eersels, B van Grinsven, TJ Cleij, (2019), Studying the Effect of Adhesive Layer Composition on MIP-Based Thermal Biosensing. *Physica Status Solidi (a)*, 216, 12, 1800941

JW Lowdon, K Eersels, **R Rogosic**, B Heidt, H Diliën, ES Redeker, M Peeters, B van Grinsven, TJ Cleij. (2019), Substrate displacement

colorimetry for the detection of diarylethylamines. *Sensors and Actuators B: Chemical*, 282, 137-144

B Heidt, **R Rogosic**, JW Lowdon, M Desmond-Kennedy, K Jurgaityte, J Ferrer Orri, TJ Cleij. (2019). Biomimetic Bacterial Identification Platform Based on Thermal Transport Analysis Through Surface Imprinted Polymers: From Proof of Principle to Proof of Application. *Physica Status Solidi A*, 216, 12, 1800688

K Eersels, H Diliën, JW Lowdon, E Steen Redeker, **R Rogosic**, B Heidt, B van Grinsven. (2018). A novel biomimetic tool for assessing vitamin K status based on molecularly imprinted polymers. *Nutrients*, 10, 6, 751

Curriculum Vitae

I obtained my master's degree in Biomechanics and Biomaterials from *Politecnico di Milano* in 2017. During my studies I had the opportunity to join a variety of research projects, spanning from the fields of endoprosthesis (surface treatments of dental implants), to bioelectronics (optical glucose meter) and regenerative medicine (development of an *in vitro* blood brain barrier). Since November 2017, I pursued my PhD in Biosensors, focusing on 3D printing, prototyping and later in my track, also on educational applications. In 2020, I had the privilege to found a start-up (Flui.Go Science) that combined my passion for product design and prototyping, with the goal of improving primary education in STEM subjects.

Acknowledgments

In this last and important section of my thesis, I would like to thank the people with whom I shared the most of the struggles and joys of my doctorate studies. From my amazing colleagues that made the working environment entertaining, to my friends and family, that supported me and helped me to reach this important goal.

Dr. Bart van Grinsven, countless times I have seen you charismatically smiling from the cover page of one of the magazines found across the campus...you are a true example to follow. In a group dominated by chemists, I shared with you the excitement of receiving a new tool kit for our engineering lab. I am grateful for being part of the Sensors Engineering group and to have witnessed the growth of a small and motivated team into a well-established research group.

Dr. Kasper Eersels, to date I still have not found a scientific field in which you are not an expert, always fuelling conversations and arguments with passion and knowledge. I must thank you for the guidance and support you gave me as my co-promoter, but what I am most thankful for, are the countless discussions about your love for Italy and Italian cuisine. Combined with your less-than-ideal politically correct humor, you made the working environment more laid-back and cheerful. My PhD would have not been as enjoyable without you.

Dr. Hanne Diliën, the shepherd that brings back to the right path the flock of sheep. Whether the sheep are your MSP students or the members of the Sensor Engineering group, I leave to interpretation (I think a bit of both). Thank you for being always available to help and answer my doubts. I will always remember your support in the early stages of Flui.Go!

Debby Hewitt, always with a smile and a positive attitude, you made all our lives easier countless times. I am sorry for consistently sending you 3 different emails in 15 minutes for ordering materials...I hope one day I will be organized and precise as you are. Thank you for guiding me through the bureaucratic hurdles of working in academia, and for your kind and caring attitude.

Prof. Dr. Thomas Cleij, thank you for putting together a state-of-the-art laboratory and for contributing to create a stimulating work environment.

Dr. Joseph Lowdon, what a journey it has been. We started our PhD together, and more than 5 years later you have become a paper factory, a real estate speculator and a soon-to-be husband. The dedication to your research, the hard work and the determination you put in your projects, are admirable. Thanks for the laughs, the drinks, the good times we had together, and for being a motivation to give more at work and not fall too far behind.

Rocio Arreguin-Campos, after overcoming your fear of bacteria (partially), you have become a brilliant researcher and an example to follow in the group. Weather by helping you in figuring out how to interpret the impedance signal of a measurement, or how to pronounce correctly pizza, I hope I have also left you some good memories about our time together.

Manlio Caldara, we formed the original Italian gang, and we are now taking over the group. Despite having quite different personalities, we somehow fit together, and we became good friends and even housemates. Everyone will agree that thanks to you, the lab is a more joyful environment and that your jokes are capable of bringing a smile even on the worst days. Thanks for your signature chicken salad that kept us going when thuisbezorgd couldn't.

Ramiro Marroquin-Garcia, thanks for being a supportive friend and for never backing up from a late night philosophical discussion. You have

many human qualities that I admire and that are rarely found. Scientist during the day, artist and husband after 17, you also have many talents, but nothing comes close to your skills as a meme-creator.

Dr. Kathia Jimenez Monroy, I remember with pleasure the ideas that we shared regarding our research activities and the highs and lows of long teaching sessions. Thank you for being a kind colleague during our time together in the lab.

Dr. Jeroen Royakkers, when one thinks of a Cambridge postgraduate, seriousness, reserve and commitment are some things that inevitably come to mind. I was pleased to discover that you might be the exception that confirms the rule. I am still waiting for a tennis rematch, in the meantime I will be ok with beating you at go-karting.

Fatemeh Ahmamdadi Tabar, you tried to teach me some Persian words but despite your patience, I am afraid I do not have a talent for languages. Thank you for trying, as well as for the good laughs and the tasty Iranian food that you always let me try.

Gil van Wissen, an incorruptible man, guided by strong moral values. Spending your days between chess and running, you are the true embodiment of *Mens sana in corpore sano*. Go and make our Yung Lean boy proud.

Margaux Frigoli, thank you for making SE more fashionable. You are part of the new SE generation, and I am sure it rests in good hands. Please stop getting into fights with Gil, but keep beating him at chess.

Francesca Bertella, good friends are rare material, and I am glad our paths brought us together. Thank you for being always supportive and most of all patient...I know sometimes it must be challenging. I would have never thought I would attend a Vasco's concert in my life, thanks to you, I can take it off my bucket list.

Xu Liu, Wei Luo, Yingyi Wu, our friendship was forged through sweat (skydiving), tears (hotpot), and joy (karaoke). Thank you for the great times we shared in the last two years, I am looking forward to many more. GANBEI!!

Nardie Fanchamps, your contribution to the Flui.Go project has been crucial. Amongst your countless professional commitments and hobbies, you always found the time to help me out. I admire the enthusiasm and the positiveness that you radiate and inevitably influence people around you.

Flui.Go team, Juliette, David, Tobi, Saga, Renée-Claire, Elias, Chris, Alex and all the others that have in their own way contributed to the Flui.Go Science project. Thank you for the incredible effort and commitment that you put in the development of Flui.Go. Despite your academic commitments, you truly went the extra mile. Without you, the Flui.Go Science experience would have been impossible.

Last on this list but first in my heart, **my mother Andelka, my father Slobodan, and my sister Lea**, the people on which I can always count on. I believe I am incredibly lucky to have you, and I will never be grateful enough for all the love and support that you show me every day.

Renato Rogosic
Maastricht
4th of April

